

**COORDINATION CHEMISTRY OF NOVEL COPPER(I) AND
SILVER(I) SCHIFF BASE COMPLEXES**



**A Thesis Submitted to the Graduate School of Naresuan University
in Partial Fulfillment of the Requirements
for the Master of Science Degree in Chemistry**

May 2017


Copyright 2017 by Naresuan University


Thesis entitled "Coordination Chemistry of Novel Copper(I) and Silver(I)
Schiff base Complexes"

by Miss Sujirat Boonlue

has been approved by the Graduate School as partial fulfillment of the requirements
for the Master of Science Degree in Chemistry of Naresuan University

Oral Defense Committee

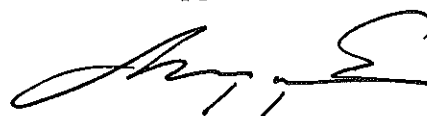

..... Chair
(Ratanon Chotima, Ph.D.)


..... Advisor
(Anchalee Sirikulakajorn, Ph.D.)


..... Co-Advisor
(Assistant Professor Kittipong Chainok, Ph.D.)


..... External Examiner
(Winya Dungkaew, Ph.D.)

Approved



.....
(Panu Putthawong, Ph.D.)

Associate Dean for Administration and Planning
for Dean of the Graduate School

1 1 1 1 1 1

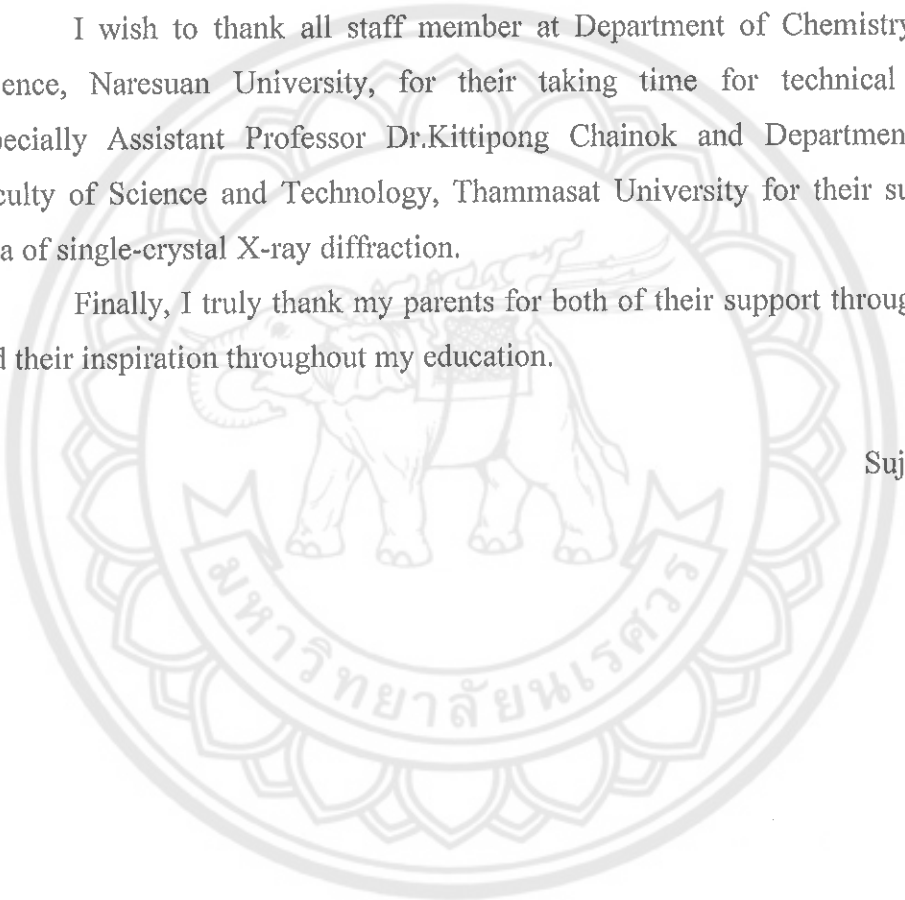
ACKNOWLEDGEMENT

First, I would like to sincerely thank my research advisor, Dr. Anchalee Sirikulkaejorn and my Co-adviser Assistant Professor Dr. Kittipong Chainok for their support, attention, patience, and throughout the completion of my research. I also would like to thank committee member Dr. winya dungkaew and Dr. ratanon chotima for their valuable insight comments and suggestions.

I wish to thank all staff member at Department of Chemistry, Faculty of Science, Naresuan University, for their taking time for technical discussions, especially Assistant Professor Dr. Kittipong Chainok and Department of physic, Faculty of Science and Technology, Thammasat University for their support of the data of single-crystal X-ray diffraction.

Finally, I truly thank my parents for both of their support throughout my life and their inspiration throughout my education.

Sujirat Boonlue



Title	COORDINATION CHEMISTRY OF NOVEL COPPER(I) AND SILVER(I) SCHIFF BASE COMPLEXES
Author	Sujirat Boonlue
Advisor	Anchalee Sirikulakajorn, Ph.D.
Co - Advisor	Assistant Professor Kittipong Chainok, Ph.D.
Academic Paper	Thesis M.S. in Science in Chemistry, Naresuan University, 2016
Keywords	Copper(I), Silver(I), Schiff base complexes, luminescence

ABSTRACT

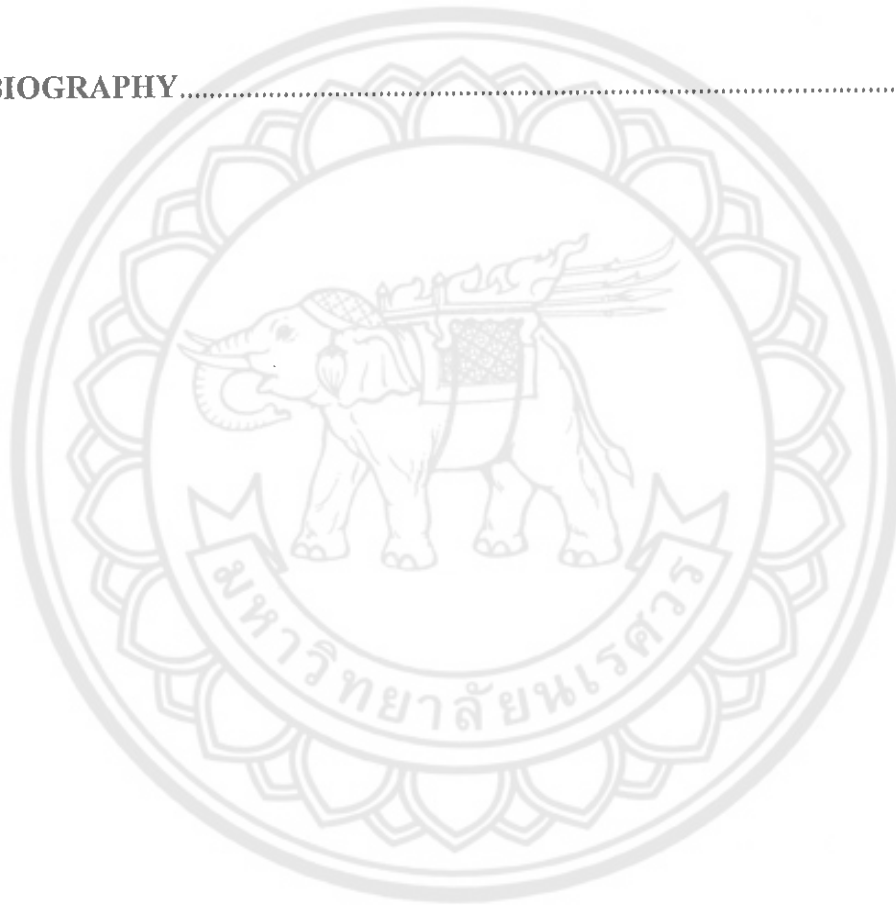
This thesis deals with the chemistry of *N,N'*-donor bidentate and bis-bidentate of Schiff base monovalence d^{10} transition metal complexes with an emphasis on the contribution to the fields of coordination chemistry, supramolecular chemistry, and crystal engineering. Eleven new luminescent Schiff base complexes of copper(I) and silver(I) with the different structural features have been synthesized and characterized by SC-XRD, elemental analysis, FT-IR, TGA, and photoluminescent spectroscopy: [Cu(PM-4-FA)(NCS)] (**Cu-1**), [Cu(PM-4-ClA)(NCS)] (**Cu-2**), [Cu(PM-4-BrA)(NCS)] (**Cu-3**), [Cu(PM-4-IA)(NCS)] (**Cu-4**), [Cu(PM-3-BrA)(NCS)] (**Cu-5**), [Cu(PM-2,3-DMA)(NCS)] (**Cu-6**), [Cu(PM-3,5-DMA)(NCS)] (**Cu-7**), [Ag(PM-IA)(NO₃)] (**Ag-1**), [Ag(PM-3,5-DMA)(SCN)] (**Ag-2**), [Ag₂(PM-PBBZ)₂][ClO₄]₂ (**Ag-3**), and [Ag₂(PM-PBBZ)(NO₃)₂] (**Ag-4**). All of the complexes are crystallized in the centrosymmetric space groups and have a diversity of structures ranging from 0D discrete mononuclear structure (**Ag-1**), 0D dinuclear structure (**Cu-3**, **Cu-4**, **Ag-3**, and **Ag-4**), tetranuclear structure (**Cu-1** and **Cu-2**), and 1D polymeric chain (**Cu-5**, **Cu-6**, **Cu-7**, and **Ag-2**). The coordination geometry of the metal ions in the copper(I) complexes is a distorted tetrahedron. While the coordination sphere of silver(I) ion is very flexible which can adopt a distorted trigonal, tetrahedral and trigonal pyramidal geometries. Complexes exhibit fluorescence emission in the solid state at room temperature due to the ligand-to-ligand charge transfer (LLCT) and show thermal stability above 150 °C.

LIST OF CONTENTS

Chapter	Page
I INTRODUCTION.....	1
Introduction to the research problem and its significance.....	1
Research objectives.....	3
Scope and limitation.....	3
Expected benefits.....	3
Research procedure.....	4
Research plan.....	5
II LITERATURE REVIEW.....	6
Fluorescence Spectroscopy.....	6
Literature reviews.....	7
III EXPERIMENTAL.....	14
Materials.....	14
Physical measurements.....	14
Synthesis of Schiff base copper(I) complexes.....	15
Synthesis of Schiff base silver(I) complexes.....	17
IV RESULTS AND DISCUSSION.....	19
Synthesis of infrared spectra.....	19
Description of crystal structure.....	21
Thermal analyses.....	58
Photoluminescent properties.....	60
V CONCLUSION.....	64

LIST OF CONTENTS (CONT.)

Chapter	Page
REFERENCES.....	66
APPENDIX.....	72
BIOGRAPHY.....	82



LIST OF TABLES

Table	Page
1 Vibrational frequencies for all copper(I) complexes and KNCS (cm^{-1})..	20
2 Crystal data and structural refinement for complexes Cu-1-Cu-4.....	21
3 Selected bond lengths (\AA) and bond angles ($^{\circ}$) for Cu-1 and Cu-2.....	24
4 Intermolecular π - π interactions (\AA , $^{\circ}$) for Cu-1 and Cu-2.....	27
5 Hydrogen bond geometry (\AA , $^{\circ}$) for Cu-1 and Cu-2.....	28
6 Selected bond lengths (\AA) and bond angles ($^{\circ}$) for Cu-3 and Cu-4.....	30
7 Intermolecular interactions (\AA , $^{\circ}$) for Cu-3 and Cu-4.....	32
8 Crystal data and structural refinement for complexes Cu-5-Cu-7.....	33
9 Selected bond lengths (\AA) and bond angles ($^{\circ}$) for Cu-5 to Cu-7.....	36
10 Geometrical parameters of π - π interactions (\AA , $^{\circ}$) for Cu-5-Cu-7.....	41
11 Crystal data and structural refinement for complexes Ag-1-Ag-4.....	42
12 Selected bond lengths (\AA) and bond angles ($^{\circ}$) for Ag-1-Ag-4.....	44
13 Hydrogen bond geometry (\AA , $^{\circ}$) for Ag-1.....	47
14 Intermolecular π - π stacking interactions (\AA , $^{\circ}$) for Ag-2.....	50
15 Hydrogen bond geometry (\AA , $^{\circ}$) for Ag-3.....	53
16 π - π stacking interactions (\AA , $^{\circ}$) for Ag-3.....	54
17 π - π stacking interactions (\AA , $^{\circ}$) for Ag-4.....	57
18 Hydrogen bond geometry (\AA , $^{\circ}$) for Ag-4.....	58
19 Solid state photoluminescent data at room temperature for some copper(I) and silver(I) complexes.....	61

LIST OF FIGURES

Figures		Page
1	The <i>N,N'</i> -donor Schiff base ligands used in the present study.....	2
2	Schematic representations for the present research procedure.....	5
3	Excitation and Emission (left) spectrum and Jablonski diagram (right)	6
4	Complex1 (Cu(SCN)(methyl nicotinate)) _n and emission spectra of solidcomplexes at room temperature: (A) (Cu(SCN)(methyl nicotinate)) _n (1) ; (B) ((ethyl isonicotinate)H)-(CuSCN) ₂ (3)	8
5	One-dimensional polymer structure of compounds (Cu(NCS) (4-Ptz)) (left), and their luminescence properties (right)	8
6	One-dimensional polymer structure.of compounds (Cu(NCS) (bipy)) (left), and their luminescence properties (right)	9
7	The asymmetric unit in the crystal structure of complex 2 (left), the 1D zigzag chains of complex 2 (right)	10
8	Crystal structures of (CuL(CH ₃ CN) ₂)ClO ₄ (left) and CuL (PPh ₃) ₂ ClO ₄ (right), L = butane-2,3-dione bis (salicylhydrazone)	10
9	X-ray structure of (CuNCS(phen)P(CH ₂ morf) ₃) (left), Normalized emission spectra of the single crystal at room temperature (right)	11
10	Perpendicular view looking directly down the channel in compound 5 (left). Photoinduced emission spectra of the multidentate Schiff base ligands 2,5-bis (3-methylpyrazinyl)-3,4-diaza-2,4-hexadiene and 2,5- bis(pyrazinyl)-3,4-diaza-2,4-hexadiene with Ag(I) salts in the solid state at room temperature (right)	12

LIST OF FIGURES (CONT.)

Figures		Page
11	Asymmetric unit of compound 1 (left), Emission spectra of ligand (2-py)-CH=N-C ₁₀ H ₆ -COOH, (Ag(HL1) ₂)(PF ₆) and (Ag(HL1) ₂)(NO ₃)(H ₂ O) (right)	13
12	Infrared spectra of all copper(I) complexes and KNCS.....	19
13	Thermal ellipsoid plot of Cu-2 as representative complex at the 50% probability level containing its asymmetric unit with atom numbering. Symmetry code: (i) 1-x, 1-y, 1-z...	23
14	Views of the 1D chain generated by π - π interactions parallel to the <i>a</i> axis (a) and the 2D sheet generated by π - π and C-H $\cdots\pi$ interactions in the <i>ab</i> plane (b) of the tetranuclear complex.....	26
15	Thermal ellipsoid plot of a dinuclear of Cu-3 as representative example at the 50% probability level containing its asymmetric unit with atom numbering and showing coordination environments of metals center. H atoms are shown as small spheres of arbitrary radii. Symmetry code: (i) 1-x, 1-y, 1-z.....	29
16	View of the two-dimensional sheet generated by a combination of π - π , C-H $\cdots\pi$, and S $\cdots\pi$ interactions (green dashed lines) in the dinuclear complex.....	31
17	A view of the weak C-H $\cdots\pi$ and C-X $\cdots\pi$ interactions in the dinuclear complex. These serve to connect the sheets into a three-dimensional architecture.....	32

LIST OF FIGURES (CONT.)

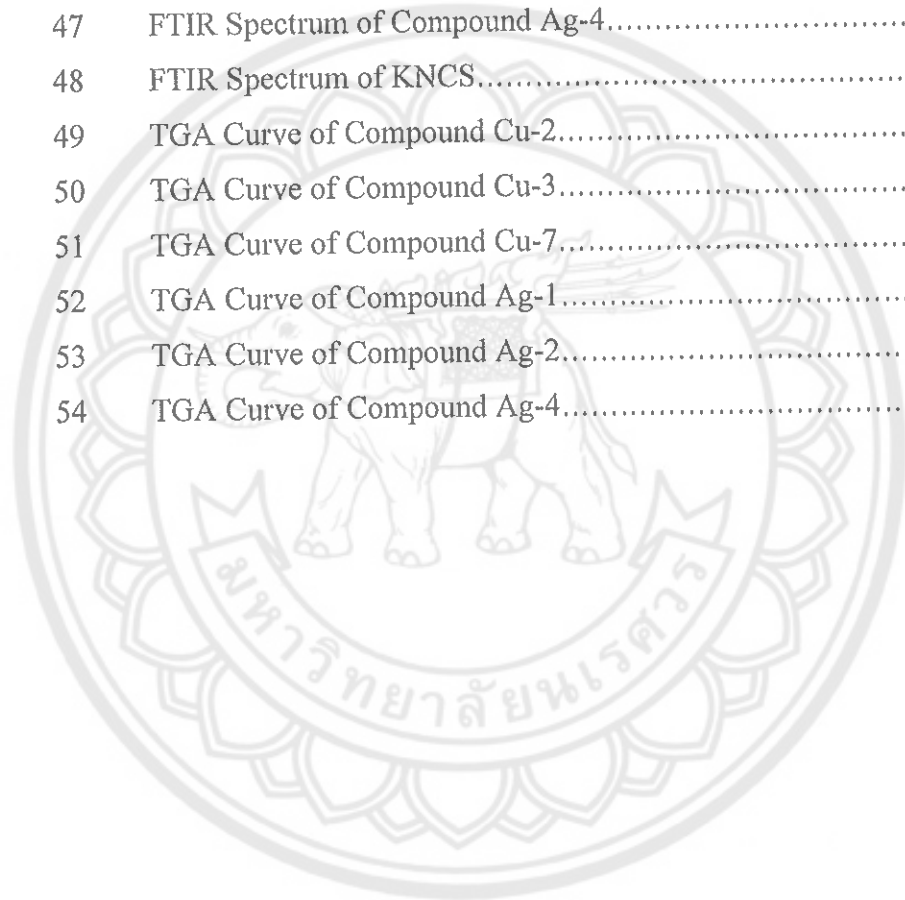
Figures		Page
18	Thermal ellipsoid plot of the polymeric complexes Cu-5 (a) Cu-6 (b) and Cu-7 at the 50% probability level containing its asymmetric unit with atom numbering and showing coordination environments of metals center. H atoms are shown as small spheres of arbitrary radii. Symmetry code: (i) $1-x, 1-y, 1-z$	35
19	Views of the one-dimensional chain in the polymeric complexes Cu-5 (a) Cu-6 (b) and Cu-7 (c)	37
20	Views of $\pi \cdots \pi$ stacking (a) and $\text{Br} \cdots \pi$ (b) interactions in Cu-5. A combination of these interactions are linked the molecules into the three-dimensional supramolecular structure.....	38
21	Views of $\pi \cdots \pi$ stacking (a) and $\text{C-H} \cdots \pi$ (b) interactions in Cu-6.....	39
22	View of two-dimensional layer structure in Cu-7 generated by aromatic $\pi \cdots \pi$ stacking interactions.....	40
23	Thermal ellipsoid plot at the 30% probability level containing its asymmetric unit with atom numbering showing environments around the metal center (a) and the two-dimensional sheets in the <i>ac</i> plane generated by the $\text{Ag} \cdots \text{I}$ contacts and $\text{C-H} \cdots \text{O}$ hydrogen bonds (b) in Ag-1..	46
24	Thermal ellipsoid plot at the 50% probability level containing its asymmetric unit with atom numbering showing environments around the metal center in Ag-2.....	48
25	View of the one-dimensional chain in Ag-2.....	48
26	View of the two-dimensional sheet in Ag-2, formed by $\pi-\pi$ stacking. Hydrogen atoms are omitted for charity.....	49

LIST OF FIGURES (CONT.)

Figures		Page
27	View of C–H··· π interactions in Ag-2.....	50
28	Thermal ellipsoid plot at the 25% probability level containing its asymmetric unit with atom numbering showing environments around the metal centres (a) and partially disordered perchlorate anions (b) in Ag-3.....	51
29	Views of the two-dimensional sheets in Ag-3 in the <i>bc</i> plane (a) and along the <i>b</i> axis.....	52
30	Crystal packing in Ag-3 view approximately along the <i>b</i> axis....	53
31	Thermal ellipsoid plot at the 30% probability level containing its asymmetric unit with atom numbering showing environments around the silver(I) centres in Ag-4.....	55
32	View of the one-dimensional chain generated by π – π stacking interaction in Ag-4.....	56
33	View of the two-dimensional double layers in Ag-4.....	57
34	TGA profiles of representative examples of Cu(I) (a) and Ag(I) (b)	59
35	The solid-state photoluminescent emission spectra of the copper(I) complexes at room temperature.....	62
36	The solid-state photoluminescent emission spectra of the silver(I) complexes at room temperature.....	63
37	FTIR Spectrum of Compound Cu-1.....	73
38	FTIR Spectrum of Compound Cu-2.....	73
39	FTIR Spectrum of Compound Cu-3.....	74
40	FTIR Spectrum of Compound Cu-4.....	74
41	FTIR Spectrum of Compound Cu-5.....	75
42	FTIR Spectrum of Compound Cu-6.....	75
43	FTIR Spectrum of Compound Cu-7.....	76

LIST OF FIGURES (CONT.)

Figures		Page
44	FTIR Spectrum of Compound Ag-1.....	76
45	FTIR Spectrum of Compound Ag-2.....	77
46	FTIR Spectrum of Compound Ag-3.....	77
47	FTIR Spectrum of Compound Ag-4.....	78
48	FTIR Spectrum of KNCS.....	78
49	TGA Curve of Compound Cu-2.....	79
50	TGA Curve of Compound Cu-3.....	79
51	TGA Curve of Compound Cu-7.....	80
52	TGA Curve of Compound Ag-1.....	80
53	TGA Curve of Compound Ag-2.....	81
54	TGA Curve of Compound Ag-4.....	81



ABBREVIATIONS

Å	=	Angstrom
θ	=	Bragg angle or scattering angle
R_1	=	Conventional crystallographic discrepancy index
°	=	Degree (angle)
°C	=	Degree Celsius
π	=	double bond
π^*	=	pi anti-bonding orbitals
μ	=	Linear absorption coefficient
a, b, c	=	Unit cell dimensions
α, β, γ	=	Unit cell angles
ν	=	Wavenumbers
λ	=	Wavelength of x-radiation
λ_{em}	=	Emission wavelength
λ_{ex}	=	Excitation wavelength
V	=	Volume of the unit cell
1D	=	One dimensional
2D	=	Two dimensional
3D	=	Three dimensional
3-abpt	=	4-amine-3,5-bis(3-pyridyl)-1,2,4-triazole
3,4,5-MeO-ba	=	<i>N,N'</i> -Bis(3,4,5-trimethoxybenzylidene)
4-ptz	=	5-(4-pyridyl)tetrazole
ACN	=	Acetonitrile
BF_4^-	=	Tetrafluoroborate
bipy	=	2,2'-bipyridine
Cg	=	Centroid
$CHCl_3$	=	Chloroform
CH_2Cl_2	=	Dichloromethane
CH_3OH	=	Methanol
ClO_4^-	=	Perchlorate

ABBREVIATIONS (CONT.)

cm ⁻¹	=	per centimeters
DCM	=	Dichloromethane
DMF	=	<i>N,N'</i> -Dimethylformamide
EDX	=	Energy dispersive X-ray spectroscopy
eg.	=	Exempli gratia, in Latin meaning “for example”
<i>et al.</i>	=	Et al ii, in Latin meaning “and others”
EtOH	=	Ethanol
FT-IR	=	Fourier transform infrared spectroscopy
HE	=	High energy
K	=	Kelvin
KNCS	=	Potassium thiocyanate
LLCT	=	Ligand to ligand charge transfer
m	=	Medium
MeOH	=	Methanol
mg	=	Milligram
MLCT	=	Metal to ligand charge transfer
mL	=	Milliliter
mm ⁻¹	=	Per millimetre
mmol	=	Millimole
mol	=	Mole
MW	=	Molecular weight
NCS	=	Thiocyanate
nm	=	Nanometer
<i>n</i> -PyHBIIm	=	2-(<i>n</i> -pyridyl)benzimidazole)
OLEDs	=	Organic light-emitting diode (OLEDs)
PF ₆ ⁻	=	Hexafluorophosphate
PM-2,3-DMA	=	<i>N</i> -(2'-pyridylmethylene)-2,3-dimethylaniline
PM-2,4-DMA	=	<i>N</i> -(2'-pyridylmethylene)-2,4-dimethylaniline
PM-3,5-DMA	=	<i>N</i> -(2'-pyridylmethylene)-3,5-dimethylaniline

ABBREVIATIONS (CONT.)

PM-4-BrA	=	<i>N</i> -(2'-pyridyl methylene)-4-bromoaniline
PM-4-ClA	=	<i>N</i> -(2'-pyridylmethylene)-4-chloroaniline
PM-4-FA	=	<i>N</i> -(2'-pyridylmethylene)-4-fluoroaniline
PM-4-IA	=	<i>N</i> -(2'-pyridylmethylene)-4-iodoaniline
phen	=	1,10-phenanthroline
PPh ₃	=	Triphenylphosphine
s	=	Strong
SCXRD	=	Single crystal X-ray diffraction
SHELXL	=	Least squares structure refinement program
SHELXS	=	Least squares structure solution program
SHELXT	=	Program for the determination of crystal structures
TGA	=	Thermogravimetric analysis
w	=	weak
Z	=	Number of formula units in the unit cell

CHAPTER I

INTRODUCTION

Introduction to the research problem and its significance

Organic light-emitting diodes (OLEDs) offer numerous advantages such as enhanced efficiency and the possibility to be manufactured on thin and lightweight substrates, which makes them highly attractive candidates for lighting and display applications (Barbieri, et al., 2008). Currently, this research area is still of great interest. It is well known that luminescent metal complexes containing noble metals such as iridium, platinum, or osmium are widely used as emitters for OLEDs. This is because of their colour tenability and high efficiencies (Barakat, et al., 2003). However, these noble metals are rather scarce and expensive, and are the main problems for their usage in high-volume products. On the other hand, luminescent complexes based on more abundant and cost-efficient metals with a d^{10} configuration such as zinc(II), cadmium(II), copper(I), silver(I) and gold(I) are currently the focus of numerous research studies with the aim of developing them for mass market applications. Of particular interests is complexes of copper(I) and silver(I), which are favoured not only because of their varied structural and photophysical properties but also the fact that they have already been successfully tested in OLEDs (Chi, et al., 2010; Cuttell, et al., 2002).

Although both copper(I) and silver(I) ions have d^{10} electron configuration, however, the coordination numbers of these metals are different. Namely, the coordination sphere of silver(I) ion is very flexible with coordination numbers usually ranging between two and six. Various geometries from linear through trigonal to tetrahedral, trigonal pyramidal, and octahedral are possible for silver(I) (Czerwieńiec, et al., 2010). Whereas, coordination number of copper(I) is usually three or four with the coordination geometry usually rigid adopting only trigonal and tetrahedral shapes (Dong, et al., 2004). Furthermore, unlike other divalent d^{10} transition metals such as zinc(II) or cadmium(II), these monovalent d^{10} metals also possess the ability to further stabilize the crystal structure through noncovalent interactions between closed-shell

$d^{10}\cdots d^{10}$ cuprophilic ($\text{Cu}^I\cdots\text{Cu}^I$) or argentophilic ($\text{Ag}^I\cdots\text{Ag}^I$) interactions. The strengths of such interactions are within the range of typical hydrogen bonds (Fahlman, et al., 2011). This unique property is perhaps the most widely applied tool for the increase of dimensionality and control of supramolecular architecture in these complexes.

A recent search from databases found that copper(I) and silver(I) complexes of Schiff base ligands have proven to be highly efficient luminescent materials for OLEDs (He, et al., 2009). However, this class of hybrid materials is surprisingly rare in the literature. Thus, the present study explores new coordination chemistry of monovalent copper and silver complexes with N,N' -donor Schiff base type ligands. It is anticipated that weak association through closed-shell $d^{10}\cdots d^{10}$ interactions, difference in coordination numbers and geometries between them, which will provide means to construct diverse architectures of various crystal structures as well as with interesting properties. The N,N' -donor Schiff base ligands used in the present study are shown in Figure 1.

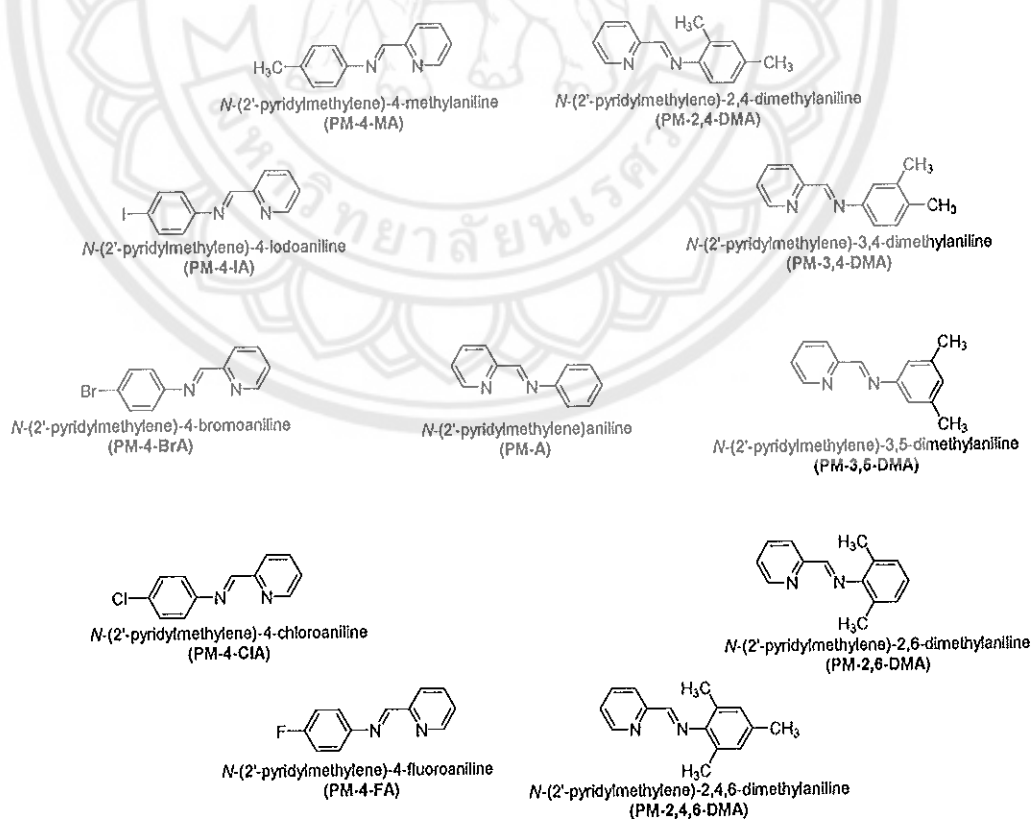


Figure 1 The N,N' -donor Schiff base ligands used in the present study

Research objectives

1. To synthesize novel monovalent metal complexes from bidentate *N*-(2'-pyridylmethylene) aniline based ligands and copper(I) and silver(I) ions.
2. To study the structures of the copper(I) and silver(I) complexes by single crystal X-ray crystallography and further characterize physical properties by various analytical techniques such as infrared spectroscopy (IR), thermogravimetric analysis (TGA) and elemental analyses (EA).
3. To study the structure with the luminescence property relationships of new copper(I) and silver(I) complexes.

Scope and limitation

This study focuses on the single crystal growth and solid state structural studies of new monovalent copper(I) and silver(I) (d^{10}) complexes containing the bidentate *N,N'*-donor ligands. Initially, this study deals with a rational synthetic strategy using the principles of crystal engineering and supramolecular chemistry for the construction of new hybrid coordination polymers containing thiocyanate anionic ligand and the neutral *N*-(2'-pyridylmethylene) aniline derivative as co-ligands. The correlations between their structures and luminescence properties will be investigated. In practice, the course of any synthesis is somewhat unpredictable and related compounds may be formed under the same synthetic reactions. These new compounds may also be considered to be within the scope of the present study.

Expected benefits

New copper(I) and silver(I) complexes of *N*-(2'-pyridylmethylene)aniline based Schiff base ligands are expected to be successfully prepared, and are also expected to show highly efficient luminescent behavior. These materials may be a new resource for electro-optic applications.

Research procedure

Schematic representation of the research procedure as well as the sample determination of the present research is depicted in Figure 2.

1. Search the crystallography literature to avoid repeating previous work and to obtain supporting knowledge for rational design of copper(I) and silver(I) complexes with *N,N'*-donor Schiff base ligands.

2. Prepare the samples of copper(I) and silver(I) complexes with Schiff base ligands using the bench top technique.

3. Obtain the sample and do preliminary examination with a optical microscope (OM). If the solid product is homogeneous go to step 4. If the solid product is heterogeneous it can often be separated by selecting on color, size, or shape of crystalline products, or by utilizing varying solubility of individual components. In the case of a crystalline product with very tiny crystals, where preliminary examination with microscope is difficult, one should examine the phase purity of the solid product by using powder X-ray diffraction technique

4. Characterize organic components by C H N elemental analysis; inorganic components by FTIR.

5. Determine structures by single crystal X-ray crystallography.

6. Determine functions and properties of prepared materials using thermogravimetric analysis and fluorescence spectroscopy.

7. Further explore supramolecular interactions such as hydrogen bonding, dipole-dipole interactions, π - π stacking, and metal-metal interactions.

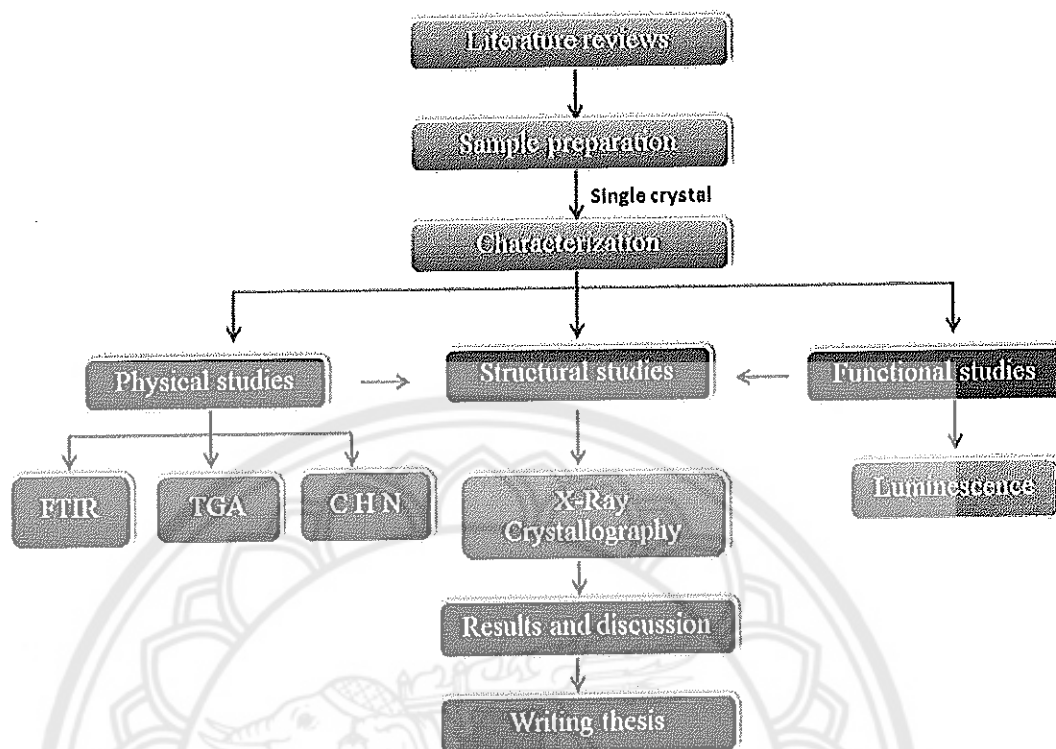


Figure 2 Schematic representations for the present research procedure

Research plan

This research was mainly performed at the Department of Chemistry, Faculty of Science, Naresuan University. The structural studies of complexes by single crystal X-ray diffraction were carried out at the Faculty of Science and Technology, Thammasat University, Rangsit campus.

CHAPTER II

LITERATURE REVIEWS

Fluorescence Spectroscopy

The light-emitting have many type, which depending the source of energy to causes electron from ground state to excite state such as electron interaction to photon of electromanetic radiation to casues "Luminescence" this can called "Photoluminescence" (Sauer, et al., 2011). Which is separate into fluorescence and phosphorescence. It both phenomena has different back to ground state process. If the molecules using energy from a chemical reaction called chemicallyluminescence. In addition, Luminescence spectroscopy is importane technique and widely used in chemical analysis, because this technique has specific and high sensitivity. Molecular Photoluminescence spectroscopy using excitation by radiation wavelength absorption or excitation wavelength and measurement emitted radiation at emission wavelength.

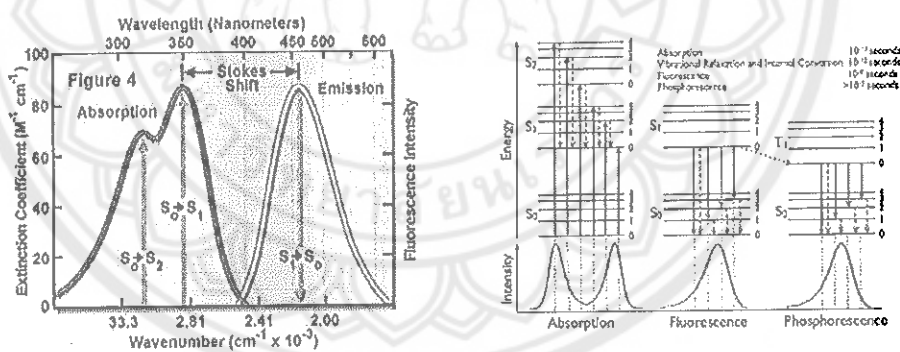


Figure 3 Excitation and Emission (left) spectrum and Jablonski diagram (right)

Fluorescence is light emission caused by irradiation with light (normally visible or ultraviolet light) and typically occurring within nanoseconds to milliseconds after irradiation. Phosphorescence is a light emission which can occur over much longer times (sometimes hours) after irradiation. It involves storage of energy in metastable states and its release through relatively slow (often thermally activated) processes. The phenomenon was discovered early on for phosphorus.

Literature reviews

The d^{10} metals group compounds such as copper(I), silver(I), zinc(II) and cadmium(II) have been developed to broad range of their structural and fluorescent properties. Herein, we focus on copper(I) and silver(I) because low cost and relative environmental friendliness. In recent years, the research has been a growing interest in luminescent complexes based on d^{10} metals beyond the platinum group, such as copper(I), silver(I), zinc(II), and cadmium(II), which are less traditional but much more abundant and cheaper. Many d^{10} metal compounds with attractive luminescence properties and potentials as new luminescence materials have been synthesized (Venkataraman, et al., 1997). The discovery of strongly luminescent copper(I) complexes containing N,N'-donor ligands by McMillin and co-workers (McMillin, et al., 1985, 1998) has been the starting point of this research. For instance, the heteroleptic CuI complexes of phenanthroline derivatives and bis (2(diphenylphosphino) phenyl) ether, which exhibited remarkably high emission quantum yields from their long lived metal-to-ligand charge-transfer (MLCT) excited states (Cuttell, et al., 2002; Rader, et al., 1981). Following this discovery, numerous examples of related heteroleptic CuI and AgI complexes have been prepared from aromatic diimine ligands.

Mohamed, et al. (2000) was success in design and synthesis three new copper(I) thiocyanato complexes $(\text{Cu}(\text{NCS})(\text{methyl nicotinate}))_n$, $(\text{Cu}(\text{NCS})(\text{ethyl nicotinate}))_n$, and $((\text{Ethyl isonicotinate})\text{H})(\text{Cu}(\text{NCS}))$. In this studied, they have interested in pseudohalide NCS^- as bridging ligand. The thiocyanate is known to coordinate to metals in both terminal and bridging modes, and can link a pair of metal centers in either end on (μ -1,1-NCS, μ -1,1-SCN) or end to end (μ -1,3-NCS) configuration. The thiocyanate ion may link a third metal atom giving rise to a μ -1,1,3 (μ -N,N,S or μ -S,S,N). The result of the emission of complexes 1-3 in the solid state at room temperature, their emission spectra exhibit a single band. Complex 1 and 2 shows λ_{max} band at 498 nm and 499 nm, respectively. Complex 3 shows λ_{max} at 575 nm. The emission of complexes 1 and 2 is attributed to the MLCT transition states and complex 3 the emission is XLTC (X=anion) transition state because ligand is protonated and not coordinated to Cu atom but complex 1 and 2 have high energy (HE) band

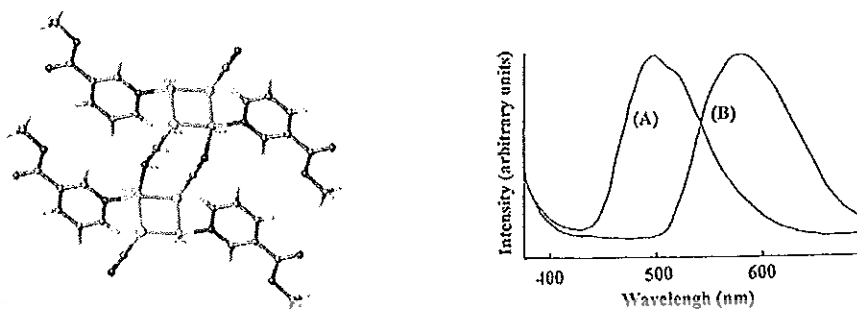


Figure 4 Complex1 ($\text{Cu}(\text{SCN})(\text{methyl nicotinate}))_n$ and emission spectra of solid complexes at room temperature: (A) ($\text{Cu}(\text{SCN})(\text{methyl nicotinate}))_n$ (1) ; (B) ((ethyl isonicotinate)H)-(CuSCN)₂ (3)

Ming-xing, et al. (2009), they report synthesis, crystal structure, and luminescent properties of thiocyanate copper(I) coordination polymers base on N-heterocyclic ligand by solvothermal method. They have got six compounds in this studied; ($\text{Cu}_5(\text{SCN})_5(3\text{-Abpt})_2$)_n (1), ($\text{Cu}(\text{SCN})(3\text{-Abpt})$)_n (2), ($\text{Cu}(\text{SCN})(4\text{-Ptz})$)_n (3), ($\text{Cu}_2(\text{SCN})_2(4\text{-PyHBIIm})$)_n (4) ($\text{Cu}_2(\text{SCN})_2(3\text{-PyHBIIm})$)_n (5) and ($\text{Cu}_2(\text{SCN})_2(3\text{-PyHBIIm})$)_n, the thiocyanate bridging ligands uni-, bi-, tri and tetradentate coordinate modes. The luminescence of copper(I) complexes exhibit yellow or blue luminescence originating from ligand-to-metal charge transfer or ligand centered emission.

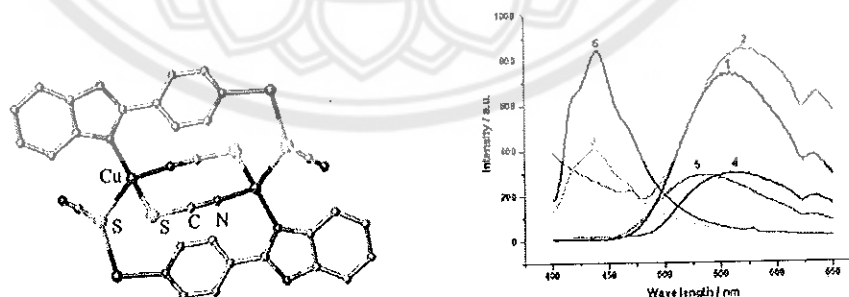


Figure 5 One-dimensional polymer structure of compounds ($\text{Cu}(\text{NCS})(4\text{-Ptz})$)_n (left), and their luminescence properties (right)

Yao, et al. (2009) have prepared new CuI complexes containing pseudohalide and neutral aromatic diimine 1,10-phenanthroline (phen) or 2,2'-bipyridine (bipy) ligands, ($\text{Cu}_2\text{Cl}_2(\text{phen})$) (1) and ($\text{Cu}(\text{NCS})(\text{bipy})$) (2), using the hydrothermal method (4). As shown in Figure 6 Compounds 1 and 2 have similar one-dimensional infinite chain structure. At room temperature, both compounds exhibit strong photoluminescence with emission maxima at 445.0 ($\lambda_{\text{ex}} = 276.5 \text{ nm}$) and 446.5 nm ($\lambda_{\text{ex}} = 278.0 \text{ nm}$) for 1 and 2, respectively.

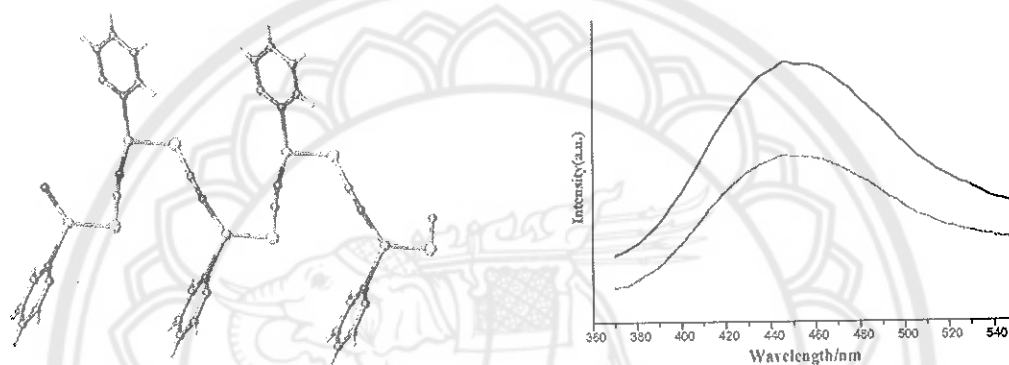


Figure 6 One-dimensional polymer structure of compounds ($\text{Cu}(\text{NCS})(\text{bipy})$) (left), and their luminescence properties (right)

Aliakbar, et al. (2009) have reported the crystal structures of two different copper(I) coordination polymers, ($\text{Cu}(\text{L}^1)(\text{SCN})_n$) (1) and ($\text{Cu}(\text{L}^2)(\text{SCN})_n$) (2). The ligand base on bidentate Schiff-base building units, ((3,4,5,-MeO-ba) $_2\text{en}(\text{L}^1)$) and (4-Me-ba) $_2\text{en}(\text{L}^2)$), and thiocyanate anion as bridging ligand. Complex 1 and 2 have common motifs and consist of one-dimensional coordination polymer chains, Cu atom are a distorted tetrahedral coordinate by two N donor atoms of the schiffbase ligand L^1 and L^2 and the N and S donor atom of two thiocyanate ligands. The Schiff-base ligands L^1 and L^2 act as chelating ligands in the complexes and SCN^- anion acts as bridging ligand. They present that the thiocyanate anion can be used for the preparation of various chiral and achiral coordination polymers containing $\text{Cu}(\text{SCN})$ and heterometallic $M\text{-Cu}(\text{I})$ complexes as building blocks.

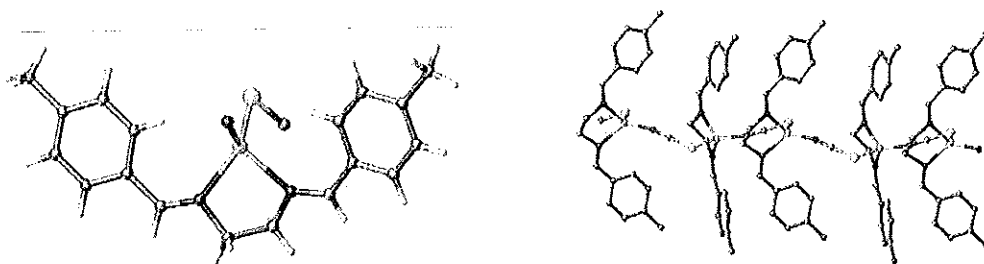


Figure 7 The asymmetric unit in the crystal structure of complex 2 (left), the 1D zigzag chains of complex 2 (right)

Mukherjee, et al. (2010) have been synthesis A flexible bis-bidentate Schiff base ligand has been used in mononuclear copper(I) complexes. For example, butane-2,3-dione bis(salicylhydrazone) (L), forms a mononuclear complexes with CuI, $(\text{CuL}(\text{CH}_3\text{CN})_2)\text{ClO}_4$ and $(\text{CuL}(\text{PPh}_3)_2)\text{ClO}_4$, Figure 8. In both complexes, the metal ion adopts a tetrahedral coordination environment. The ligand is weakly fluorescent in dichloromethane, however, the emission is quenched in the copper(I) complexes.

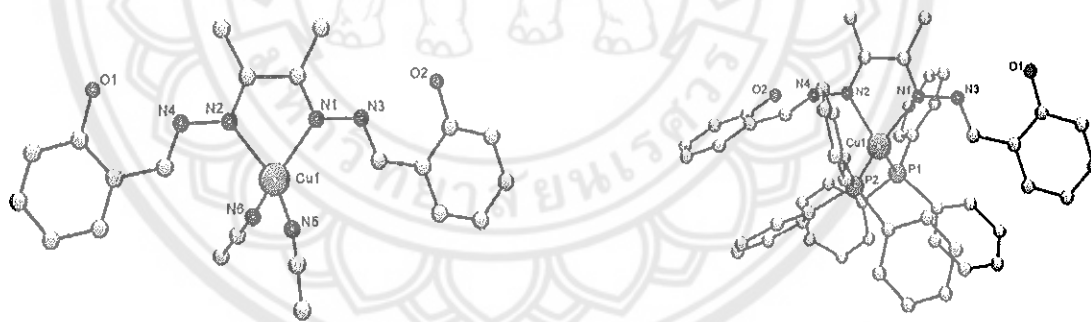


Figure 8 Crystal structures of $(\text{CuL}(\text{CH}_3\text{CN})_2)\text{ClO}_4$ (left) and $\text{CuL}(\text{PPh}_3)_2\text{ClO}_4$ (right), L = butane-2,3-dione bis(salicylhydrazone)

Radoslaw, et al. (2012) have investigated aliphatic tris(aminomethyl) phosphanes and their Cu(I) complexes. They synthesis $(\text{CuNCS}(\text{phen}0\text{P}(\text{CH}_2\text{N}(\text{CH}_2\text{CH}_2)_2\text{O})_3))$ complex of copper(I) isothiocyanate with 1,10-phenanthroline and tris(aminomethyl)phosphane derived from morpholine . X-ray structure of the complex shows that the Cu(I) atom is distorted tetrahedral, the Cu atom has coordinating with N atom form thiocyanate, the phosphane molecule coordinating by

P atom and two N atoms of phenanthroline acting as a bidentate ligand to the Cu center. The complex crystallizes as the discrete centrosymmetric dimers bound by π -stacking interactions between the phen molecules. In this research, they have study photophysical properties by solid state luminescence at room temperature and LN temperature. At room temperature, the main emission band consists of three transitions at 617, 663 and 721 nm. At 77 K the maximum of emission is shifted to 735 nm and most probably comes from a single transition. They discussed PL spectra are an evidence for a complex mechanism of the luminescence of the Cu(I) complexes, the result show that the most probably all the ligands are involved into the forming of the absorption and photoluminescence bands.

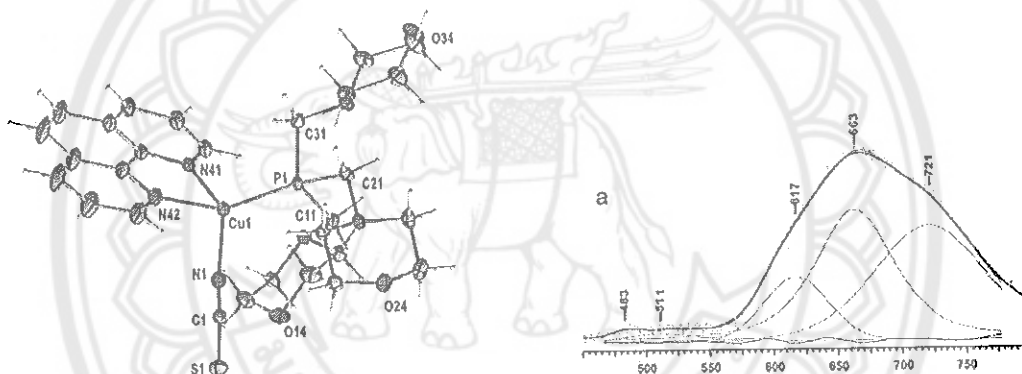


Figure 9 X-ray structure of $(\text{CuNCS}(\text{phen})\text{P}(\text{CH}_2\text{morf})_3)$ (left), Normalized emission spectra of the single crystal at room temperature (right)

The coordination chemistry of the multidentate Schiff base ligands 2,5-bis(3-methylpyrazinyl)-3,4-diaza-2,4-hexadiene (L1) and 2,5-bis(pyrazinyl)-3,4-diaza-2,4-hexadiene (L2) with Ag(I) salts has been investigated by the group of Dong et al. (Dong, et al., 2004). Five new silver (I) compounds $(\text{Ag}(\text{L1}))\text{ClO}_4 \cdot 0.5\text{CH}_3\text{OH}$, $(\text{Ag}(\text{L1}))\text{PF}_6 \cdot 0.5\text{CH}_3\text{OH}$, $(\text{Ag}(\text{L2}))\text{SbF}_6 \cdot 0.5\text{CH}_3\text{OH}$, $(\text{Ag}(\text{L2}))(\text{BF}_4) \cdot 0.5\text{CH}_3\text{OH}$, and $(\text{Ag}_4(\text{L2})_4) \cdot (\text{PF}_6)_4 \cdot \text{CHCl}_3$ have been prepared. The first and fourth compounds were crystallized in an orthorhombic system with a three-dimensional structure. Each AgI center is coordinated with four N-donors of the ligand. In a later compound, AgI center consists of three N-donors from the ligand and forms tetrahedral building

blocks. These building blocks are then linked together into an infinite one-dimensional structure. In the solid state, all compounds are luminescent as shown in Figure 10.

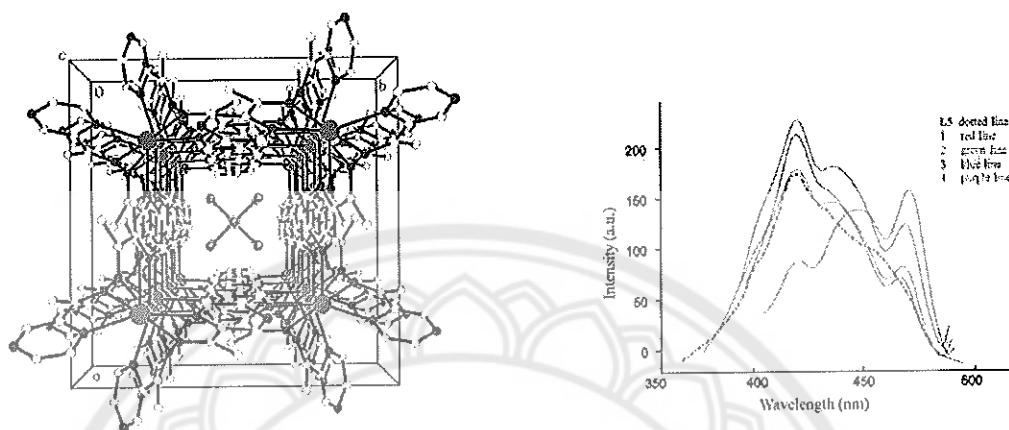


Figure 10 Perpendicular view looking directly down the channel in compound **5** (left). Photoinduced emission spectra of the multidentate Schiff base ligands 2,5-bis(3-methylpyrazinyl)-3,4-diaza-2,4-hexadiene and 2,5-bis(pyrazinyl)-3,4-diaza-2,4-hexadiene with Ag(I) salts in the solid state at room temperature (right)

Other examples of silver(I) (Lee, et al., 2013) compounds with Schiff base ligand exhibiting luminescent properties are $(\text{Ag}(\text{HL}1)_2)(\text{PF}_6)$ and $(\text{Ag}(\text{HL}1)_2)(\text{NO}_3)(\text{H}_2\text{O})$, $\text{HL}1 = (2\text{-py})\text{-CH=N-C}_{10}\text{H}_6\text{-COOH}$. (7) Both compounds form a dimeric structure by the intermolecular $\text{O-H}\cdots\text{O}$ hydrogen bonds between two carboxylate terminals of two adjacent molecules. Ligand HL1 exhibited a 437 nm ($\lambda_{\text{ex}} = 330\text{nm}$). Compounds 1 and 2 show two peak strong bands at 467 nm and shoulder at 485 nm ($\lambda_{\text{ex}} = 330$). They propose that the emission peak at 467 nm stems from the intraligand $\pi^* \rightarrow n$ transition in the complexes. The band at 485 nm may arise from the charge transfer from the Ag^+ (d^{10}) ion to ligand HL^1 (π^* orbital), as shown in Figure 11.

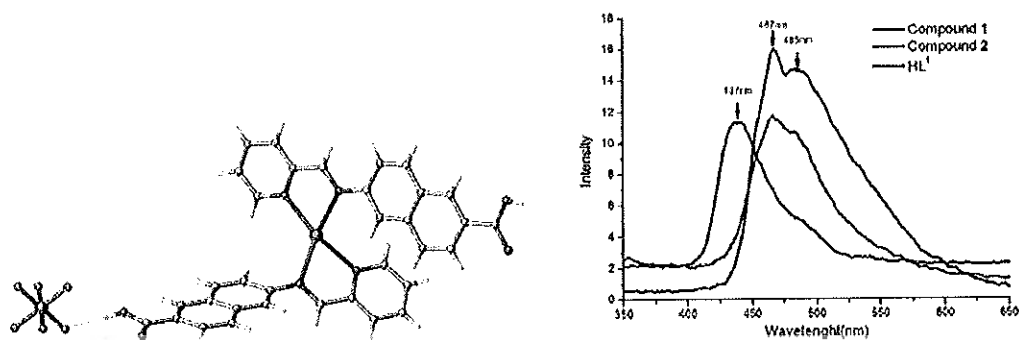


Figure 11 Asymmetric unit of compound 1 (left), Emission spectra of ligand (2-py)-CH=N-C₁₀H₆-COOH, (Ag(HL1)₂)(PF₆) and (Ag(HL1)₂)(NO₃)(H₂O) (right)

CHAPTER III

EXPERIMENTAL

Materials

Commercially available reagents *viz.* acetonitrile (ACN, RCI Labscan, ACS for analysis, minimum assay 99.9%, residue on evaporation 0.0002%, acidity 0.0005%, water 0.02%), dichloromethane (DCM, RCI Labscan, ACS for analysis, minimum assay 99.8%, residue on evaporation 0.001%, acidity 0.0003%, water 0.02%), dimethylformamide (DMF, RCI Labscan, ACS for analysis minimum assay 99.8%, residue on evaporation 0.001%, acidity 0.0005%, water 0.07%), methanol (MeOH, RCI Labscan, ACS for analysis, minimum assay 99.9%, residue on evaporation 0.001%, acidity 0.0003, water 0.05%), and all other chemicals *viz.* copper(II) nitrate trihydrates ($\text{Cu}(\text{NO}_3)_2 \cdot 3\text{H}_2\text{O}$, Sigma-Aldrich, 99.999% trace metals basis) and silver nitrate (AgNO_3 , Acros Organics, minimum assay 99.85%), potassium thiocyanate (KNCS, FERAK, minimum assay 97%), potassium selenocyanate (KNCSe , Acros Organics, minimum assay 99%), were used as received without further purification. All Schiff base type ligands *viz.* *N*-(2'-pyridylmethylene)-2,3-dimethylaniline (PM-2,3-DMA), *N*-(2'-pyridylmethylene)-2,4-dimethylaniline (PM-2,4-DMA), *N*-(2'-pyridylmethylene)-3,5-dimethylaniline (PM-3,5-DMA), *N*-(2'-pyridylmethylene)-4-bromoaniline (PM-BrA), *N*-(2'-pyridylmethylene)-4-chloroaniline (PM-ClA), *N*-(2'-pyridylmethylene)-4-fluoroaniline (PM-FA), *N*-(2'-pyridylmethylene)-4-iodoaniline (PM-IA) were synthesized according to the reported procedures (Chanthee, 2015).

Physical measurements

1. Single Crystal X-Ray Diffraction (SCXRD)

Single crystals of all complexes were mounted to the end of a hollow glass fiber. X-ray intensity data were measured at 296(2) K on a Bruker D8 QUEST diffractometer with graphite-monochromatic $\text{Mo } K_\alpha$ radiation ($\lambda = 0.71073 \text{ \AA}$). Data reductions and absorption corrections were performed with the SAINT and SADABS

software packages (Bruker, 2014) respectively. The structures were solved using SHELXT and refined on F^2 using SHELXL (Sheldrick, 2015). Crystallographic figures were prepared using OLEX2 (Dolomanov, et al., 2009). All non-hydrogen atoms were refined anisotropically. The hydroxide H atom was located in a difference Fourier map and positional parameters were refined with $U_{\text{iso}}(\text{H}) = 1.5U_{\text{eq}}(\text{O})$.

2. Fourier Transform Infrared Spectroscopy (FTIR)

Infrared spectra of the samples were recorded using a diamond-Universal Attenuated Total Reflectance (UATR) cell on a Perkin-Elmer spectrum 100 in the range of 600-4000 cm^{-1} (50 scans, resolution 4 cm^{-1}).

3. Thermogravimetric Analysis (TGA)

Thermogravimetric analyses (TGA) for complexes were performed using a Mettler Toledo 851e to characterize. The sample was heated from room temperature to 800 °C under N_2 atmosphere with a heating rate of 10 °C/min.

4. Photoluminescence Spectroscopy (PL)

The solid-state photoluminescent spectra were measured at room temperature on a Horiba FluoroMax-4 & FluoroMax-4P.

5. C H N Elemental analyses (EA)

Elemental analyses for C, H and N were measured on a CHN-O-Rapid analyzer and an ElementarVario MICRO analyzer.

Synthesis of Schiff base copper(I) complexes

1. Synthesis of $(\text{Cu}_4(\text{PM-4-FA})_4(\text{NCS})_4)$ (Cu1)

To a dry CH_2Cl_2 solution (2 mL) of PM-4-FA (70 mg, 0.35 mmol) in a test tube (14 mL capacity), a mixture $\text{CH}_3\text{CN}/\text{CH}_2\text{Cl}_2$ (1:1) solution (7 mL) was carefully added on the top. A dry CH_3CN solution (2 mL) of $\text{Cu}(\text{NO}_3)_2 \cdot 3\text{H}_2\text{O}$ (24.1 mg, 0.1 mmol) and KNCS (19.4 mg, 0.2 mmol) was then carefully layered on the top of a mixture $\text{CH}_3\text{CN}/\text{CH}_2\text{Cl}_2$ solution. Upon slow diffusion at room temperature for 3 days, dark blue block-shaped single crystals of **Cu1** were obtained in 76% yield (18.32 mg) base on copper source. Found (calcd) for $\text{C}_{52}\text{H}_{36}\text{Cu}_4\text{F}_4\text{N}_{12}\text{S}_4$ (Mw = 1287.33 g/mol): C, 48.53 (48.52); H, 2.82 (2.92); N, 13.06 (13.06). IR ($\nu_{\text{max}}/\text{cm}^{-1}$): 3454br, 2122s, 1500s, 1240m, 800m, 587w.

2. Synthesis of $(\text{Cu}_4(\text{PM-4-CIA})_4(\text{NCS})_4)$ (Cu2)

The complex **Cu2** was prepared using the same procedure performed in the preparation of **Cu1** except that PM-4-FA ligand was replaced by PM-4-CIA (75.8 mg, 3.5 mmol). Green brown block shaped single crystals of **Cu2** were obtained. Yield: 81% (19.52 mg) based on copper source. Found (calcd) for $\text{C}_{52}\text{H}_{36}\text{Cl}_4\text{Cu}_4\text{N}_{12}\text{S}_4$ (Mw = 1353.17 g/mol): C, 46.17 (46.83); H, 2.37 (2.93); N, 12.42 (13.06). IR ($\nu_{\text{max}}/\text{cm}^{-1}$): 3465br, 2112s, 1589w, 828m, 770m.

3. Synthesis of $(\text{Cu}_2(\text{PM-4-BrA})_2(\text{NCS})_2)$ (Cu3)

The complex **Cu3** was prepared using the same procedure performed in the preparation of **1** except that PM-4-FA ligand was replaced by PM-4-BrA (91.0 mg, 3.5 mmol). Green brown block shaped single crystals of **Cu3** were obtained. Yield: 84% (20.24 mg) based on copper source. Found (calcd) for $\text{C}_{26}\text{H}_{18}\text{Br}_2\text{Cu}_2\text{N}_6\text{S}_2$ (Mw = 765.48g/mol): C, 40.81 (40.25); H, 2.37 (2.94), N; 10.98 (11.76). IR ($\nu_{\text{max}}/\text{cm}^{-1}$): 3486br, 2112s, 1589m, 829m, 767m, 533w.

4. Synthesis of $(\text{Cu}_2(\text{PM-4-IA})_2(\text{NCS})_2)$ (Cu4)

The complex **Cu4** was prepared using the same procedure performed in the preparation of **Cu1** except that PM-4-FA ligand was replaced by PM-4-IA (107 mg, 3.5 mmol). Dark blue block shaped single crystals of **Cu4** were obtained. Yield: 87% (20.96 mg) based on copper source. Found (calcd) for $\text{C}_{26}\text{H}_{18}\text{Cu}_2\text{I}_2\text{N}_6\text{S}_2$ (Mw = 859.48g/mol): C, 36.34 (36.71); H, 2.11 (2.09); N, 9.78 (9.88). IR ($\nu_{\text{max}}/\text{cm}^{-1}$): 3481w, 2091s, 1474w, 827m 544w.

5. Synthesis of $(\text{Cu}(\text{PM-2,3-DMA})(\text{NCS}))$ (Cu5)

The complex **Cu6** was prepared using the same procedure performed in the preparation of **Cu1** expect that PM-4-FA ligand was replaced by PM-2,3-DMA (14.7 mg, 7.0 mmol). Dark brown block shaped single crystals of **Cu6** were obtained. Yield: 64% (15.35 mg) based on copper source. Found (calcd) for $\text{C}_{15}\text{H}_{14}\text{CuN}_3\text{S}$ (Mr = 331.89 g/mol): C, 54.11 (54.28); H, 4.20 (4.25); N, 12.55 (12.66). IR ($\nu_{\text{max}}/\text{cm}^{-1}$): 3435br, 2107s, 1591w, 1467w, 784w, 772m.

6. Synthesis of $(\text{Cu}(\text{PM-2,4-DMA})(\text{NCS}))$ (Cu6)

The complex **Cu7** was prepared using the same procedure performed in the preparation of **Cu1** expect that PM-4-FA ligand was replaced by PM-2,4-DMA (14.7 mg, 7.0. mmol). Dark brown block shaped single crystals of **Cu7** were obtained.

Yield: 86% (20.72 mg) based on copper source. Found (calcd) for $C_{15}N_3H_{13}SCu$. (Mw = 330.89 g/mol): C, 54.24 (54.28); H, 4.29 (4.25); N, 12.67 (12.66). IR (ν_{max}/cm^{-1}): 3436br, 2109s, 1491w, 813m, 781m.

7. Synthesis of (Cu(PM-3,5-DMA)(NCS)) (Cu7)

The complex **Cu8** was prepared using the same procedure performed in the preparation of **Cu1** expect that PM-4-FA ligand was replaced by PM-3,5-DMA (14.7 mg, 7.0 mmol). Dark brown block shaped single crystals of **Cu8** were obtained. Yield: 87% (20.96 mg) based on copper source. Found (calcd) for $C_{15}H_{14}CuN_3S$ ((Mw = 330.89 g/mol): C, 54.30 (54.28); H, 4.20 (4.25); N, 12.60 (12.66). IR (ν_{max}/cm^{-1}): 3430br, 2912w, 2100s, 1585w, 1466w, 849w, 769m.

Synthesis of Schiff base silver(I) complexes

1. Synthesis of (Ag(PM-4-IA)(NO₃)) (Ag1)

To a dry MeOH/EtOH (1:1, v:v, 2 ml) solution of PM-4-BrA (43.3 mg, 2 mmol) in a test tube (14 mL capacity), a mixture MeOH/EtOH solution (7 mL) was carefully added on the top. A dry mixture MeOH/EtOH solution (2 mL) of AgNO₃ (16.9 mg, 1 mmol) and KNCS (19.4 mg, 2 mmol) was then carefully layered on the top of a mixture MeOH/EtOH solution. Upon slow diffusion at room temperature for 2 days, yellow rod-shaped single crystals of **Ag1** were obtained in 86% yield (14.53 mg) base on copper source. Found (calcd) for $C_{12}H_9AgIN_3O_3$ (Mw = 477.99 g/mol): C, 30.04 (30.15); H, 1.95 (1.90); N, 8.75 (8.80). IR (ν_{max}/cm^{-1}): 3416br, 3065w, 2319w, 1591m, 1419m, 1159m, 822m, 787m, 540s.

2. Synthesis of (Ag(PM-3,5-DMA)(NCS)) (Ag2)

To a dry CH₃CN (5 ml) solution of AgNO₃ (16.9 mg, 1 mmol) in a test tube (14 mL capacity), KNCS (97 mg, 1 mmol) was carefully added and a mixture solution was stirred for 30 minute at room temperature. A white solid of AgNCS precursor complex was filtered off and washed several times by Et₂O. The AgNCS complex (41.4 mg, 0.25 mmol) was dissolved in DMF (2 mL) and was then added in a test tube (14 mL capacity). A dry MeOH solution (2 mL) of PM-3,5-DMA (52.5 mg, 0.25 mmol) was then carefully layered on the top. Upon slow diffusion at room temperature for 4 weeks, dark yellow block-shaped single crystals of **Ag2** were obtained in 83% yield (14.0 mg) based on silver source. Found (calcd) for

$C_{15}H_{14}AgN_3S$ ($M_w = 376.22$ g/mol): C, 47.85 (47.89); H, 3.74 (3.75); N, 11.20 (11.17). IR (ν_{max}/cm^{-1}): 3436br, 2913br, 2107s, 1585m, 856m, 771m, 685m.

3. Synthesis of (Ag(PM-PBBZ)(NO₃)) (Ag3)

To a dry CH_2Cl_2 solution (2 mL) of PM-PBBZ (47.0 mg, 1 mmol) in a test tube, a mixture of $CH_2Cl_2/MeOH$ (1:1, v:v) solution (7 mL) was added on the top of ligand. A dry MeOH solution (2 mL) of $AgNO_3$ (16.9 mg, 1 mmol) was then carefully layered on the top of a mixture $CH_2Cl_2/MeOH$ solution. Upon slow diffusion at room temperature for 2 weeks, yellow block-shaped single crystals of Ag3 were obtained in 62% yield (10.5 mg) based on silver source. Found (calcd) for $C_{30}H_{22}Ag_2N_6O_8$ ($M_r = 810.27$ g/mol): C, 44.45 (44.47); H, 2.77 (2.74); N, 11.36 (11.37). IR (ν_{max}/cm^{-1}): 3438br, 3063w, 1592m, 1483s, 1234s, 1083s, 840m, 615m.

4. Synthesis of (Ag(PM-PBBZ)(ClO₄)) (Ag4)

In a similar manner, to a dry CH_2Cl_2 solution (2 mL) of PM-PBBZ (94.0 mg, 0.2 mmol) in a test tube, a mixture of $CH_2Cl_2/MeOH$ (1:1, v:v) solution (7 mL) was added on the top of ligand. A dry MeOH solution (2 mL) of $Ag(ClO_4)$ (41.4 mg, 0.2 mmol) was then carefully layered on the top of a mixture $CH_2Cl_2/MeOH$ solution. Upon slow diffusion at room temperature for 5 days, orange block-shaped single crystals of Ag4 were obtained in 82% yield (34.0 mg) based on silver source. Found (calcd) for $C_{60}H_{44}Ag_2Cl_2N_8O_{12}$ ($M_r = 1355.67$ g/mol): C, 53.20 (53.16); H, 3.22 (3.27); N, 8.27 (8.23). IR (ν_{max}/cm^{-1}): 3445br, 3054w, 1584m, 1492s, 1234s, 833m, 624m.

CHAPTER IV

RESULTS AND DISCUSSION

Synthesis of infrared spectra

All complexes were successfully synthesized in good yields by slow diffusion method at room temperature using different a protic solvent (see synthesis section in Chapter III). In the presence of NCS solution, the synthetic processes for all the copper(I) complexes involve the spontaneous reduction of Cu^{II} to Cu^{I} to form complex precursor of the composition (CuNCS) . The reactions of (CuNCS) precursor with N,N' -donor Schiff base type ligands in a 1:3.5 mole ratio afforded eight new copper(I) complexes, which show structural diversity ranging from discrete complexes of tetranuclear (**Cu-1**, **Cu-2**) and dinuclear (**Cu-3**, **Cu-4**) species, and one-dimensional coordination polymers (**Cu-5** - **Cu-8**). These complexes show characteristic vibration absorptions of thiocyanate at *ca.* $2060\text{--}2100\text{ cm}^{-1}$, which are shifted to higher wavenumbers by about 20 cm^{-1} compared to the free KNCS, indicating a NCS group is bridged by $\mu_{1,3}$ mode *via* N and S atoms to a second Cu(I) ion. These results are consistent with the single crystal X-ray studies. Comparison of the infrared spectral patterns for all copper(I) complexes and the free KNCS are shown in Figure 12 The assignments of the vibrational bands of these complexes are given in the Table 1.

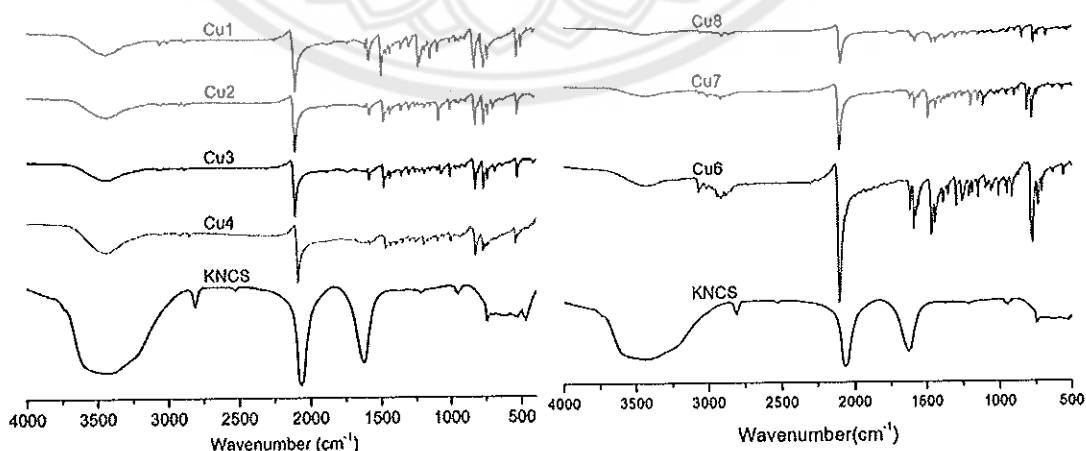


Figure 12 Infrared spectra of all copper(I) complexes and KNCS

Table 1 Vibrational frequencies for all copper(I) complexes and KNCS (cm^{-1})

Complex	IR (cm^{-1})			
	$\nu_{\text{C=N}}$	ν_{NCS}	$\nu_{\text{C=C(Ar)}}$	$\nu_{\text{C-XA}}^{\xi}$
Cu-1	3096	2122	1509	587
Cu-2	3080	2121	1564	899
Cu-3	3086	2110	1587	837
Cu-4	3097	2109	1573	963
Cu-5	3085	2110	1586	835
Cu-6	3435	2107	1467	
Cu-7	3436	2109	1491	
Cu-8	3436	2100	1466	
KNCS		2100		

ξ X = F, Cl, Br, I

The complex Ag-1 was synthesized in a similar manner to those copper(I) complexes by react AgNCS with PM-3,5-DMA ligand using a mixture MeOH/DMF solution. Brown plate like single crystals were obtained in good yield. The thiocyanate characteristic absorption appears at 2107 cm^{-1} , which is higher stretching frequency than the free thiocyanate, also indicating the NCS group is bridging. When the reactions were performed in absence of thiocyanate solution, the reactions of silver(I) nitrate or silver(I) perchlorate with bidentate or bis-bidentate Schiff base ligands afforded three new discrete complexes of Ag-2 – Ag-4. The infrared spectra of these complexes have higher stretching frequency than the free Schiff base ligands, indicating all the ligands are coordinated to the metal ions. These results are consistent with the single crystal X-ray studies. The infrared spectra for all silver(I) complexes are shown in Figure S1-S3, Appendix A of this thesis.

Description of crystal structure

Summary of crystallographic data and details of data collection for copper(I) complexes **Cu-1-Cu-4** and **Cu-5-Cu-7** are given in Tables 2 and 8, respectively. The selected bond lengths and bond angles for the tetranuclear complexes (**Cu-1**, **Cu-2**), dinuclear complexes (**Cu-3**, **Cu-4**), and the polymeric complexes (**Cu-5-Cu-7**) are also provided in Tables 3, 6 and 9, respectively.

Table 2 Crystal data and structural refinement for complexes **Cu-1-Cu-4**

Complex	Cu-1	Cu-2
Identify code	KCSB2	KCCT12
Empirical formula	C ₁₃ H ₉ CuFN ₃ S	C ₁₃ H ₉ ClCuN ₃ S
Formula weight	321.83	338.28
Temperature (K)	296(2)	296(2)
Crystal system	triclinic	triclinic
Space group	<i>P</i> -1	<i>P</i> -1
<i>a</i> (Å)	10.3361(5)	10.4283(8)
<i>b</i> (Å)	11.4207(5)	11.7760(9)
<i>c</i> (Å)	12.1221(6)	12.2077(9)
α (°)	109.8700(15)	111.203(2)
β (°)	93.8430(15)	94.175(2)
γ (°)	92.4060(16)	91.985(3)
<i>V</i> (Å ³)	1339.54(11)	1390.96(18)
<i>Z</i>	4	4
<i>D</i> _{calcd} (g cm ⁻³)	1.596	1.615
μ (mm ⁻¹)	1.785	1.899
Reflections collected/unique	24446/4699	36482/6739
Goodness of Fit on <i>F</i> ²	1.110	1.002
<i>R</i> _{int} , <i>R</i> _{sigma}	0.031, 0.023	0.049, 0.045
<i>R</i> ₁ ^a , <i>wR</i> ₂ ^b [<i>I</i> > 2σ(<i>I</i>)]	0.051, 0.100	0.040, 0.082
<i>R</i> ₁ ^a , <i>wR</i> ₂ ^b (all data)	0.062, 0.107	0.086, 0.097
Maximum/minimum residual (e Å ⁻³)	1.36/-0.55	0.58/-0.34

Table 2 (cont.)

Complex	Cu-3	Cu-4
Identify code	KCCT10	KCCT11
Empirical formula	C ₂₆ H ₁₈ Br ₂ Cu ₂ N ₆ S ₂	C ₂₆ H ₁₈ Cu ₂ I ₂ N ₆ S ₂
Formula weight	765.48	859.46
Temperature (K)	296(2)	296(2)
Crystal system	triclinic	triclinic
Space group	<i>P</i> -1	<i>P</i> -1
<i>a</i> (Å)	9.0931(7)	9.0997(4)
<i>b</i> (Å)	9.2969(6)	9.4284(5)
<i>c</i> (Å)	9.7681(6)	9.8504(4)
α (°)	110.786(2)	111.0670(10)
β (°)	107.736(2)	106.4380(10)
γ (°)	104.674(2)	106.0020(10)
<i>V</i> (Å ³)	672.04(8)	685.87(6)
<i>Z</i>	1	1
<i>D</i> _{calcd} (g cm ⁻³)	1.891	2.081
μ (mm ⁻¹)	4.740	3.982
Reflections collected/unique	14934/3302	16577/3375
Goodness of Fit on <i>F</i> ²	1.038	1.039
<i>R</i> _{int} , <i>R</i> _{sigma}	0.027, 0.022	0.026, 0.021
<i>R</i> ₁ ^{<i>a</i>} , <i>wR</i> ₂ ^{<i>b</i>} [<i>I</i> > 2σ(<i>I</i>)]	0.029, 0.058	0.027, 0.055
<i>R</i> ₁ ^{<i>a</i>} , <i>wR</i> ₂ ^{<i>b</i>} (all data)	0.039, 0.062	0.039, 0.059
Maximum/minimum residual (e Å ⁻³)	0.56/−0.69	1.00/−0.58

Computer programs: *APEX3* (Bruker, 2014), *SAINT* (Bruker, 2014), *SHELXT* (Sheldrick, 2015), *SHELXL* (Sheldrick, 2015), *DIAMOND* (Brandenburg, 2006), *publCIF* (Westrip, 2010), *enCIFer* (Allen, et al., 2004), and *Olex2* (Dolomanov, et al., 2009)

1. Crystal structure of the tetranuclear complexes

The single crystal X-ray diffraction analysis revealed that **Cu-1** and **Cu-2** are isotopic and represent a discrete tetranuclear complex. They crystallize in the triclinic space group *P*-1 with one formula unit in the unit cell. The asymmetric unit contains half of a tetranuclear unit that reside on a center of symmetry, consisting two crystallographic independent copper(I) atoms (**Cu1** and **Cu2**), two neutral Schiff base ligands, and four thiocyanate anion. A view of the asymmetric unit with the atom-labeling scheme of **Cu-2** as representative is shown in Figure 13 Both Cu(I) centers in these complexes are four-coordinated by two nitrogen atoms from Schiff base ligands, one nitrogen atom from thiocyanate anion, and one sulfur atom from other thiocyanate anion, adopting in a slightly tetrahedral geometry. The Cu–N bond lengths range from 1.904(4) to 2.157(3) Å and 1.907(3) to 2.145(2) Å for **Cu-1** and **Cu-2**, respectively. Whereas, the Cu–S bond lengths are 2.2876(12) and 2.3466(14) Å for **Cu-1**, and 2.2951(8) and 2.3307(10) Å for **Cu-2**. The (CuN₃S) bond angles range from 79.46(13) to 127.81(16)° and 79.28(9) to 126.30(10)° for **Cu-1** and **Cu-2**, respectively. The bond lengths and angles around the Cu(I) center at 296(2) K, Table 3, are typical and comparable to those observed in other four-coordinated copper(I) complexes with N,S-donor ligands (Li, et al., 2009).

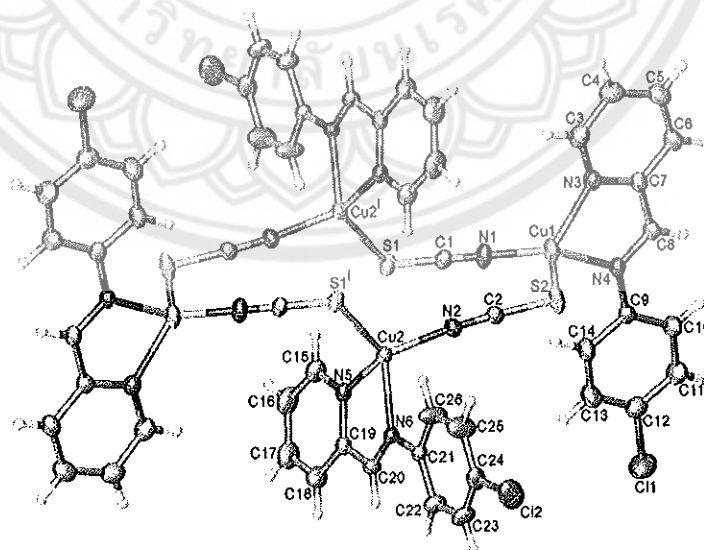


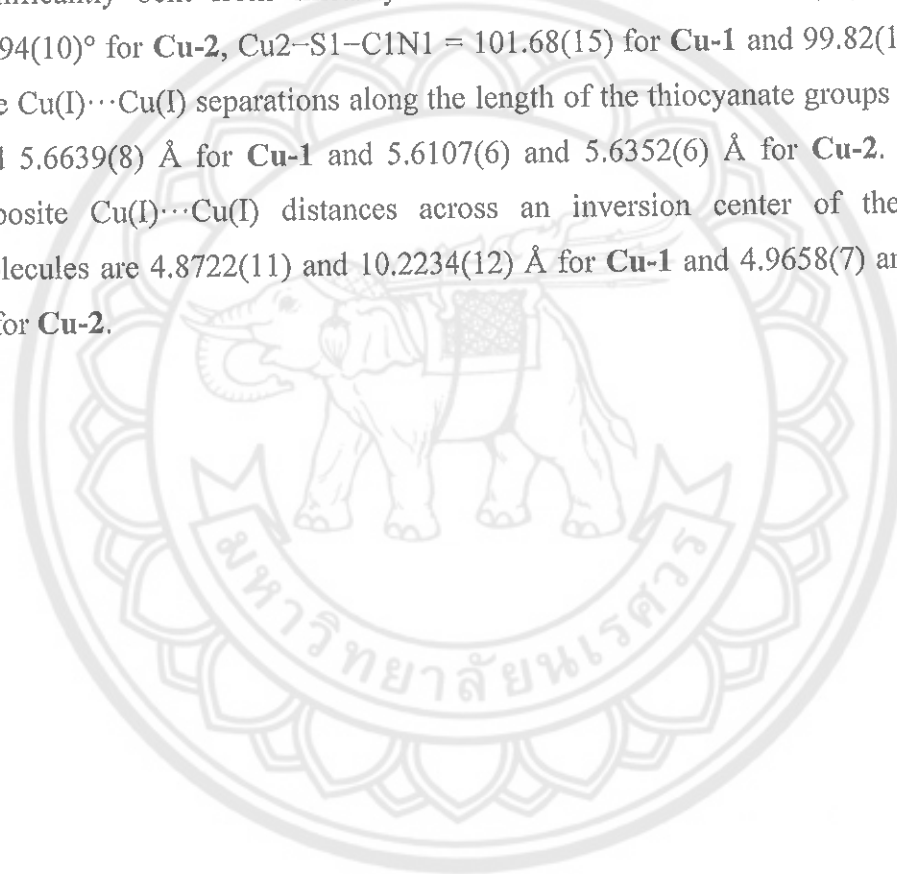
Figure 13 Thermal ellipsoid plot of **Cu-2** as representative complex at the 50% probability level containing its asymmetric unit with atom numbering. Symmetry code: (i) $1-x, 1-y, 1-z$.

Table 3 Selected bond lengths (Å) and bond angles (°) for Cu-1 and Cu-2

	Cu-1	Cu-2
Cu1–N1	1.904(4)	1.907(3)
Cu1–N3	2.061(3)	2.068(2)
Cu1–N4	2.116(3)	2.105(2)
Cu1–S2	2.3466(14)	2.3307(10)
Cu2–N2	1.928(3)	1.921(2)
Cu2–N5	2.036(3)	2.041(2)
Cu2–N6	2.157(3)	2.145(2)
Cu2–S1 ⁱ	2.2876(12)	2.2951(8)
N1–Cu1–S2	109.73(12)	111.31(8)
N1–Cu1–N3	127.81(16)	124.31(11)
N1–Cu1–N4	121.41(15)	119.67(10)
N3–Cu1–S2	107.42(10)	110.10(7)
N3–Cu1–N4	79.46(13)	79.89(9)
N4–Cu1–S2	106.82(10)	107.38(7)
N2–Cu2–S1 ⁱ	109.13(11)	110.37(7)
N2–Cu2–N5	127.32(14)	126.30(10)
N2–Cu2–N6	105.90(13)	106.46(9)
N5–Cu2–S1 ⁱ	113.95(9)	113.48(6)
N5–Cu2–N6	79.52(12)	79.28(9)
N6–Cu2–S1 ⁱ	117.68(9)	117.22(6)

Symmetry code: (i) 1–x, 1–y, 1–z.

In both **Cu-1** and **Cu-2** complexes, the thiocyanates act as $\mu_{1,3}$ -end-to-end bridge to coordinate copper(I) ions through nitrogen and sulfur atoms to form a discrete neutral tetranuclear species containing eight-membered Cu–N–C–S heterocycles in which the four copper(I) atoms and four sulfur atoms occupy in the corners. Within the tetranuclear molecule, the Cu–N–CS angles are almost linear *viz.* Cu1–N1–C1S1 = 176.8(4) for **Cu-1** and 179.5(3)° for **Cu-2**, Cu2–N2–C2S2 = 175.9(3) for **Cu-1** and 179.5(3)° for **Cu-2**. While, the Cu–S–CN angles are significantly bent from linearity *viz.* Cu1–S2–C2N2 = 99.00(14) for **Cu-1** and 98.94(10)° for **Cu-2**, Cu2–S1–C1N1 = 101.68(15) for **Cu-1** and 99.82(10)° for **Cu-2**. The Cu(I)⋯Cu(I) separations along the length of the thiocyanate groups are 5.6611(8) and 5.6639(8) Å for **Cu-1** and 5.6107(6) and 5.6352(6) Å for **Cu-2**. Whereas, the opposite Cu(I)⋯Cu(I) distances across an inversion center of the tetranuclear molecules are 4.8722(11) and 10.2234(12) Å for **Cu-1** and 4.9658(7) and 10.0902(9) Å for **Cu-2**.



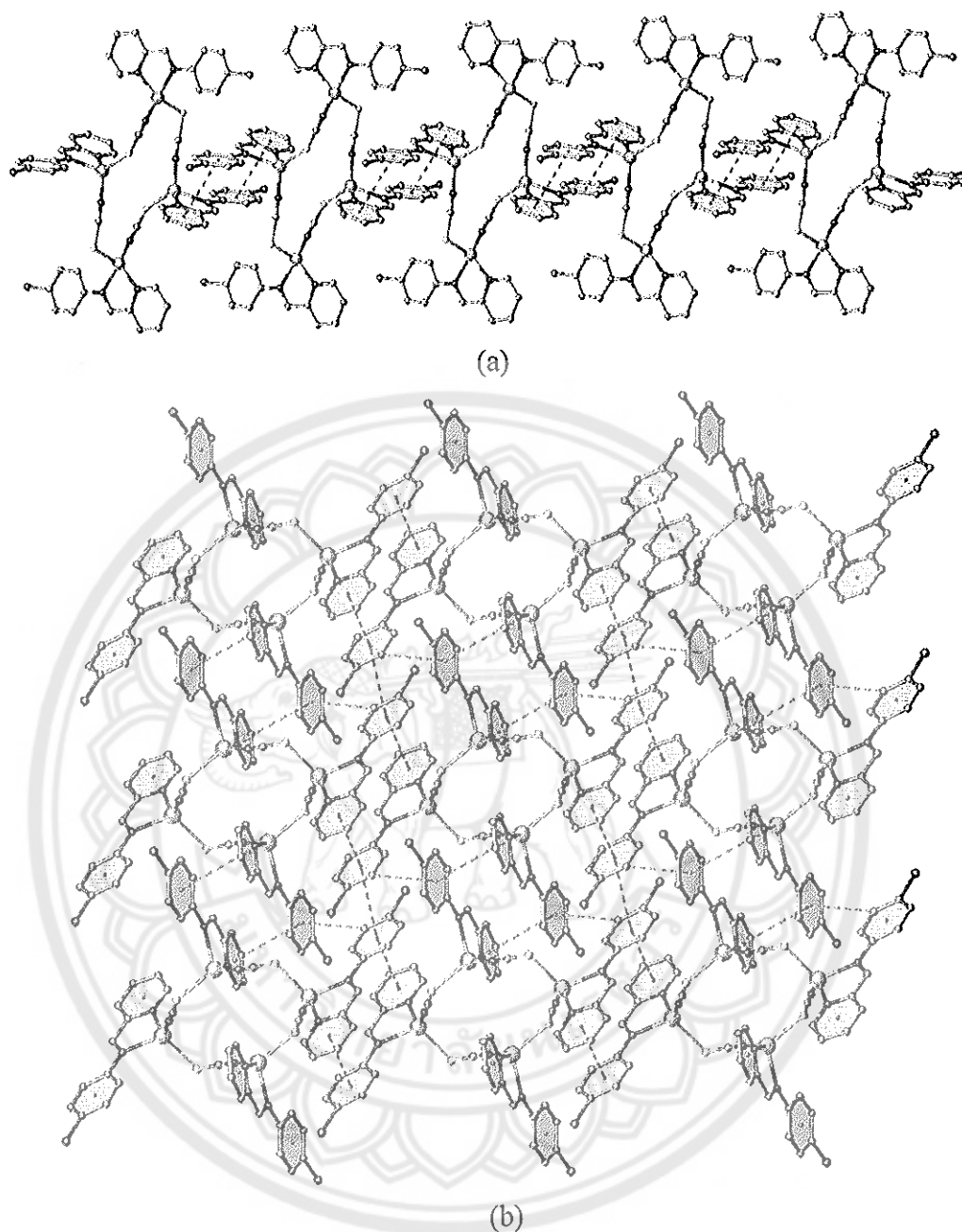


Figure 14 Views of the 1D chain generated by π - π interactions parallel to the a axis (a) and the 2D sheet generated by π - π and C-H \cdots π interactions in the ab plane (b) of the tetranuclear complex

The chelated Schiff base molecules in the tetranuclear core are almost perpendicular to each other, with a dihedral angle of 80.53(6) and 80.53(6) $^\circ$ for **Cu-1** and **Cu-2**, respectively. In crystal of the tetranuclear complexes, adjacent tetranuclear

complexes are connected *via* intermolecular face-to-face (*ff*) π - π interactions involving the pyridyl (N1/C3-C7)-phenyl (C9-C14) and phenyl (C9-C14)-phenyl (C9-C14) rings of the Schiff base ligands, generating a one-dimensional chain running parallel to the *a* axis as shown in Figure 14. Parallel to the *b* axis, other intermolecular *ff* π - π interactions between the aromatic rings of Schiff base ligands along with edge-to-face (*ef*) C-H $\cdots\pi$ interactions involving the phenyl ring hydrogen atom (H13) and the phenyl ring (C9-C14) of the Schiff base ligands are also observed. These *ff* π - π and *ef* C-H $\cdots\pi$ interactions are further connected the chains into the two-dimensional sheets extending in the *ab* plane. Other C-H $\cdots\pi$ interactions involving the pyridyl hydrogen atom (H16) and the phenyl ring of Schiff base ligands and between the imine hydrogen atom (H20) and the mid-point of the carbon-nitrogen double bonds (C2=N2) of the bridging thiocyanate groups are present and provide the link between the adjacent sheets resulting in the formation of the three-dimensional supramolecular structure. It should be noted that no halogen bonding interactions observed in these tetranuclear complexes. Details of all intermolecular interactions in **Cu-1** and **Cu-2** are given in Tables 4 and 5.

Table 4 Intermolecular π - π interactions (\AA , $^\circ$) for **Cu-1** and **Cu-2**

π - π	Centroid to Centroid Distance		Dihedral angle	
	Cu-1	Cu-2	Cu-1	Cu-2
$Cg1\cdots Cg2^i$	3.886(3)	3.848(3)	8.49(17)	6.02(14)
$Cg2\cdots Cg2^{ii}$	3.651(5)	3.825(4)	0.0(6)	0.0(5)
$Cg3\cdots Cg4^{iii}$	3.820(3)	3.947(2)	9.67(8)	13.97(16)

$Cg1$, $Cg2$, $Cg3$, and $Cg4$ are the centroid of the N1/C3-C7, C9-C14, N5/C15-C19, and C21-C26 rings, respectively. Symmetry codes: (i) $1-x, -y, -z$; (ii) $x-1, y, z$; (iii) $-x, 1-y, 1-z$.

Table 5 Hydrogen bond geometry (Å, °) for **Cu-1** and **Cu-2**

D–H···A	D–H	H···A	D···A	D–H···A
Cu-1				
C13–H13···Cg1 ⁱ	0.93	3.200(2)	4.034(6)	149.9
C16–H16···Cg2 ⁱⁱ	0.93	2.9221(18)	3.784(6)	165.8
C20–H20···Cg3 ^{iv}	0.93	2.819(3)	3.740(3)	160.6
Cu-2				
C13–H13···Cg1 ⁱ	0.93	3.2346(14)	4.048(4)	147.3
C16–H16···Cg2 ⁱⁱ	0.93	3.0398(13)	3.926(4)	159.8
C20–H20···Cg3 ^{iv}	0.93	2.819(3)	3.740(3)	160.6

Cg1, Cg2, and Cg3 are the centroid of the C21–C26 and N3/C3–C7 rings, and C=N bonds, respectively. Symmetry codes: (i) 1+x, y, z; (ii) 1–x, 1–y, –z; (iii) x–1, 1+y, z.

2. Crystal structure of the dinuclear copper(I) complexes

Using the same solvent and stoichiometric ratio of the (Cu(NCS)) complex precursor and Schiff base ligand as in the tetranuclear complexes **Cu-1** and **Cu-2**, unexpectedly, discrete dinuclear complexes of **Cu-3** and **Cu-4** were obtained and characterized by single crystal X-ray diffraction. Both complexes are isostructural and crystallize in the triclinic space group *P*-1 with one formula unit in the unit cell (*Z* = 1). As shown in Figure 15, the asymmetric of the dinuclear species consists of one crystallographically independent copper(I) cation, one neutral Schiff base ligand, and one thiocyanate anion. Each copper(I) cation is doubly bridged by thiocyanate anions in $\mu_{1,3}$ -end-to-end coordination modes and the chelated Schiff base ligand, giving a centrosymmetric dinuclear neutral species, in which the copper(I) center has a distorted tetrahedral coordination geometry similar to that observed in the tetranuclear complexes **Cu-1** and **Cu-2**. The Cu(I)···Cu(I) intramolecular separation through the $\mu_{1,3}$ bridging thiocyanato anions is 5.0965(2) and 5.1185(2) Å for **Cu-3** and **Cu-4**, respectively. The Cu–N bond lengths range from 1.936(2) to 2.105(2) Å for **Cu-3** and 1.941(2) to 2.117(2) Å for **Cu-4**, whereas, the Cu–S bond lengths are 2.3237(7) and 2.3303(8) Å for **Cu-3** and **Cu-4**, respectively. The CuN₃S bond angles are in the range

(dihedral angle = 0.00(3)°) for **Cu-4** (*Cg*1 is the centroid of N2/C2-C6 ring; symmetry code: (i) 1-x, -y, 1-z), leading to the formation of a one-dimensional chain running

Table 6 Selected bond lengths (Å) and bond angles (°) for Cu-3 and Cu-4

	Cu-3	Cu-4
Cu1-N1	1.936(2)	1.941(2)
Cu1-N2	2.075(2)	2.079(2)
Cu1-N3	2.105(2)	2.117(2)
Cu1-S1 ⁱ	2.3237(7)	2.3303(8)
N1-Cu1-S1 ⁱ	106.60(6)	105.95(7)
N1-Cu1-N2	126.16(8)	127.55(10)
N1-Cu1-N3	117.81(7)	117.27(9)
N2-Cu1-S1 ⁱ	110.89(5)	109.79(7)
N2-Cu1-N3	79.38(7)	79.27(8)
N3-Cu1-S1 ⁱ	114.26(5)	115.65(6)

Symmetry code: (i) 2-x, 1-y, 1-z

parallel to the *b* axis. These chains are extended into the two-dimensional sheets in the *bc* plane via *ef* C-H... π interactions involving the phenyl ring hydrogen atom (H12) and the pyridyl ring of the Schiff base ligands along with S... π interactions between thiocyanate sulfur atom (S1) and the phenyl ring of the Schiff base ligands. It is interesting to note that S... π interactions occurred frequently in the protein system, however, only observed in the thiocyanate metal complex (xxxx) (ref).

Moreover, C-X... π and C-H... π interactions, Figure 17, involving the halogen atom or the pyridyl hydrogen atom (H3) and the mid-point of the C=N double bonds of the thiocyanate groups as well as additional C-H... π interactions between the pyridyl hydrogen atom (H4) and the pyridyl ring of the Schiff base ligands are present. These interactions help to consolidate the stacking of the sheets as well as to increase

structural dimensionality into the three-dimensional supramolecular architecture. It should be also note that no halogen-halogen interactions observed in these dinuclear complexes. Details of all intermolecular interactions in **Cu-3** and **Cu-4** are given in Table 7.

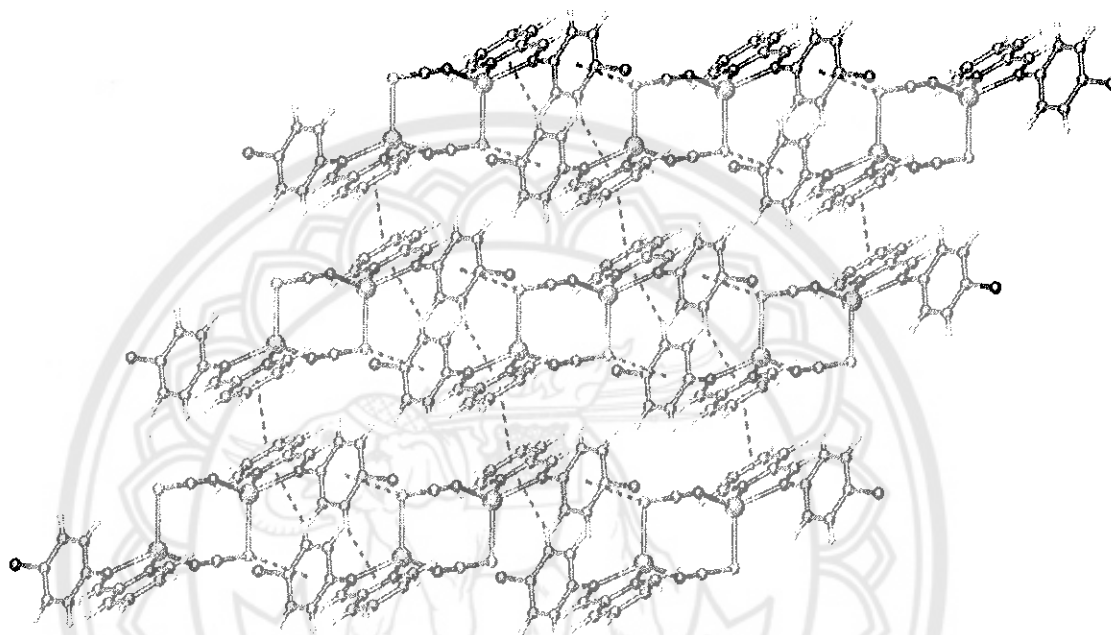


Figure 16 View of the two-dimensional sheet generated by a combination of π - π , $C-H\cdots\pi$, and $S\cdots\pi$ interactions (green dashed lines) in the dinuclear complex

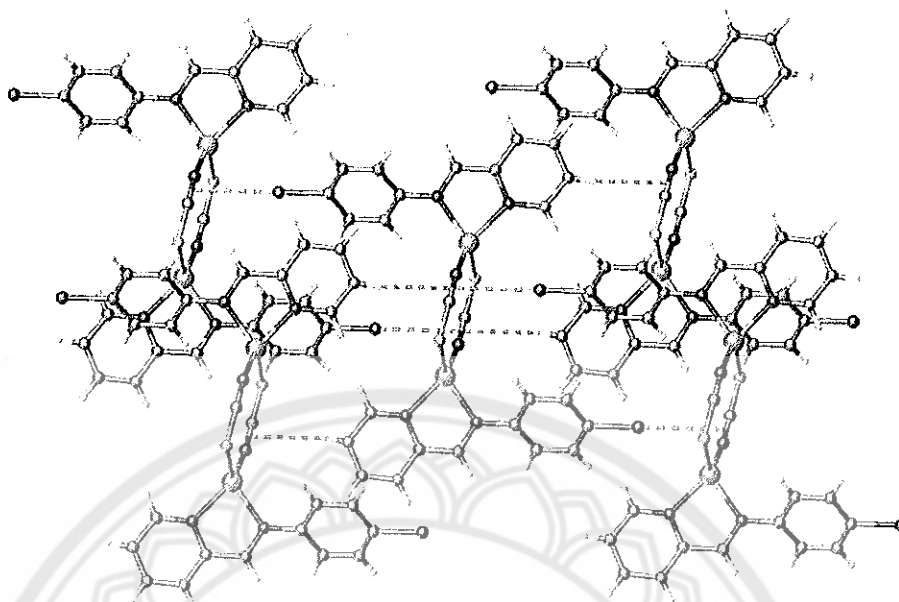


Figure 17 A view of the weak C–H $\cdots\pi$ and C–X $\cdots\pi$ interactions in the dinuclear complex. These serve to connect the sheets into a three-dimensional architecture

Table 7 Intermolecular interactions (Å, °) for Cu-3 and Cu-4

D–X \cdots A	D–X	X \cdots A	D \cdots A	D–X \cdots A
Cu-3				
C3–H3 \cdots Cg1 ⁱ	0.93	2.8003(2)	3.7213(2)	170.9
C4–H4 \cdots Cg2 ⁱ	0.93	2.9930(2)	3.4949(2)	50.7
C12–H12 \cdots Cg3 ⁱⁱ	0.93	2.8311(2)	3.5618(2)	47.2
C11–Br1 \cdots Cg1 ⁱⁱⁱ	1.8956(2)	3.3215(2)	5.2168(4)	178.8
Cu-4				
C3–H3 \cdots Cg1 ⁱ	0.93	2.79239(10)	3.71674(13)	172.7
C4–H4 \cdots Cg2 ⁱ	0.93	2.98149(11)	3.47787(12)	52.3
C12–H12 \cdots Cg3 ⁱⁱ	0.93	2.90159(12)	3.64316(15)	47.8
C11–I1 \cdots Cg1 ⁱⁱⁱ	2.09742(8)	3.38148(13)	5.4788(2)	179.4

Cg1, Cg2, and Cg3 are the centroid of the C1=N1 double bonds, C8–C13 and N2/C2–C6 rings, respectively. Symmetry codes: (i) $x-1, y, z$; (ii) $2-x, 1-y, 2-z$; (iii) $1+x, y, 1+z$.

3. Crystal structure of the polymeric copper(I) complexes

The polymers **Cu-5**, **Cu-6**, and **Cu-7** crystallize in the monoclinic system and their asymmetric unit contain one copper(I) ion, one neutral Schiff base ligand and one thiocyanate anion as shown in Figure 18. Each copper(I) atom is four-coordinated by two nitrogen atoms from the Schiff base ligand, one nitrogen atom from thiocyanate anion, and one sulfur atom from other thiocyanate anion, adopting a distorted tetrahedral geometry. The Cu–N bond lengths range from 1.909(2) to 2.112(2) Å for **Cu-5**, 1.901(5) to 2.123(4) Å for **Cu-6** and 1.935(2) to 2.115(2) Å for **Cu-7**, whereas the Cu–S bond lengths in **Cu-5**, **Cu-6** and **Cu-7** are 2.3285(10), 2.3365(18), and 2.3006(9) Å, respectively. The CuN₃S bond angles are in the range 79.38(7) to 126.16(8)°, 79.27(8) to 127.55(10)° and 80.16(8) to 117.99(10)° for **Cu-5**, **Cu-6** and **Cu-7**, respectively. Indeed, the bond lengths and bond angles in both polymeric complexes, Table 8, are typical for thiocyanate Schiff base-based complex with a formal oxidation state of copper(I) such as the tetranuclear complexes of **Cu-1** and **Cu-2** and the dinuclear complexes **Cu-3** and **Cu-4** and other four-coordinated copper(I) complexes with N,S-donor ligands (Li, et al., 2009).

Table 8 Crystal data and structural refinement for complexes **Cu-5-Cu-7**

Complex	Cu-5	Cu-6	Cu-7
Identify code	KCBR207	KCSB26	KCSB8
Empirical formula	C ₁₃ H ₉ BrCuN ₃ S	C ₁₅ H ₁₄ CuN ₃ S	C ₁₅ H ₁₄ CuN ₃ S
Formula weight	382.74	331.89	331.89
Temperature (K)	296(2)	296(2)	296(2)
Crystal system	monoclinic	monoclinic	monoclinic
Space group	<i>P2₁/n</i>	<i>P2₁/n</i>	<i>P2₁/c</i>
<i>a</i> (Å)	9.5706(5)	11.2655(18)	9.6460(4)
<i>b</i> (Å)	10.4245(5)	10.6100(17)	9.8210(3)
<i>c</i> (Å)	14.5520(6)	12.5140(20)	16.1651(6)
<i>a</i> (°)	90	90	90
<i>β</i> (°)	105.623(2)	101.495(3)	104.8510(11)

Table 8 (cont.)

Complex	Cu-5	Cu-6	Cu-7
γ ($^{\circ}$)	90	90	90
V (\AA^3)	1398.20(12)	1465.8(4)	1480.22(9)
Z	4	4	4
D_{calcd} (g cm^{-3})	1.818	1.504	1.489
μ (mm^{-1})	4.556	1.624	1.608
2θ range for data	5.90 to 51.45	5.88 to 50.14	6.02 to 52.74
Reflections	18114/2659	13561	41597/3019
Goodness of Fit on F^2	1.020	1.051	1.043
$R_{\text{int}}, R_{\text{sigma}}$	0.058, 0.033	0.159, 0.091	0.038, 0.015
R_1^a, wR_2^b ($I > 2\sigma(I)$)	0.031, 0.063	0.056, 0.092	0.037, 0.088
R_1^a, wR_2^b (<i>all data</i>)	0.050, 0.069	0.131, 0.114	0.049, 0.095
Max/min residual (e \AA^{-3})	0.40/−0.51	0.44/−0.51	0.52/−0.18

Computer programs: *APEX2* (Bruker, 2014), *SAINT* (Bruker, 2014), *SHELXT* (Sheldrick, 2015), *SHELXL* (Sheldrick, 2015), *DIAMOND* (Brandenburg, 2006), *publCIF* (Westrip, 2010), *enCIFer* (Allen *et al.*, 2004), and *Olex2* (Dolomanov, *et al.*, 2009).

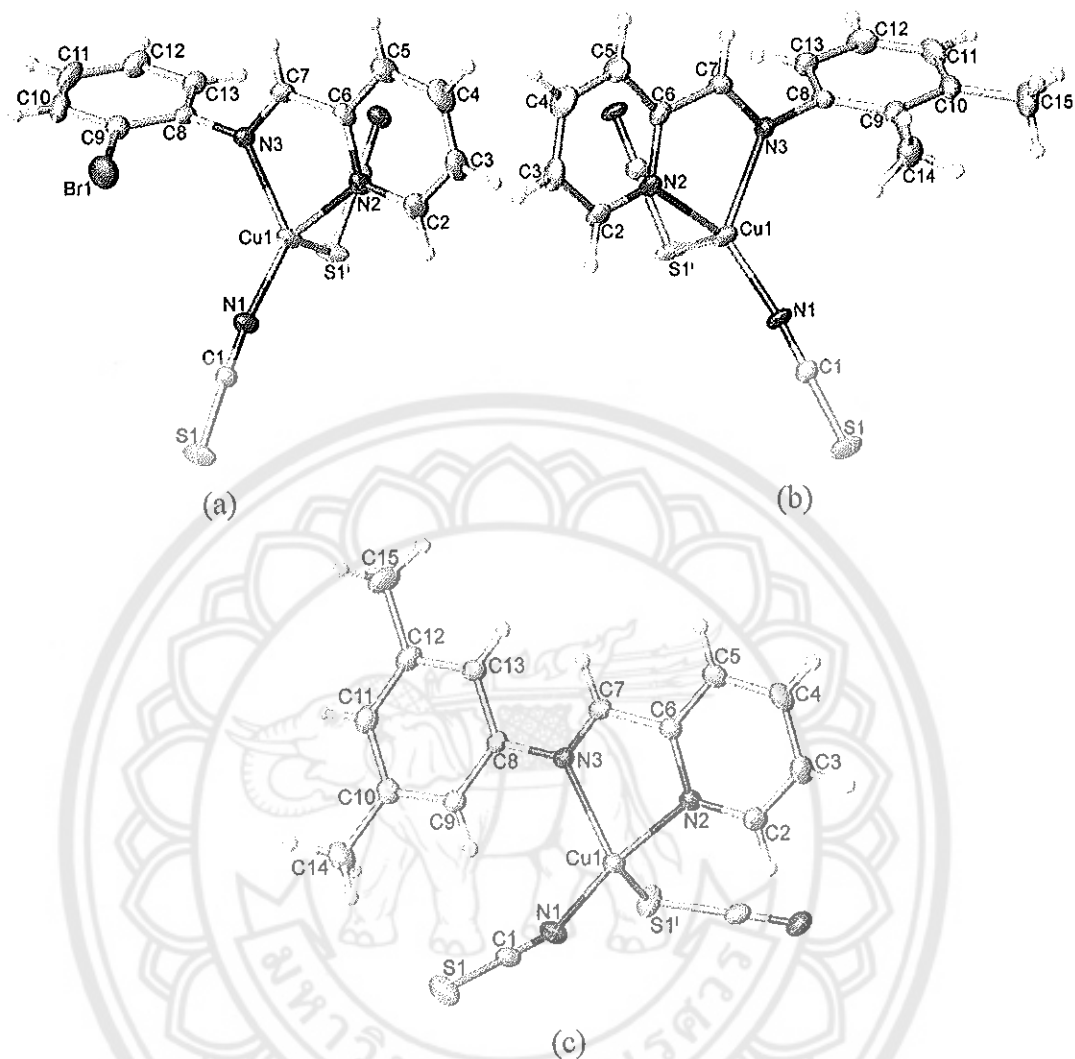


Figure 18 Thermal ellipsoid plot of the polymeric complexes Cu-5 (a) Cu-6 (b) and Cu-7 at the 50% probability level containing its asymmetric unit with atom numbering and showing coordination environments of metals center. H atoms are shown as small spheres of arbitrary radii. Symmetry code: (i) $1-x, 1-y, 1-z$

Table 9 Selected bond lengths (Å) and bond angles (°) for **Cu-5** to **Cu-7**

	Cu-5	Cu-6	Cu-7
Cu1–N1	1.909(2)	1.901(5)	1.935(2)
Cu1–N2	2.084(2)	2.079(4)	2.065(2)
Cu1–N3	2.112(2)	2.123(4)	2.115(2)
Cu1–S1 ⁱ	2.3285(10)	2.3365(18)	2.3006(9)
N1–Cu1–S1 ⁱ	109.35(8)	112.67(14)	116.05(8)
N1–Cu1–N2	122.07(10)	122.45(18)	117.99(10)
N1–Cu1–N3	127.24(10)	124.94(18)	111.43(9)
N2–Cu1–S1 ⁱ	111.40(7)	108.57(13)	115.75(6)
N2–Cu1–N3	78.75(9)	78.93(17)	80.16(8)
N3–Cu1–S1 ⁱ	104.35(7)	104.16(12)	109.43(6)

Symmetry code: (i) $-x, y-1/2, 1/2-z$.

As can be seen in Figure 19, the copper(I) cations in all the polymeric complexes are each bridged by two thiocyanate anions in a μ -1,3-coordination mode, resulting in the formation of a corrugated one-dimensional chain with the intrachain Cu \cdots Cu separation *via* the thiocyanate bridging ligands being 5.5514(4), 5.5888(10), and 5.5697(3) Å for **Cu-5**, **Cu-6**, and **Cu-7**, respectively. Although all the polymeric complexes have similar the chain motifs, however, their crystal packing are different due to the effect of bromine or methyl groups substitute on the benzene ring of the Schiff base ligands which enable different types of intermolecular interactions. This is also evident through the dihedral angles between the mean plane of pyridyl and phenyl rings of the Schiff base ligands which being 80.3(2), 75.1(2), and 12.06(9)°, for **Cu-5**, **Cu-6**, and **Cu-7**, respectively. In the crystal of **Cu-5**, the adjacent chains are stacked into the two-dimensional sheets along the crystallographic *a* axis *via* symmetry related π - π interactions between the pyridyl/pyridyl and phenyl/pyridyl rings as shown in Figure 20. Alternatively, the interchain halogen $\cdots\pi$ interactions involving the bromine

atom and the phenyl ring of the Schiff base ligand is observed along the *c* axis with a $\text{Br}\cdots\text{Cg}$ (*Cg* is centroid of C8-C13 ring) distance of 3.5115(13) Å. A combination of this type of interactions and $\pi\cdots\pi$ stacking in **Cu-5** are linked the chains into the three-dimensional supramolecular architecture.

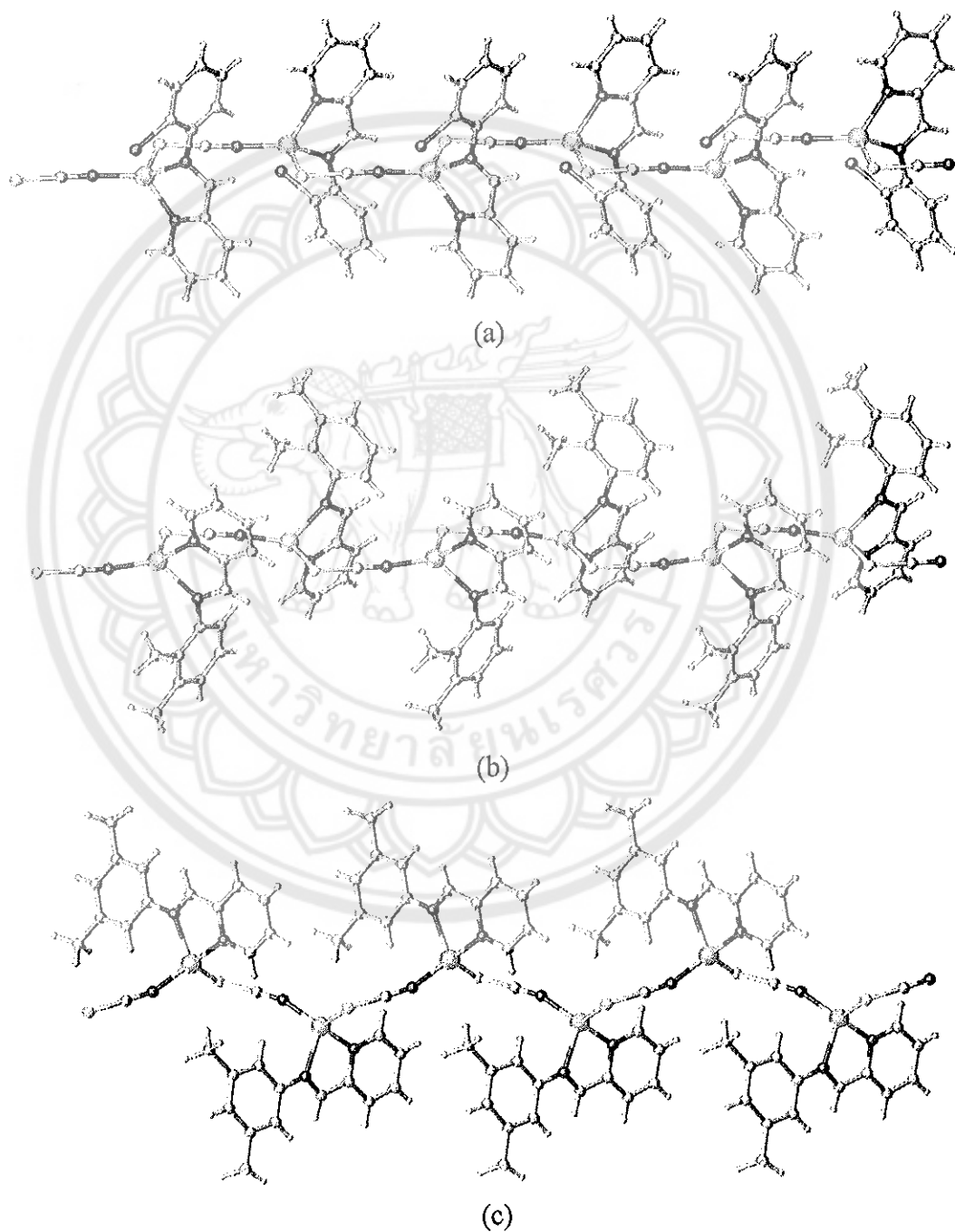


Figure 19 Views of the one-dimensional chain in the polymeric complexes **Cu-5** (a) **Cu-6** (b) and **Cu-7** (c)

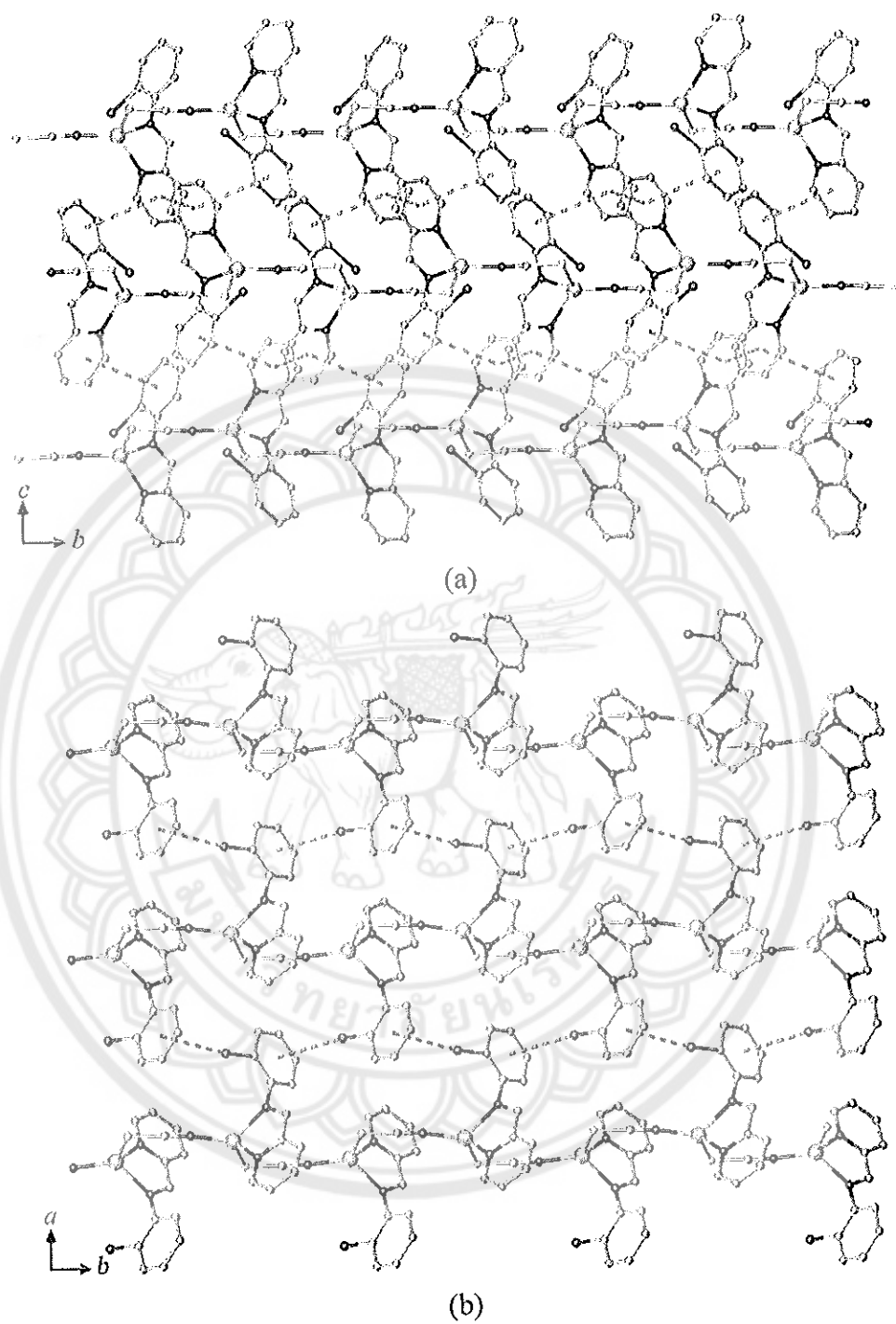


Figure 20 Views of $\pi \cdots \pi$ stacking (a) and $\text{Br} \cdots \pi$ (b) interactions in Cu-5.

A combination of these interactions are linked the molecules into the three-dimensional supramolecular structure

The substitution of the methyl groups in the *ortho* and *para* positions on the benzene ring with respect to the bromine atom, the crystal packing in **Cu-6** is similar to that described for **Cu-5**, Figure 21, except that weak C–H \cdots π (H15c \cdots Cg1 = 3.134(2) Å; Cg1 is the centroid of the N2/C2–C6 ring) interaction is recognized.

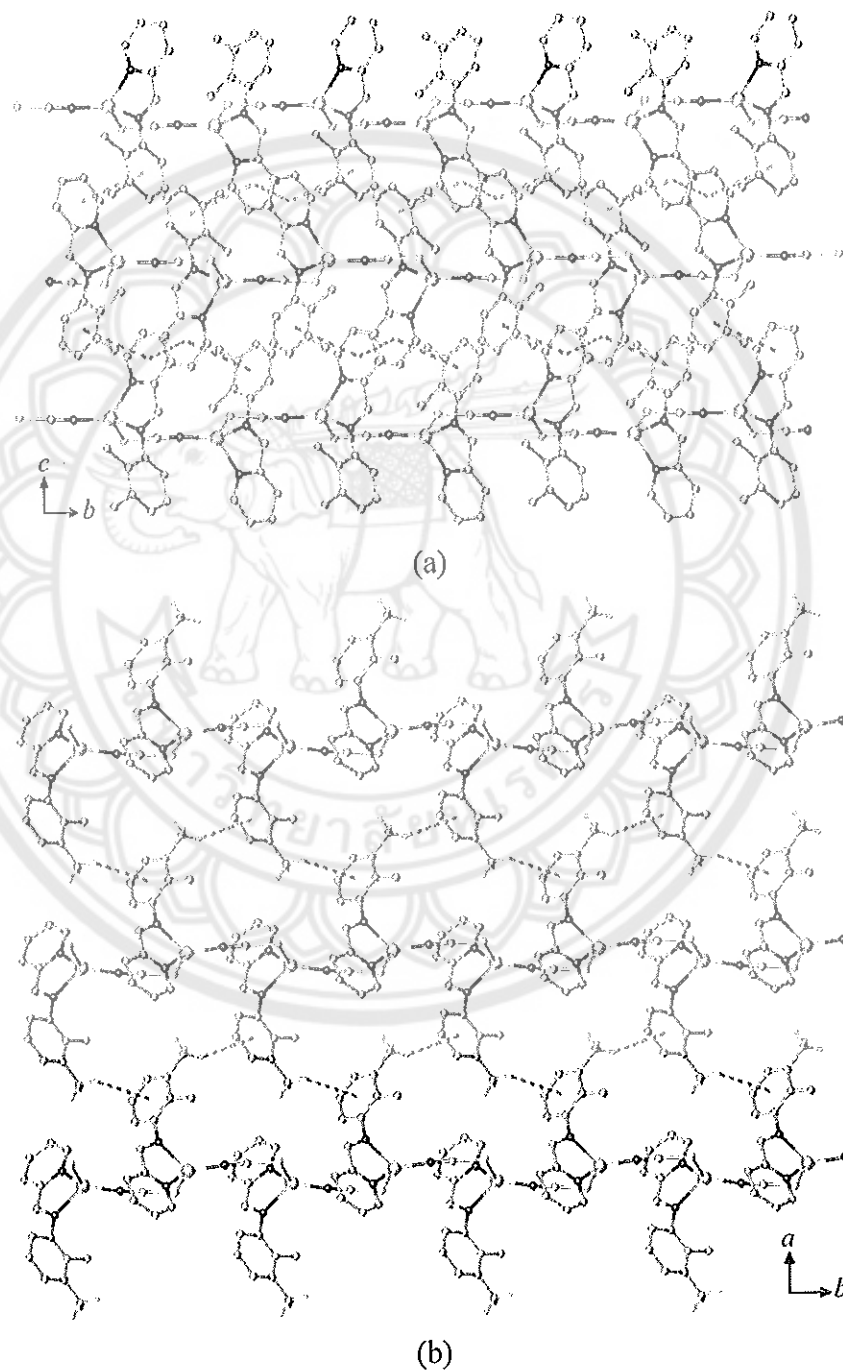


Figure 21 Views of $\pi\cdots\pi$ stacking (a) and C–H \cdots π (b) interactions in **Cu-6**

For **Cu-7**, the three-dimensional supramolecular structure is mainly built by aromatic $\pi \cdots \pi$ interactions of the Schiff base ligands. As can be seen in Figure 22, adjacent one-dimensional chains generated by a 2_1 screw axis are linked to each other by symmetry-related phenyl/phenyl and pyridyl/pyridyl $\pi \cdots \pi$ stacking, generating the two-dimensional layer structure along the crystallographic a axis. Other aromatic $\pi \cdots \pi$ stacking between phenyl/phenyl rings is present, and further link the layers into the three-dimensional supramolecular structure. It should be noted that no $C-H \cdots \pi$ interactions are observed in this complex. Geometrical parameters of $\pi-\pi$ interactions for all the polymeric complexes **Cu-5-Cu-7** are listed in Table 10. It should be noted that no $Cu^I \cdots Cu^I$ ($d^{10} \cdots d^{10}$) interactions are observed among the Schiff base copper(I) complexes in the present study.

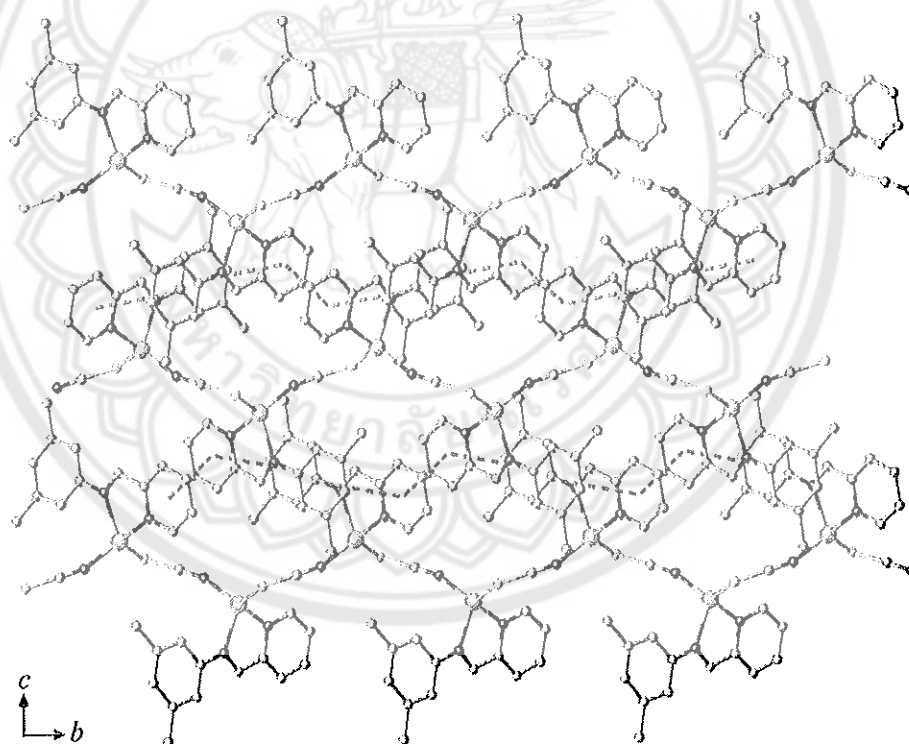


Figure 22 View of two-dimensional layer structure in **Cu-7** generated by aromatic $\pi \cdots \pi$ stacking interactions

Table 10 Geometrical parameters of π - π interactions (\AA , $^\circ$) for Cu-5-Cu-7

	Centroid to Centroid Distance	Dihedral Angle
Cu-5		
Cg1...Cg1 ⁱ	3.842(3)	0.00(17)
Cg1...Cg2 ⁱⁱ	4.010(2)	14.15(11)
Cu-6		
Cg1...Cg1 ⁱⁱⁱ	3.678(5)	0.0(5)
Cg1...Cg2 ^{iv}	3.883(4)	12.07(19)
Cu-7		
Cg1...Cg1 ^v	3.592(2)	0.00(3)
Cg1...Cg2 ^{vi}	3.8557(15)	12.06(9)

Cg1 and Cg2 are the centroid of pyridyl N2/C2-C6 and phenyl C8-C13 rings, respectively. Symmetry codes: (i) $-x, 2-y, 1-z$; (ii) $x-1/2, 3/2-y, z-1/2$; (iii) $2-x, -y, 1-z$; (iv) $1/2+x, 1/2-y, 1/2+z$; (v) $-x, -y, 1-z$; (vi) $-x, 1-y, -z$

4. Crystal structure of the silver(I) complexes

Summary of crystallographic data and details of data collection for silver(I) complexes **Ag-1-Ag-4** are given in Table 11. The selected bond lengths and bond angles for all silver(I) complexes are also provided in Table 12.

Ag-1: The complex **Ag-1** crystallizes in the centrosymmetric triclinic space group $P-1$ with two formula unit per the unit cell. The asymmetric unit of **Ag-1** contains one Ag(I) ion, one PM-IA Schiff base ligand, and one NO_3 anion as shown in Figure 22. The unique Ag(I) cation is coordinated by two nitrogen atoms from the PM-IA ligand and one oxygen atom of nitrate anion in a distorted trigonal-planar geometry. The Ag-N bond lengths in **Ag-1** are 2.386(2) and 2.313(2) \AA while the Ag-O bond length is 2.301(3) \AA . The AgN_2O bond angles in **Ag-1** are in the range 71.96(8) to 146.94(8) $^\circ$ (Table 12). One interesting feature in **Ag-1** is the formation of a $\text{Ag}\cdots\text{I}$ contact at 3.1474(8) \AA . This contact is well below the sum of the van der Waals radii (1.72 (Ag) + 1.98 (I) = 3.70 \AA) (Bondi, 1964), and considered to be a weak

interaction. The Ag...I contacts along with the C-H... π interactions involving the hydrogen pyridyl atom (C1) and the phenyl ring (C7-C12) are linked adjacent molecules into a one-dimensional chain running parallel to the crystallographic *a* direction.

Table 11 Crystal data and structural refinement for complexes Ag-1-Ag-4

Complex	Ag-1	Ag-2
Identify code	KCSB18	KCSB25
Empirical formula	C ₁₂ H ₉ AgIN ₃ O ₃	C ₁₅ H ₁₄ AgN ₃ S
Formula weight	477.99	376.22
Temperature (K)	296(2)	296(2)
Crystal system	triclinic	monoclinic
Space group	<i>P</i> -1	<i>P</i> 2 ₁ / <i>n</i>
<i>a</i> (Å)	8.601(2)	12.2529(15)
<i>b</i> (Å)	9.378(2)	7.6782(9)
<i>c</i> (Å)	9.524(3)	16.450(2)
α (°)	80.104(9)	90
β (°)	69.459(8)	103.316(4)
γ (°)	74.068(9)	90
<i>V</i> (Å ³)	689.3(3)	1506.0(3)
<i>Z</i>	2	4
<i>D</i> _{calcd} (g cm ⁻³)	2.303	1.659
μ (mm ⁻¹)	3.71	1.469
Reflections collected/unique	22336/3422	43781/2792
Goodness of Fit on <i>F</i> ²	1.03	1.03
<i>R</i> _{int} , <i>R</i> _{sigma}	0.040, 0.026	0.063, 0.021
<i>R</i> ₁ ^{<i>a</i>} , <i>wR</i> ₂ ^{<i>b</i>} (<i>I</i> > 2 σ (<i>I</i>))	0.028, 0.054	0.031, 0.062
<i>R</i> ₁ ^{<i>a</i>} , <i>wR</i> ₂ ^{<i>b</i>} (all data)	0.047, 0.059	0.048, 0.067
Maximum/minimum residual (e Å ⁻³)	0.92/-0.93	0.58/-0.54

Table 11 (cont.)

Complex	Ag-3	Ag-4
Identify code	KCSB22	KCSB19
Empirical formula	C ₆₀ H ₄₄ Ag ₂ Cl ₂ N ₈ O ₁₂	C ₃₀ H ₂₂ Ag ₂ N ₆ O _{8.53}
Formula weight	1355.67	818.67
Temperature (K)	296(2)	296(2)
Crystal system	triclinic	monoclinic
Space group	<i>P</i> -1	<i>P</i> 2/ <i>n</i>
<i>a</i> (Å)	10.5410(6)	13.5524(5)
<i>b</i> (Å)	14.8988(8)	11.9643(4)
<i>c</i> (Å)	18.9219(11)	18.8566(8)
α (°)	81.801(2)	90
β (°)	88.631(2)	111.0320(10)
γ (°)	72.675(2)	90
<i>V</i> (Å ³)	2807.3(3)	2853.81(19)
<i>Z</i>	2	4
<i>D</i> _{calcd} (g cm ⁻³)	1.604	1.905
μ (mm ⁻¹)	0.87	1.440
Reflections collected/unique	9947/4165	87415/5433
Goodness of Fit on <i>F</i> ²	1.00	1.070
<i>R</i> _{int} , <i>R</i> _{sigma}	0.143, 0.140	0.046, 0.114
<i>R</i> ₁ ^{<i>a</i>} , <i>wR</i> ₂ ^{<i>b</i>} (<i>I</i> > 2σ(<i>I</i>))	0.075, 0.144	0.070, 0.128
<i>R</i> ₁ ^{<i>a</i>} , <i>wR</i> ₂ ^{<i>b</i>} (all data)	0.204, 0.190	0.039, 0.059
Maximum/minimum residual (e Å ⁻³)	0.77/-0.78	0.59/-0.61

Computer programs: *APEX3* (Bruker, 2014), *SAINT* (Bruker, 2014), *SHELXT* (Sheldrick, 2015), *SHELXL* (Sheldrick, 2015), *DIAMOND* (Brandenburg, 2006), *publCIF* (Westrip, 2010), *enCIFer* (Allen *et al.*, 2004), and *Olex2* (Dolomanov, *et al.*, 2009)

Table 12 Selected bond lengths (Å) and bond angles (°) for Ag-1-Ag-4

Ag-1			
Ag1-O1	2.301(3)	Ag1-N2	2.386(2)
Ag1-N1	2.313(2)	Ag1-I1 ⁱ	3.1474(8)
O1-Ag1-N1	140.56(9)	O1-Ag1-N2	146.94(8)
N1-Ag1-N2	71.96(8)		
Ag-2			
Ag1-S1	2.5091(11)	Ag1-N2	2.331(2)
Ag1-S1 ⁱⁱ	2.5478(11)	Ag1-N3	2.397(2)
S1-Ag1-S1 ⁱⁱ	120.020(17)	N2-Ag1-N3	71.51(8)
N2-Ag1-S1 ⁱⁱ	110.66(7)	N3-Ag1-S1 ⁱⁱ	108.64(6)
N2-Ag1-S1	119.68(6)	N3-Ag1-S1	116.31(6)
Ag1-S1-Ag1 ⁱⁱⁱ	130.72(5)		
Ag-3			
Ag1-N1	2.336(8)	Ag2-N3	2.394(7)
Ag1-N2	2.393(7)	Ag2-N4	2.304(7)
Ag1-N5	2.371(8)	Ag2-N7	2.307(7)
Ag1-N6	2.385(7)	Ag2-N8	2.395(8)
N1-Ag1-N2	71.3(3)	N3-Ag2-N8	135.7(2)
N1-Ag1-N5	104.7(3)	N4-Ag2-N3	72.1(3)
N1-Ag1-N6	170.9(2)	N4-Ag2-N7	161.7(3)
N5-Ag1-N2	134.2(2)	N4-Ag2-N8	105.9(3)
N5-Ag1-N6	71.7(3)	N7-Ag2-N3	122.9(2)
N6-Ag1-N2	117.3(2)	N7-Ag2-N8	71.6(3)

Table 12 (cont.)

Ag-4			
Ag1-N1	2.268(3)	Ag2-N4	2.240(3)
Ag1-N2	2.371(4)	Ag2-O7A	2.379(10)
Ag1-O3	2.230(4)	Ag2-O6A	2.412(10)
Ag2-N3	2.394(4)	Ag2-O6B	2.17(2)
N1-Ag1-N2	72.72(12)	N3-Ag2-O6B	133.9(7)
N1-Ag1-O3	145.70(14)	N3-Ag2-O7A	114.8(3)
N2-Ag1-O3	134.89(16)	N4-Ag2-O6A	146.4(2)
N3-Ag2-N4	72.99(12)	N4-Ag2-O6B	144.3(4)
N3-Ag2-O6A	123.8(4)	N4-Ag2-O7A	153.2(2)

Symmetry codes: (i) $x-1, y, z$; (ii) $-x+1/2, y+1/2, -z+1/2$; (iii) $-x+1/2, y-1/2, -z+1/2$

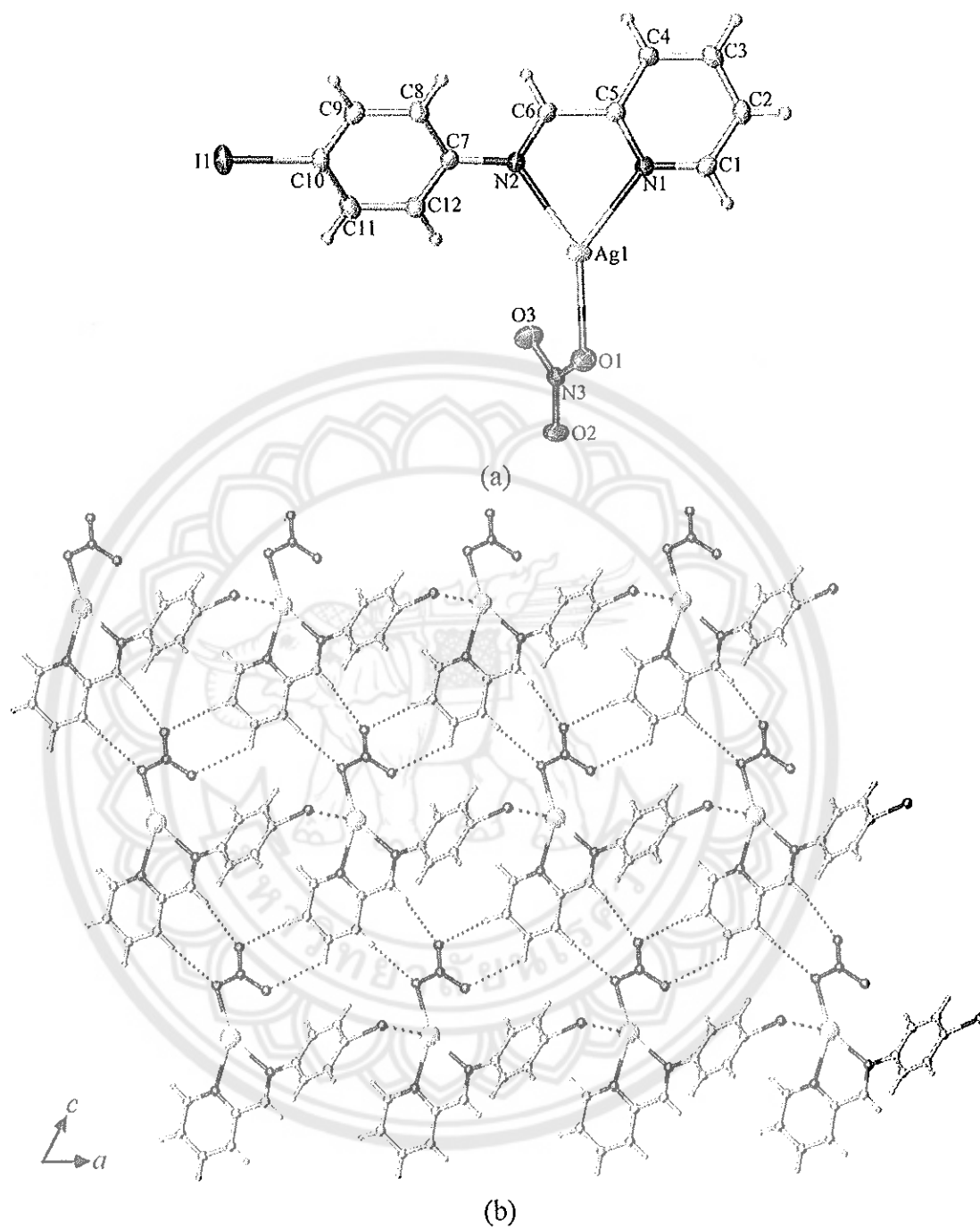


Figure 23 Thermal ellipsoid plot at the 30% probability level containing its asymmetric unit with atom numbering showing environments around the metal center (a) and the two-dimensional sheets in the *ac* plane generated by the Ag...I contacts and C-H...O hydrogen bonds (b) in Ag-1

The adjacent one-dimensional supramolecular chains are connected through weak C–H⋯O hydrogen bonds involving the nitrate and phenyl or imine groups, forming the two-dimensional sheet structure (Figure 22b). The sheets are further linked *via* the symmetry-related π – π stacking between the C=N imine group and the pyridyl ring (centroid to centroid distance = 3.5350(15) Å) and additional weak C–H⋯ π interactions involving the hydrogen phenyl atom (C9) and the pyridyl ring (N1/C1–C5), completing the three-dimensional supramolecular structure. All the hydrogen bonds information in Ag-1 is listed in Table 13.

Table 13 Hydrogen bond geometry (Å, °) for Ag-1

D–H⋯A	D–H	H⋯A	D⋯A	D–H⋯A
C1–H1⋯Cg2 ⁱ	0.93	3.0062(14)	3.639(4)	142
C2–H2⋯O2 ⁱⁱ	0.93	2.40	3.324(4)	170
C3–H3⋯O3 ⁱⁱ	0.93	2.89	3.534(4)	127
C4–H4⋯O1 ⁱⁱⁱ	0.93	2.62	3.543(4)	175
C4–H4⋯O2 ⁱⁱⁱ	0.93	2.76	3.451(4)	132
C6–H6⋯O2 ⁱⁱⁱ	0.93	2.58	3.294(4)	134
C9–H9⋯Cg1 ^{iv}	0.93	2.7934(13)	3.452(3)	135

Cg1 and Cg2 are centroid of the N1/C1–C5 and C7–C12 rings, respectively. Symmetry codes: (i) $x-1, y, z$; (ii) $x-1, y, z+1$; (iii) $x, y, z+1$; (iv) $-x, 1-y, 1-z$

Ag-2: X-ray crystallographic analysis revealed that complex Ag-2 crystallizes in the centrosymmetric space group $P2_1/n$ and the asymmetric unit contains one silver(I) atom, one Schiff base PM-3,5-DMA ligand and one thiocyanate anion. The silver(I) center is four-connected by two nitrogen atoms from the Schiff base ligand and two sulfur atoms from two different thiocyanate anions, adopting a distorted tetrahedral geometry as shown in Figure 23. The Ag–N bond lengths of *viz.* 2.331(2) and 2.397(2) Å are significantly shorter than the Ag–S bond lengths *viz.* 2.5091(11) and 2.5478(11) Å. The bond angles around the silver(I) metal center range from 71.51(8) to 120.020(17)° (Table 12).

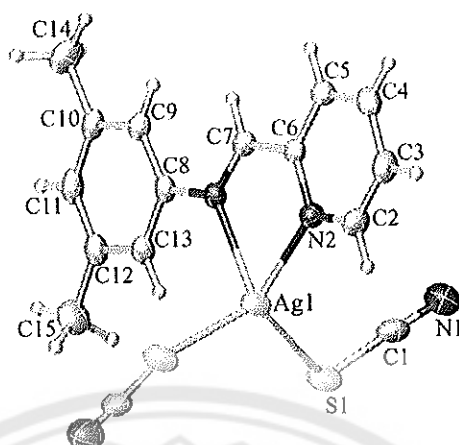


Figure 24 Thermal ellipsoid plot at the 50% probability level containing its asymmetric unit with atom numbering showing environments around the metal center in Ag-2

Due to the extremely soft metal's nature, adjacent silver(I) atoms are linked through the sulfur atom of thiocyanate anions, led to the formation of a one-dimensional chain running parallel to the *b* axis. Alternatively, the structure can be describe as the sulfur atom of thiocyanate anion acts as μ_2 -bridging ligand, linking the adjacent $(\text{Ag}(\text{PM-3,5-DMA}))^+$ cation related by a 2_1 screw axis into a one-dimensional chain with the $\text{Ag}\cdots\text{Ag}$ separation of 4.5964(5) Å.

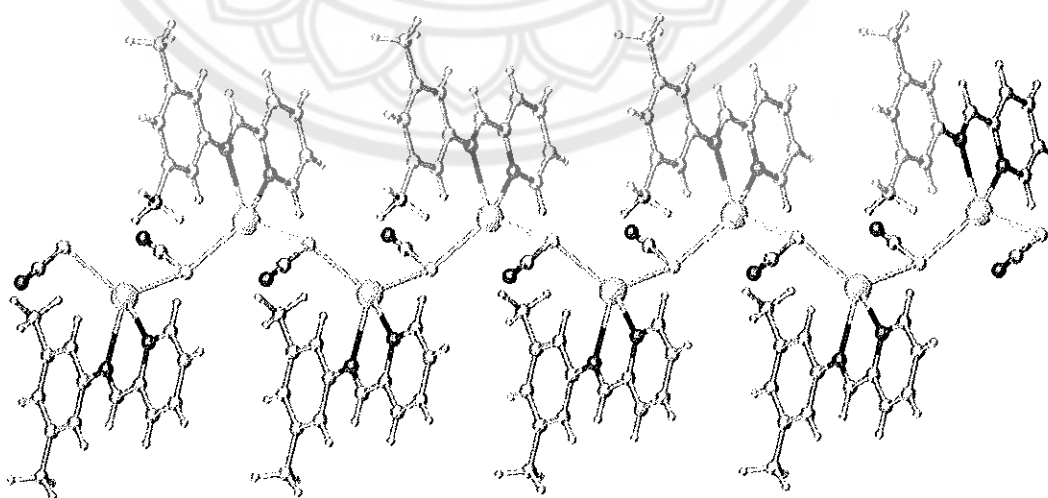


Figure 25 View of the one-dimensional chain in Ag-2

In the crystal of **Ag-2**, the neighboring one-dimensional chains are connected together in the *bc* plane *via* aromatic π - π stacking between the symmetry related pyridyl and phenyl rings or pyridyl rings of the PM-3,5-DMA ligands, generating the two-dimensional sheets as shown in Figure 25. The details of intermolecular π - π stacking interactions in **Ag-2** is provided in Table 14. Moreover, weak C-H \cdots π interaction involving H11 atom and the centroid of the phenyl ring (C8-C15) at 3.0130(13) Å is observed as shown in Figure 26. This type of intermolecular interactions help to stabilize the crystal structure by link the two-dimensional layers to complete the three-dimensional supramolecular structure.

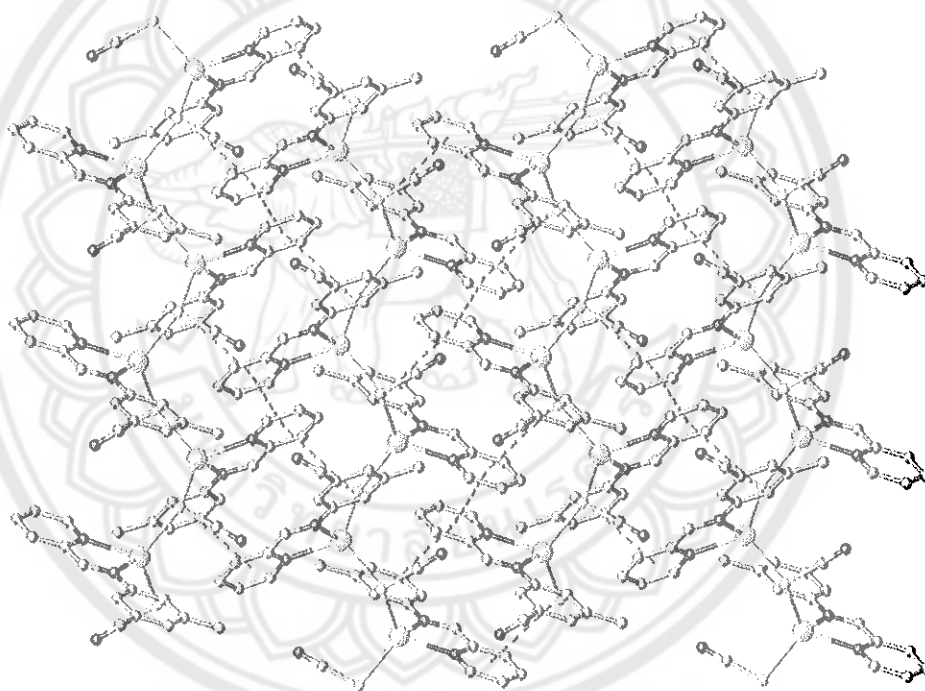
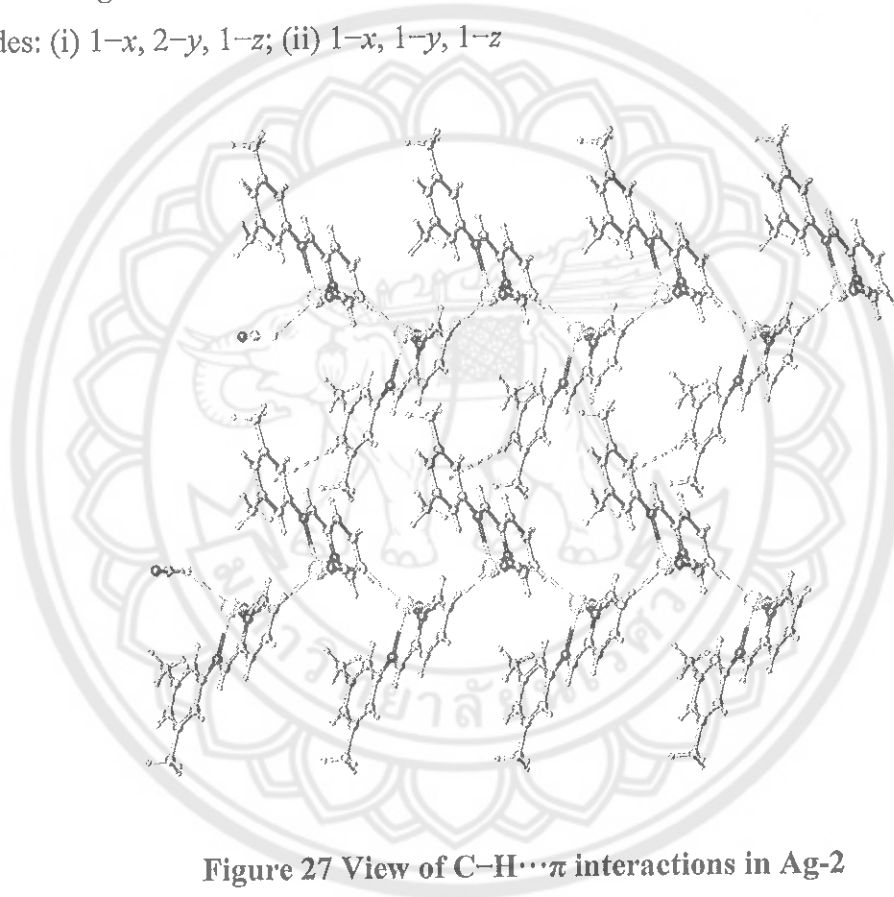


Figure 26 View of the two-dimensional sheet in **Ag-2**, formed by π - π stacking.
Hydrogen atoms are omitted for clarity

Table 14 Intermolecular π - π stacking interactions (\AA , $^\circ$) for Ag-2

π - π	Centroid-to-Centroid Distance	Dihedral Angle
$Cg1 \cdots Cg1^i$	3.786(3)	0.0(5)
$Cg1 \cdots Cg2^{ii}$	3.7127(18)	4.7(3)

$Cg1$ and $Cg2$ are centroid of the N2/C2-C6 and C8-C13 rings, respectively. Symmetry codes: (i) $1-x, 2-y, 1-z$; (ii) $1-x, 1-y, 1-z$

**Figure 27 View of C-H \cdots π interactions in Ag-2**

Ag-3: At room temperature, reaction of bis-bidentate Schiff base PM-BBZ ligand with silver(I) perchlorate using mixed $\text{CH}_3\text{OH}/\text{CH}_2\text{Cl}_2$ solvent yielded new a discrete dinuclear silver(I) complex of **Ag-3**. As shown in Figure 27, the asymmetric unit contains two crystallographic independent silver(I) atoms, two PM-PBBZ Schiff base ligands, and two disordered perchlorate anions. Each Ag(I) centres are four-coordinated with four nitrogen atoms from two different bis-bidentate Schiff base ligands with the Ag-N bond lengths range from 2.304(7) to 2.395(8) \AA (Table 12). Indeed, both Ag(I) ions have weakly bonded by oxygen atom from a perchlorate anion

with the Ag–O bond lengths of 2.731(18) and 2.960(19) Å for Ag1–O5a (Ag1–O5b = 2.915(15) Å) and Ag2–O9a, respectively. Thus, the coordination geometry around the Ag(I) ions in **Ag-3** could be best described as a pseudo trigonal prismatic arrangement, where the N–Ag–N bond angles are in the range 71.3(3) to 170.9(2)° (Table 12). The bond lengths and bond angles around the silver(I) centre in **Ag-3** are typical and comparable to the related silver(I) complexes (Dong, et al., 2006).

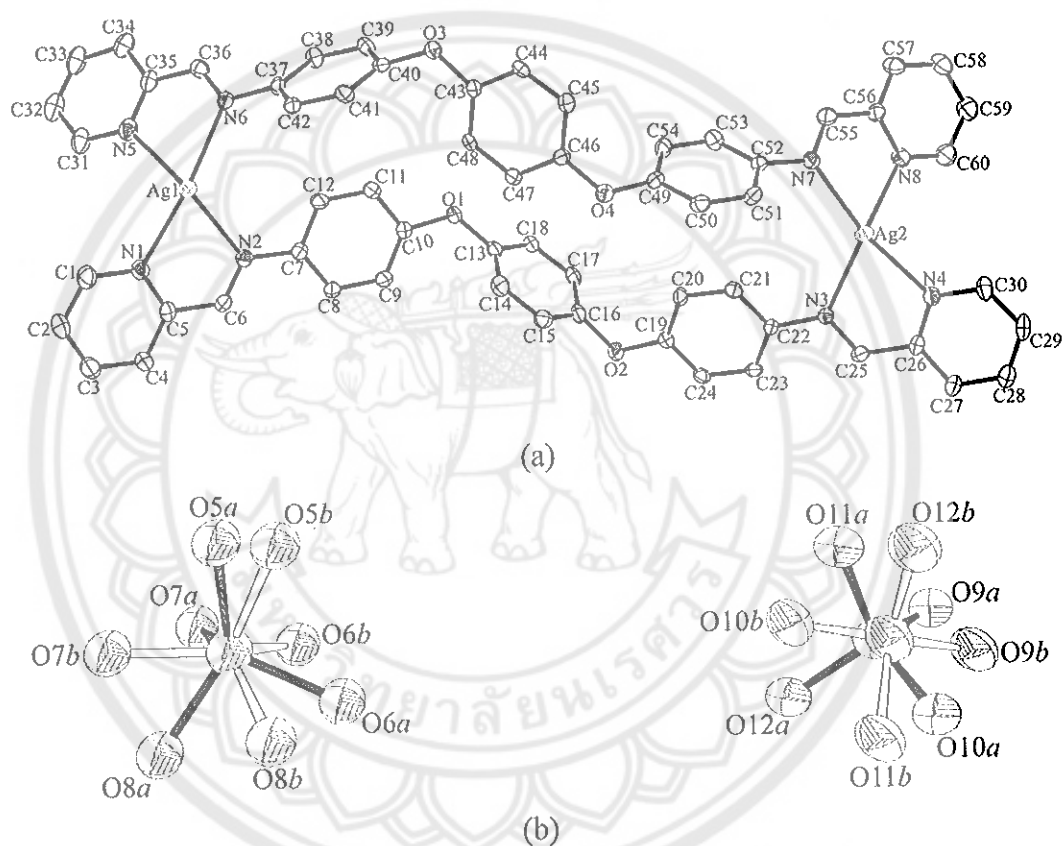


Figure 28 Thermal ellipsoid plot at the 25% probability level containing its asymmetric unit with atom numbering showing environments around the metal centres (a) and partially disordered of perchlorate anions (b) in **Ag-3**

The PM-PBBZ Schiff base acts as a bis-bidentate chelating ligand to Ag(I) ions, forming a zero-dimensional discrete dinuclear $(\text{Ag}_2(\text{PM-PBBZ})_2)^{2+}$ cationic complex with the Ag \cdots Ag separation along the length of the ligands is 16.8598(11) Å. The twist angle between the bis-bidentate ligands is 29.1(3)°. In the crystal, the

discrete cationic complexes are linked through C–H \cdots π interactions and π – π stacking into a one-dimensional chain with no directional intermolecular interactions between them. It should be noted that there also exists intramolecular C–H \cdots π interactions in the discrete cationic complex. In the *bc* plane, the chains are extended *via* symmetry related weak π – π stacking between the (2-pyridylmethalene)amine units of ligands, giving the two-dimensional corrugated sheet as shown in Figure 28.

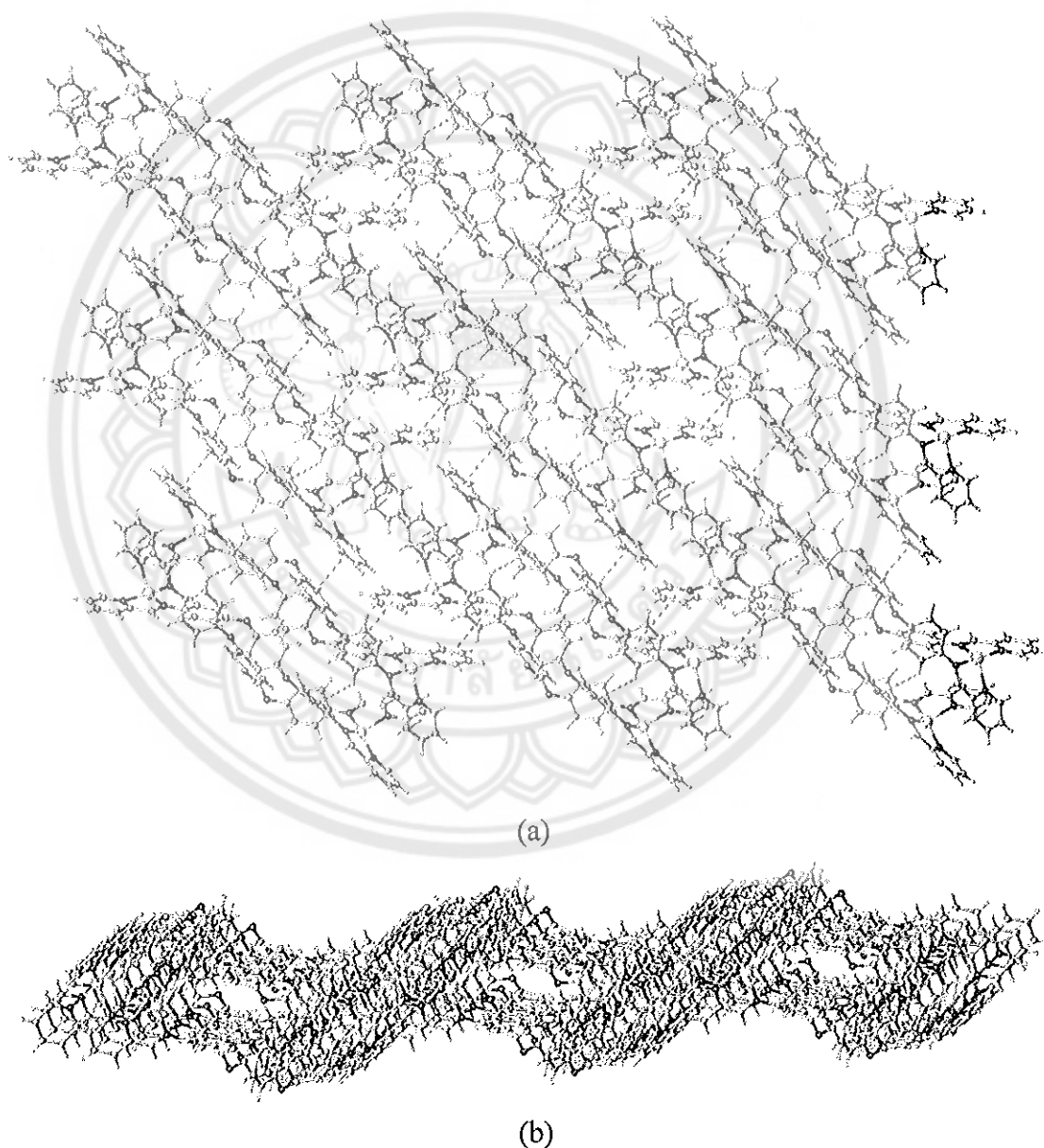


Figure 29 Views of the two-dimensional sheets in Ag-3 in the *bc* plane (a) and along the *b* axis

Indeed as can be seen in Figure 29, the disordered perchlorate anions are connected to the discrete dinuclear cationic complexes as well as stabilize the crystal packing of the three-dimensional supramolecular structure *via* intramolecular C–H $\cdots\pi$ interactions between the central rings of the PM-PBBZ ligand and C–H \cdots O hydrogen bonds involving the ligands and the perchlorate anions. All relevant interactions in **Ag-3** are listed in Tables 15 and 16.

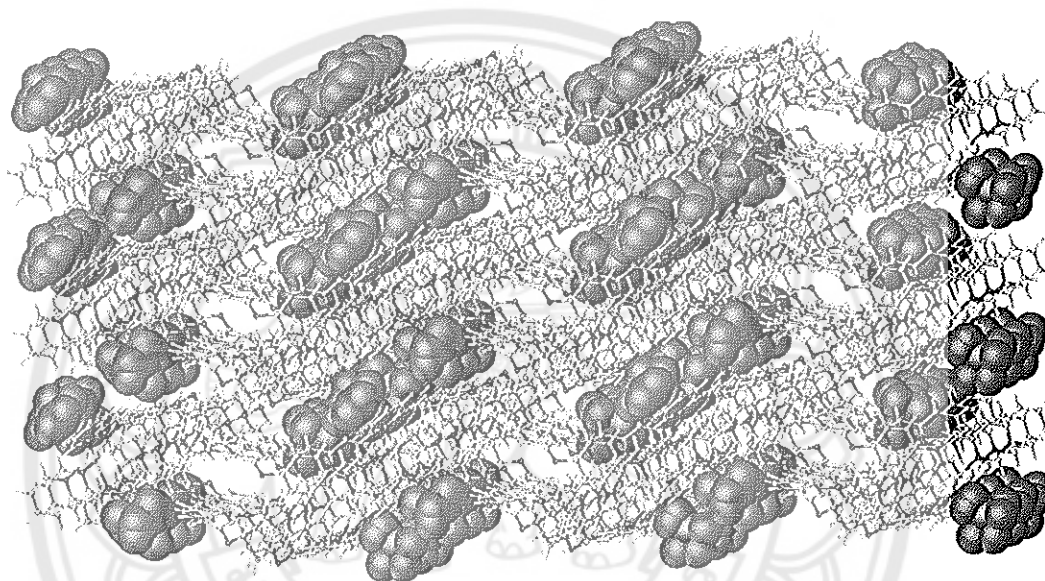


Figure 30 Crystal packing in **Ag-3** view approximately along the *b* axis

Table 15 Hydrogen bond geometry (Å, °) for **Ag-3**

D–H \cdots A	D–H	H \cdots A	D \cdots A	D–H \cdots A
C4–H4 \cdots O5B ⁱ	0.93	2.37	3.133(16)	139
C12–H12 \cdots O6A ⁱ	0.93	2.39	3.187(14)	144
C28–H28 \cdots O6A ⁱⁱ	0.93	2.36	3.187(15)	148
C33–H33 \cdots O7A ⁱⁱⁱ	0.93	2.39	3.196(16)	146
C38–H38 \cdots Cg1 ^{iv}	0.93	2.964(4)	3.646(9)	147
C41–H41 \cdots O8B ^v	0.93	2.33	3.067(15)	136
C42–H42 \cdots O5A	0.93	2.25	3.150(15)	163
C44–H44 \cdots Cg2 ^{vi}	0.93	2.891(3)	3.632(8)	152

Table 15 (cont.)

D-H...A	D-H	H...A	D...A	D-H...A
C58-H58...O7B ^{vii}	0.93	2.32	3.039(17)	133
C60-H60...Cg3 ^{iv}	0.93	3.043(4)	3.794(9)	148

Cg1, Cg2, and Cg3 are centroid of the C19-C24, C13-C18, and N5/C31-36 rings, respectively. Symmetry codes: (i) $-x+1, -y+1, -z$; (ii) $x-1, y+1, z+1$; (iii) $-x+2, -y, -z$; (iv) $1-x, 1-y, 1-z$ (v) $-x+2, -y+1, -z$; (vi) $1+x, y, z$; (vii) $-x+2, -y+1, -z+1$

Table 16 π - π stacking interactions (\AA , $^\circ$) for Ag-3

π - π	Centroid-to-Centroid Distance	Dihedral Angle
Cg1...Cg2 ⁱ	3.790(6)	5.2(3)
Cg3...Cg3 ⁱⁱ	3.610(8)	0.0(13)
Cg4...Cg5 ⁱⁱⁱ	4.226(6)	4.3(3)

Cg1, Cg2, Cg3, Cg4, and Cg5 are centroid of the N4/C26-C30, C43-C48, N5/C31-C35, N1/C1-C5, and C7-C12 rings, respectively. Symmetry codes: (i) $1-x, 2-y, 1-z$; (ii) $2-x, -y, -z$; (iii) $1-x, 1-y, -z$

Ag-4: Using the same crystallization solvents and stoichiometric ratio of the metal and ligand as in **Ag-3**, but the silver(I) perchlorate was replaced by silver(I) nitrate, a discrete dinuclear silver(I) complex of **Ag-4** was isolated with substitutional disorder of the oxygen atoms (from water) bonded to the carbon imine group. As shown in Figure 30, the asymmetric unit of **Ag-4** contains two crystallographic unique of silver(I) atoms, one bis-bidentate PM-PBBZ ligand, two nitrate anions, and two substitutional disorder of the oxygen atoms with occupancy of 0.25 (O9) and 0.275 (O10). It should be noted that one of nitrate anion is disordered over two positions with an occupancy ration of 0.31(2): 0.69(2).

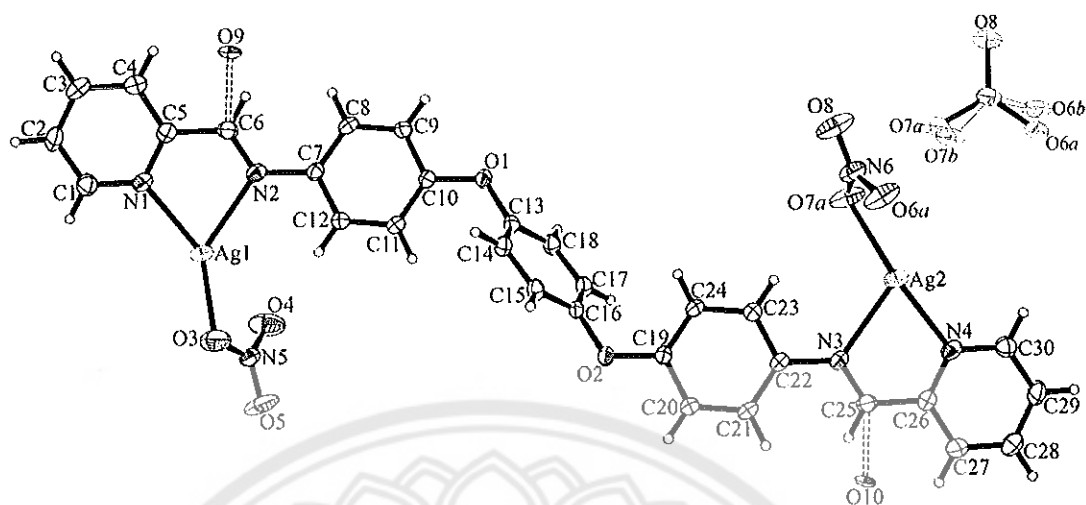


Figure 31 Thermal ellipsoid plot at the 30% probability level containing its asymmetric unit with atom numbering showing environments around the silver(I) centres in Ag-4

Each Ag(I) centres are three-coordinated by two nitrogen atoms from the PM-PBBZ ligand and an oxygen atom from nitrate anion, adopting a distorted trigonal planar with the N–Ag–N and N–Ag–O bond angles range from 72.72(12) to 146.4(2) $^{\circ}$ (Table 12). The Ag–N and Ag–O bond lengths (Table 12) are comparable to the values in Ag-3 and other three-coordinated silver(I) complexes (Yang, et al., 2010). Similar observation was found in Ag-3, the PM-PBBZ acts as bis-bidentate chelating ligand toward the Ag(I) ions with the Ag \cdots Ag separation along the length of the bis-bidentate ligand in Ag-4 of 16.897(4) Å, which comparable to that found in Ag-3.

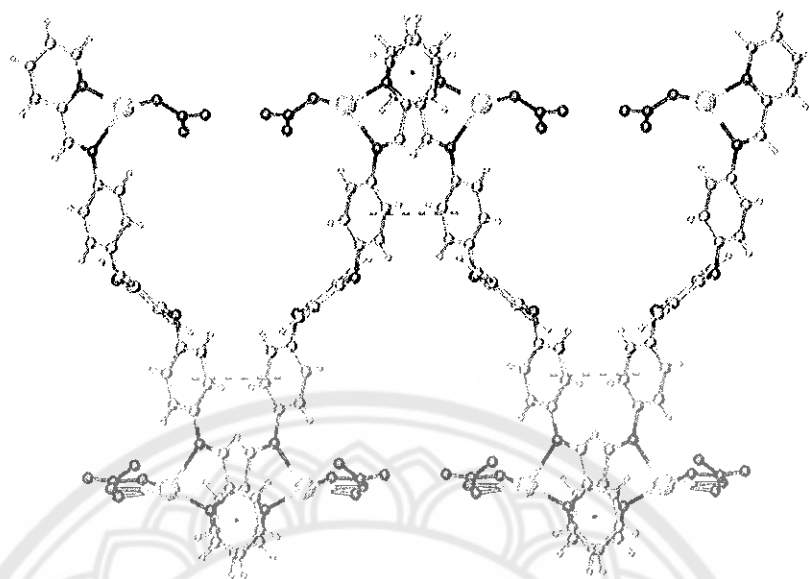


Figure 32 View of the one-dimensional chain generated by π - π stacking interaction in Ag-4

Significantly, the replacement of perchlorate anion by nitrate anion makes difference to the solid state crystal structure of bis-bidentate silver(I) complexes. In the crystal, the dinuclear complexes are linked by symmetry related weak π - π between the aromatic pyridyl rings or the phenyl rings of the PM-PBBZ ligands led to the formation of a one-dimensional zigzag chain along the a axis as shown in Figure 31. Adjacent chains are extended *via* weak C-H \cdots O hydrogen bonds involving the hydrogen atom of the imine group and the nitrate anion, forming the two-dimensional double layers in the bc plane as shown in Figure 32. Finally, the three-dimensional supramolecular architecture in Ag-4 is achieved by extensive intermolecular C-H \cdots O hydrogen bonds (between the carbon atoms of the bis-bidentate ligands and nitrate anions) and C-H \cdots π interactions (involving the bis-bidentate ligands) connect the adjacent double layers. All relevant intermolecular π - π stacking and hydrogen bonding interactions in Ag-4 are listed in Tables 17 and 18, respectively. Noted that no Ag^I \cdots Ag^I interactions were observed in the Schiff base silver(I) complexes.

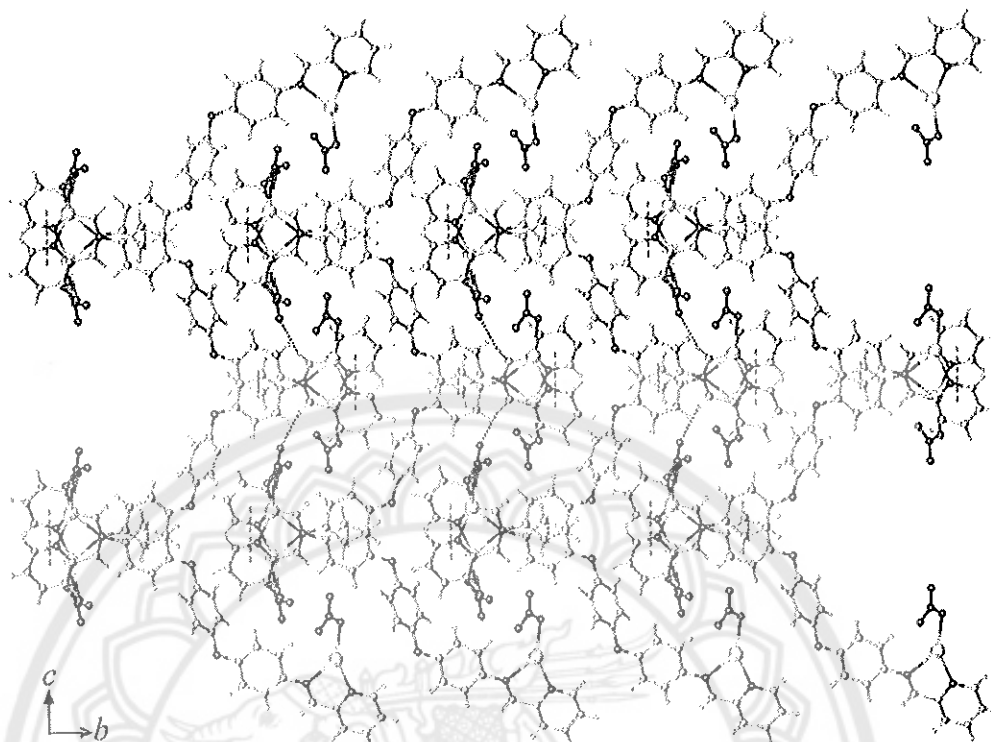


Figure 33 View of the two-dimensional double layers in Ag-4

Table 17 π - π stacking interactions (\AA , $^\circ$) for Ag-4

π - π	Centroid-to-Centroid Distance	Dihedral Angle
$Cg1 \cdots Cg1^i$	4.145(9)	3.3(6)
$Cg2 \cdots Cg2^i$	4.057(8)	5.7(7)
$Cg3 \cdots Cg3^{ii}$	4.138(8)	2.6(7)
$Cg4 \cdots Cg4^{ii}$	4.040(9)	4.5(6)

$Cg1$, $Cg2$, $Cg3$, and $Cg4$ are centroid of the N1/C1-C5, C7-C12, N4/C26-C30, and C19-C24 rings, respectively. Symmetry codes: (i) $2-x, y, 1/2-z$; (ii) $2-x, -y, -z$

Table 18 Hydrogen bond geometry (Å, °) for Ag-4

D-H...A	D-H	H...A	D...A	D-H...A
C2-H2...O6A ⁱ	0.93	2.60	3.370(16)	141
C3-H3...Cg1 ⁱⁱ	0.93	2.955(7)	3.632(8)	145
C6-H6...O8 ^{iviii}	0.93	2.40	3.291(6)	160
C9-H9...O6A ^{iv}	0.93	2.57	3.196(7)	125
C11-H11...O7A ^v	0.93	2.73	3.333(8)	123
C14-H14...O6A ^{vi}	0.93	2.71	3.448(12)	137
C15-H15...O8 ^{vi}	0.93	2.78	3.372(6)	123
C17-H17...O4 ^{vii}	0.93	2.71	3.411(6)	133
C20-H20...O4 ^{viii}	0.93	2.65	3.312(6)	129
C21-H21...O5 ^{ix}	0.93	2.55	3.457(6)	166
C21-H21...O10	0.93	2.77	3.443(12)	130
C23-H23...O7B	0.93	2.51	3.43(2)	175
C24-H24...O3 ^x	0.93	2.73	3.397(6)	129
C25-H25...O5 ^{xi}	0.93	2.41	3.302(6)	162
C28-H28...Cg1 ^{xii}	0.93	2.967(8)	3.617(8)	151
C29-H29...O4 ^{xiii}	0.93	2.57	3.309(7)	137

Cg1 is centroid of the C13-C18 ring. Symmetry codes: (i) $x-1/2, -y+1, z-1/2$; (ii) $3/2-x, 1+y, 1-z$; (iii) $-x+3/2, y+1, -z+1/2$; (iv) $x-1/2, -y, z-1/2$; (v) $x, y+1, z$; (vi) $-x+2, -y, -z+1$; (vii) $-x+1, -y+1, -z+1$; (viii) $x+1/2, -y+1, z+1/2$; (x) $x, y-1, z$; (xi) $-x+3/2, y-1, -z+3/2$; (xii) $3/2-x, -1+y, 3/2-z$; (xiii) $x+1/2, -y, z+1/2$

Thermal analyses

To examine the thermal stabilities of the complexes in the present study, thermogravimetric analyses (TGA) were carried out from room temperature to 800 °C at a heating rate of 10 °C min⁻¹ under a nitrogen atmosphere. The TGA profiles for the tetranuclear complex **Cu-2**, the dinuclear complex **Cu-3**, and the polymeric complex **Cu-7** as a representative example are shown in Figure 33a. As expected, the polymeric complex has highest thermal stability among them. For **Cu-2**, there are three stages of

weight losses and the structure decomposed at 150 °C. While, **Cu-3** and **Cu-7** exhibit quite similar the TGA profiles with two stages of weight losses and the removal of the organic (Schiff base ligands and thiocyanate anions) occurs at 175 °C for **Cu-3** and at 190 °C for **Cu-7**. However, it is difficult to determine these weight losses accurately. The TGA curves for complexes **Ag-1**, **Ag-2**, and **Ag-3** are shown in Figure 33b, and are stable up to 190, 140, and 280 °C, respectively. After these temperatures, the complexes begin to decompose upon further heating.

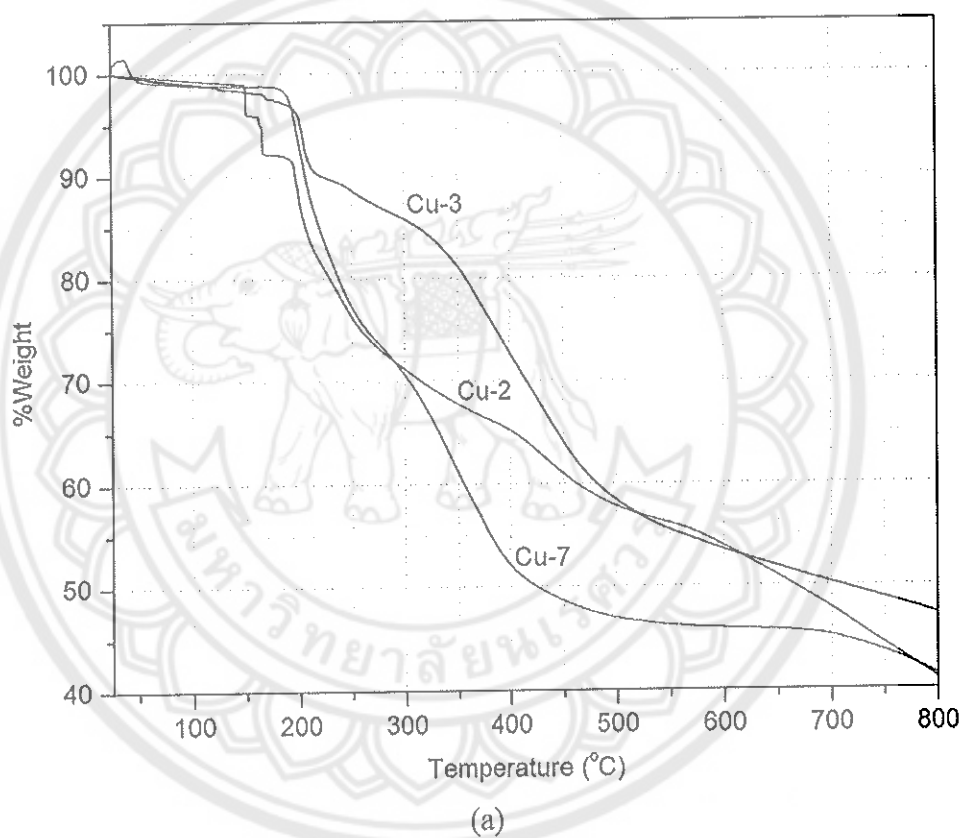
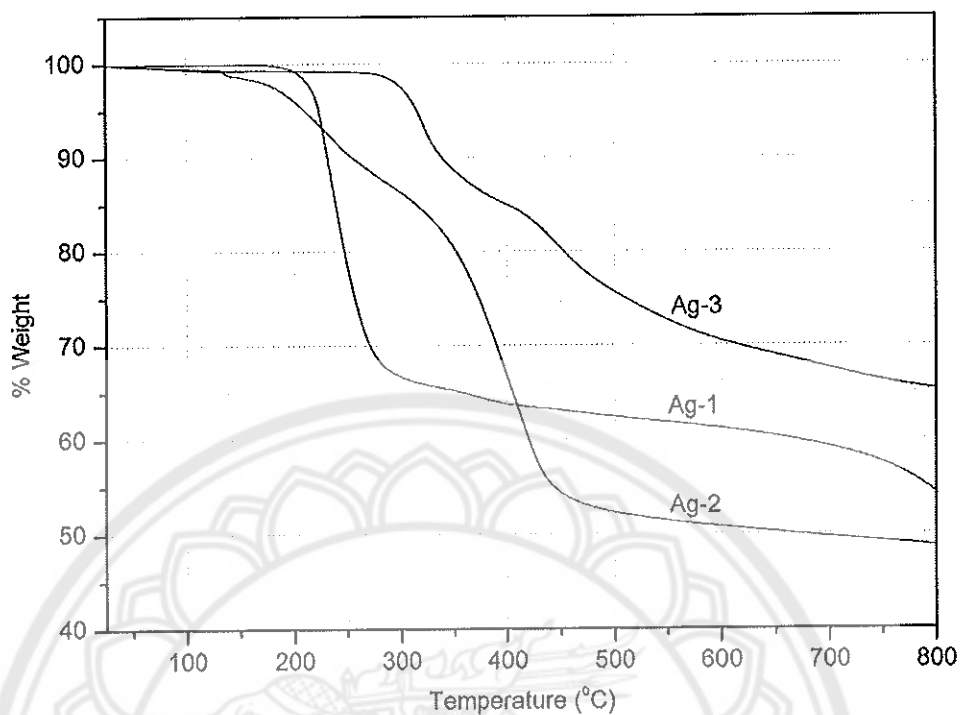


Figure 34 TGA profiles of representative examples of Cu(I) (a) and Ag(I) (b)



(b)

Figure 34 (cont.)

Photoluminescent properties

The luminescent properties of d^{10} metal ions containing Schiff base ligands system have been investigated widely and can possibly be applied as chemical probes and photoactive materials. In the present study, the photoluminescent properties of some copper(I) and silver(I) complexes have been explored in the solid state at room temperature and are shown in Figures 34 and 35, respectively. Also, their photoluminescent characteristics are summarized in Table 19.

Table 19 Solid state photoluminescent data at room temperature for some copper(I) and silver(I) complexes

Complex	$\lambda_{\text{excitation}}(\text{nm})$	$\lambda_{\text{emission}}(\text{nm})$
Cu-1	340	455
Cu-2	340	453
Cu-3	340	419
Cu-4	340	452
Cu-6	320	425
Cu-7	320	422
Ag-1	360	473
Ag-2	360	471
Ag-4	360	470

Because the emission profiles of the copper(I) and silver(I) complexes are similar to that of the free ligand (Theppitak, 2015), the luminescence behavior of these complexes may be attributed mainly to ligand-to-ligand charge transfer (LLCT), which is mixed with metal-to-ligand charge transfer (MLCT) and metal-to-ligand charge transfer (MCLT). The complexes, however, exhibit slightly different their emission bands, presumably due to a result of intermolecular interactions among them.

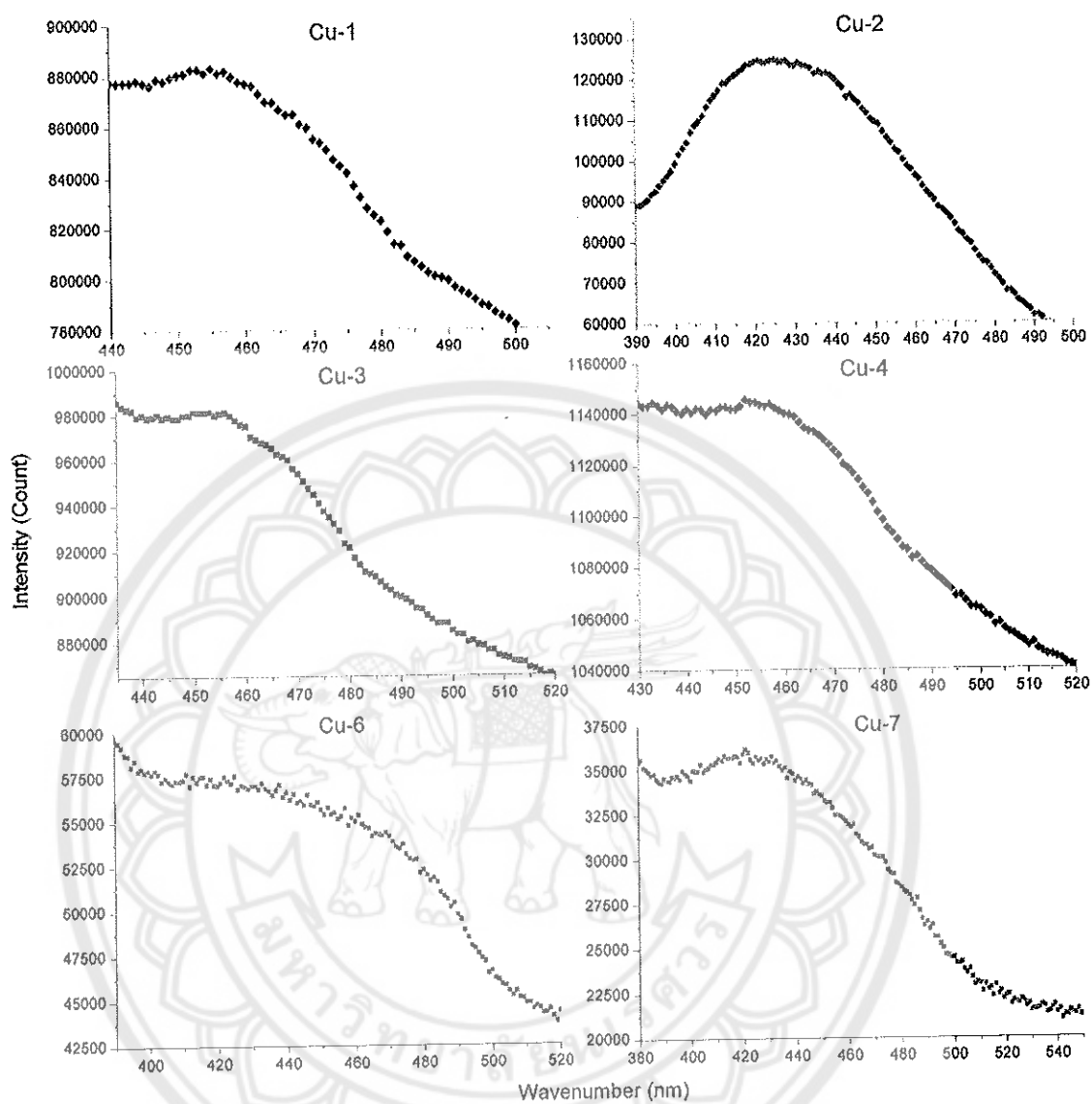


Figure 35 The solid-state photoluminescent emission spectra of the copper(I) complexes at room temperature

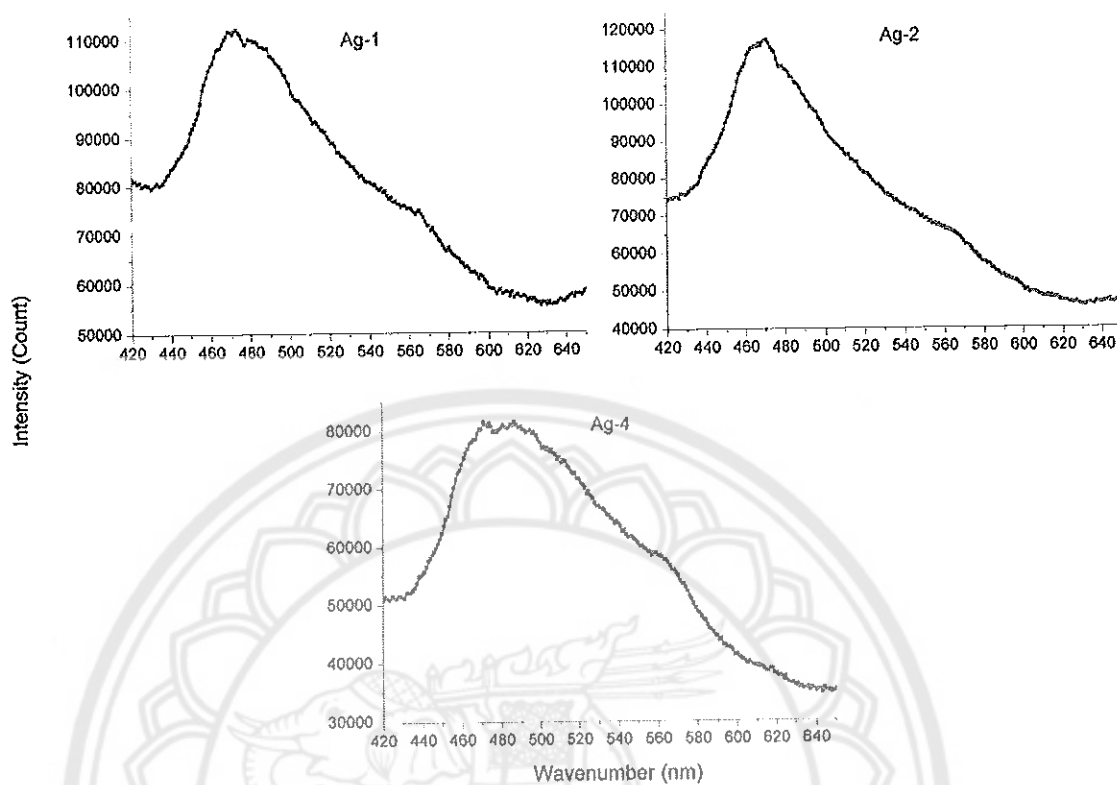


Figure 36 The solid-state photoluminescent emission spectra of the silver(I) complexes at room temperature

CHAPTER V

CONCLUSIONS

Eleven new copper(I) and silver(I) metal complexes containing bidentate and bis-bidentate *N*-donor Schiff base ligands have been synthesized by conventional methods at room temperature and characterized by various analytical methods. The complexes are structurally diverse, including four main structural motifs *viz.* zero-dimensional dinuclear, zero-dimensional dinuclear metallocycles, zero-dimensional tetranuclear metallocycles, and one-dimensional chains. In crystal of the complexes, the different substituents groups as well as the conformation of Schiff base ligands have influence on several types of intermolecular interactions involving hydrogen bonds, halogen bonds, metal- π , and π - π interactions. These interactions are responsible for the formation of various structural topologies as well as supramolecular architectures. This study clearly demonstrates that hard-soft acid-base metals, ligand conformations, the solvent system, and synthetic conditions found to be of much importance in directing the synthetic pathway in the systems.

Reactions of copper(II) ions with newly synthesized Schiff base ligands in the presence of thiocyanate as co-ligand led to the formation of seven copper(I) complexes with variety of structures ranging from the discrete zero-dimensional complexes *viz.* tetranuclear metallocycle {[Cu(PM-4-FA)(NCS)] (Cu-1) and [Cu(PM-4-CIA)(NCS)] (Cu-2)}, dinuclear metallocycle {[Cu(PM-4-BrA)(NCS)] (Cu-3) and [Cu(PM-4-IA)(NCS)] (Cu-4)} and the one-dimensional chain *viz.* {[Cu(PM-3-BrA)(NCS)] (Cu-5), [Cu(PM-2,3-DMA)(NCS)] (Cu-6) and [Cu(PM-3,5-DMA)(NCS)] (Cu-7)}. All copper complexes, the spontaneous reduction of Cu^{II} to Cu^I were observed and found to crystallize in the centrosymmetric system in which the Cu^I center displays a distorted tetrahedral geometry. On the other hand, reactions of the Schiff base ligands with Ag^I ions yielded new silver(I) complexes: discrete zero-dimensional structure {[Ag(PM-IA)(NO₃)] (Ag-1), [Ag₂(PM-PBBZ)₂][ClO₄]₂ (Ag-3) and [Ag₂(PM-PBBZ)(NO₃)₂] (Ag-4)} and one-dimensional chain structure [Ag(PM-3,5-DMA)(SCN)] (Ag-2). The coordination geometry of the metal center in the silver(I) complexes are somewhat

flexible which can adopt a distorted trigonal (**Ag-1** and **Ag-4**), tetrahedral (**Ag-2**) and trigonal pyramidal (**Ag-3**). Photoluminescent studies indicate that the complexes exhibit fluorescence emission in the solid state at room temperature and show thermal stabilities above 150 °C.





REFERENCES

REFERENCES

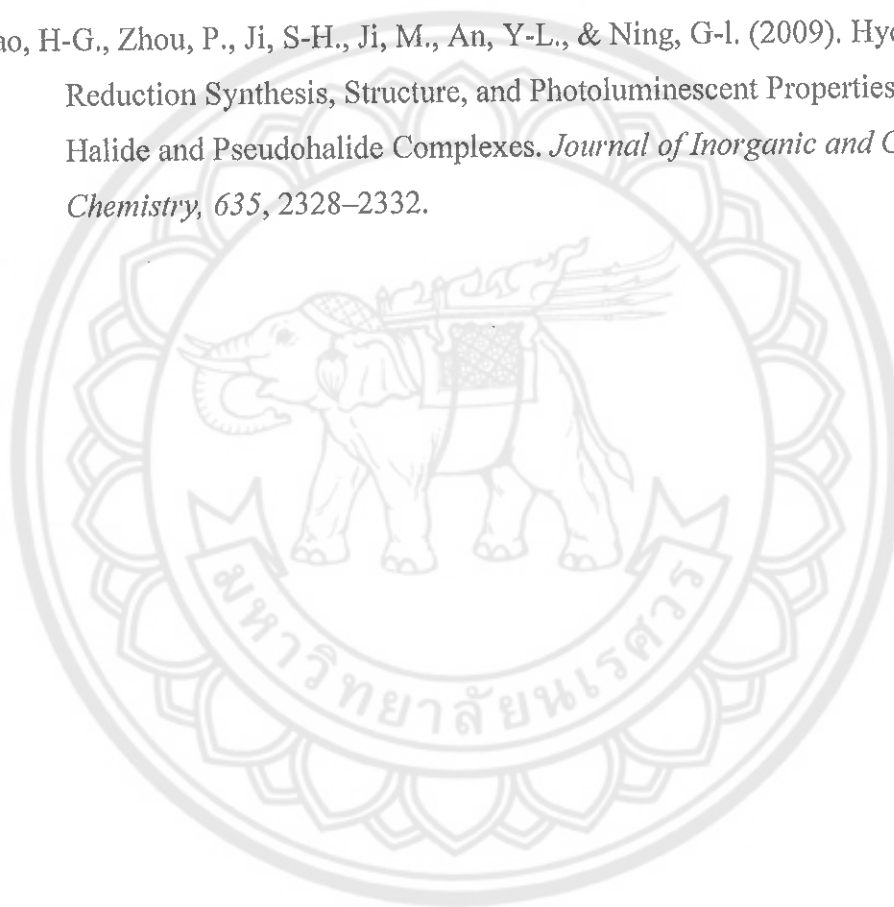
- Barakat, A.R., Schunk, R.W., & Demars, H.G. (2003). Seasonal and solar activity dependence of the generalized polar wind with low altitude auroral ion energization. *Journal of Geophysical Research*, *108*, 148-227.
- Barbieri, A., Accorsi, G., & Armaroli, N. (2008). Luminescent complexes beyond the platinum group: The d¹⁰ avenue. *Chemical Communications*, *2008*, 2185-2193.
- Bruker. (2014). *Apex2, Sadabs and Saint*. USA: Bruker AXS, Madison, Wisconsin.
- Chi, Z., Zhang, X., Yang, Z., Chen, M., Xu, B., Wang, C., ... Xu, J. (2010). A multi-sensing fluorescent compound derived from cyanoacrylic acid. *Journal of Materials Chemistry*, *20*, 292-298.
- Colacio, E., Kivekas, R., Lloret, F., Sunberg, M., Varela, J.S., Bardaji, M., & Laguna A. (2002). Architecture Dependence on the Steric Constrains of the Ligand in Cyano-Bridged Copper(I) and Copper(II)-Copper(I) Mixed-Valence Polymer Compounds Containing Diamines: Crystal Structures and Spectroscopic and Magnetic Properties. *Inorg. Chem*, *41*, 5141-5149.
- Cuttell, D. G., Kuang, S-M., Fanwick, P. E., McMillin, D. R., & Walton, R. A. (2002). Simple Cu(I) Complexes with Unprecedented Excited-State Lifetimes. *Journal of American Chemical Society*, *124*(1), 6-7.
- Czerwieniec, R., Hofbeck, T., Crespo, O., Laguna, A., Gimeno, M. C., & Yersin, H. (2010). The Lowest Excited State of Brightly Emitting Gold(I) Triphosphine Complexes. *Inorganic Chemistry*, *49*(8), 3764-3767.
- Dolomanov, O. V., Bourhis, L. J., Gildea, R. J., Howard, J. A. K., & Puschmann, H. (2009). *OLEX2*: A complete structure solution, refinement and analysis program. *Journal of Applied Crystallography*, *42*, 339-341.
- Dong, Y-B., Zhao, X., & Huang, R-Q. (2004). New Ag(I)-Containing Coordination Polymers Generated from Multidentate Schiff-Base Ligands. *Inorganic Chemistry*, *43*, 5603-5612.
- Fahlman, B.D. (2011). *Materials chemistry* (2nd ed.). Netherlands: Springer.

- Graham, A. Bowmaker, John, V. Hanna, Scott, P. King, Fabio Marchetti, Claudio Pettinari, Adriano Pizzabiocca, ... Allan, H. White. (2014). Complexes of Copper(I) Thiocyanate with Monodentate Phosphine and Pyridine Ligands and the *P,N*-Donor Diphenyl(2-pyridyl)phosphine. *European Journal of Inorganic Chemistry*, 2014, 6104-6116.
- He, G., Rothe, C., Murano, S., Werner, A., Zeika, O., & Birstock, J. (2009). White-stacked OLED with 38 lm/W and 100,000-hour lifetime at 1000 cd/m² for display and lighting applications. *Journal of the Society for Information Display*, 17(2), 159-165.
- Hsu, PP., Kang, SA., Rameseder, J., Zhang, Y., Ottina, KA., Lim, D., ... Sabatini, DM. (2011). The mTOR-regulated phosphoproteome reveals a mechanism of mTORC1-mediated inhibition of growth factor signaling. *American Association for the Advancement of Science*, 332, 1317-1322.
- Khalaji, A.D., Weil, M., Hadadzadeh, H., & Daryanavard, M., (2009). Two different 1D-chains in the structures of the copper(I) coordination polymers based on bidentate Schiff-base building units and thiocyanate anions as bridging ligands. *Inorganica Chimica Acta*, 362, 4837-4842.
- Lee, Y, J., & Lee, S, W. (2013). Ligands containing pyridyl-carboxylate terminals and their discrete silver and polymeric cadmium compounds: (n-py)-CH=; N-C₁₀H₆-COOH (n = 2 (HL¹), 3 (HL²)), (Ag(HL¹)₂)(PF₆), (Ag(HL¹)₂) (NO₃) (H₂O), and (Cd(L²)₂)_∞. *Polyhedron*, 53, 10 103-112.
- Leo, K., Meerheim, R., & Nitsche, R. (2008). High-efficiency monochrome organic light emitting diodes employing enhanced microcavities. *Applied Physics Letters*, 93, 04331.
- Li, M-X., Wang, H, Liang, S-W., Shao, M., He, X., Wang, Z-X., & Zhu, S-R. (2009). Solvothermal Synthesis and Diverse Coordinate Structures of a Series of Luminescent Copper(I) Thiocyanate Coordination Polymers Based on N-Heterocyclic Ligands. *Crystal Growth and Design*, 9(11), 4626-4633.
- Lowry, M, S., & Bernhard, S. (2006). Synthetically Tailored Excited States: Phosphorescent, Cyclometalated Iridium (III) Complexes and Their Applications. *Chemistry - A European Journal*, 12(31), 7970-7977.

- McMillin, D. R., & Cunningham, K. L. (1998). Reductive quenching of photoexcited Cu(dipp)(2)(+) and Cu(tptap)(2)(+) by ferrocenes (dipp = 2,9-diisopropyl-1,10-phenanthroline and tptap = 2,3,6,7-tetraphenyl-1,4,5,8-tetraazaphenanthrene). *Inorganic Chemistry*, 37, 4114-4119.
- McMillin, D. R., Kirchoff, J. R., Robinson, W. R., Powell, D. R., McKenzie, A. T., & Chen, S. (1985). Steric effects and the behaviour of Cu(NN)(PPh₃)²⁺ systems in fluid solution – crystal and molecular-structures of (Cu(dmp)(PPh₃)₂)NO₃ and (Cu(phen)(pPh₃)₂)NO₃.11/2EtOH. *Journal of the American Chemical Society*, 107(23), 3928-3933.
- Miller, A. J. M., Labinger, J. A., & Bercaw J. E. (2011). Trialkylborane-Assisted CO₂ Reduction by Late Transition Metal Hydrides. *Journal of Organometallics Chemistry*, 30, 4308-4314.
- Ming-Xing Li, Hui Wang, Sheng-Wen Liang, Min Shao, Xiang He, Zhao-Xi ang, & Shou-Rong Zhu. (2009). Solvothermal Synthesis and Diverse Coordinate Structures of a Series of Luminescent Copper(I) Thiocyanate Coordination Polymers Based on N-Heterocyclic Ligands. *Crystal Growth & Design*, 9, 4626-4633.
- Mitschke, U., & Bäuerle, P. (2000). The electroluminescence of organic materials. *Journal of Materials Chemistry*, 10, 1471-1507.
- Mohamed, A.S. Goher, Qing-Chuan Yang, & Thonas, C.W. Mak. (2000). Synthesis, structural and spectroscopic study of polymeric copper(I) thiocyanate complexes (Cu(NCS))_n (L=methyl nicotinate and ethyl nicotinate) and (HL)(Cu(NCS)₂) (HL=H-ethyl isonicotinate). *Polyhedron*, 19, 615-621.
- Mukherjee, A., Chakrabarty, R., Ng, S. W., & Patra, G. K. (2010). The syntheses, characterizations, X-ray crystal structures and properties of Cu(I) complexes of a bis-bidentate schiff base ligand. *Inorganica Chimica Acta*, 363, 1707-712.
- Pettinari, C., Di Nicola, C., Marchetti, F., Pettinari, R., Skelton, B.W., Somers, N., ... Nervi, C. (2008). Synthesis, Characterization, Spectroscopic and Photophysical and Photophysical Properties of New [Cu(NCS){(L-N)₂ or (L'-N N)}(PPh₃)] Complexes (L-N, L'-N N= Aromatic Nitrogen Base). *European Journal of Inorganic Chemistry*, 12, 1974-1984.

- Phillips, DL., Che, CM., Leung, KH., Mao, Z., & Tse, MC. (2005). A comparative study on metal-metal interaction in binuclear two- and three-coordinated d^{10} -metal complexes Spectroscopic investigation of M(I)-M(I) interaction in the $^1[d\sigma^*p\sigma]$ excited state of $[M_2(dcpm)_2]^{2+}$ (dcpm=bis(dicyclohexylphosphino)methane) (M=Au, Ag, Cu) and $[M_2(dmpm)_3]^{2+}$ (dmpm = bis-(dimethylphosphino)methane) (M = Au, Ag, Cu) complexes. *Coord Chem Rev*, 249, 1476-1490.
- Rader, R, A., McMillin, D, R., Buckner, M, T., Matthews, T, G., Casadonte, D, J., Lengel, R, K., ... Lytle, F, E. (1981). Photostudies of 2,2'-bipyridine bis(triphenylphosphine)copper(1+), 1,10-phenanthroline bis(triphenylphosphine)copper(1+), and 2,9-dimethyl-1,10-phenanthroline bis(triphenylphosphine)copper(1+) in solution and in rigid, low-temperature glasses. Simultaneous multiple emissions from intraligand and charge-transfer states. *Journal of American Chemical Society*, 103(19), 5906-5912.
- Radoslaw Starosta, Urszula K Komarnicka, Marcin Sobczyk, & Maciej Barys. (2012). Laser induced multi-component luminescence of (CuNCS(1,10-phen)-(CH₂N(CH₂CH₂O)₃) the first example of CuNCS complexes with diimines and tris(aminomethyl) phosphanes. *Journal of Luminescence*, 132, 1842-1847.
- Sauer, M., Hofkens, J., & Enderlein, J. (2011). *Handbook of fluorescence spectroscopy and imaging*. KGaA, Weinheim: Wiley-vch Verlag GmbH and Co.
- Sheldrick, G. M. (2015). *Shelxt* - Integrated space-group and crystal-structure determination. *Acta Crystallographica Section A: Foundations*, A71, 3-8.
- Susanne Wöhlert, Lothar Fink, Martin U. Schmidt, & Christian Näther. (2013). Synthesis and Characterization of New 2D Coordination Polymers based on Mn(NCS)₂ and Ni(NCS)₂ with 1,2-Bis(4-pyridyl)-ethane as Co-Ligand. *Z. Anorg. Allg. Chem*, 639(12-13), 2186-2194.
- Tsuzuki, T., & Tokito, S. (2007). Highly Efficient and Low-Voltage Phosphorescent Organic Light-Emitting Diodes Using an Iridium Complex as the Host Material. *Advanced Materials*, 19(2), 276-280.

- Venkataraman, D., Du, Y., Wilson, S. R., Hirsch, K. A., Zhang, P., & Moore, J. S. (1997). A Coordination Geometry Table of the d-Block Elements and Their Ions. *Journal of Chemical Education*, 74, 915.
- Yang, X., Wang, Z., Madakuni, S., Li, J., & Jabbour, G. E. (2008). Efficient Blue- and White-Emitting Electrophosphorescent Devices Based on Platinum(II) (1,3-Difluoro-4,6-di(2-pyridinyl)benzene) Chloride. *Advanced Materials*, 20(12), 2405–2409.
- Yao, H-G., Zhou, P., Ji, S-H., Ji, M., An, Y-L., & Ning, G-l. (2009). Hydrothermal Reduction Synthesis, Structure, and Photoluminescent Properties of Copper(I) Halide and Pseudohalide Complexes. *Journal of Inorganic and General Chemistry*, 635, 2328–2332.





APPENDIX

APPENDIX A FOURIER TRANSFORM INFRARED SPECTROSCOPY

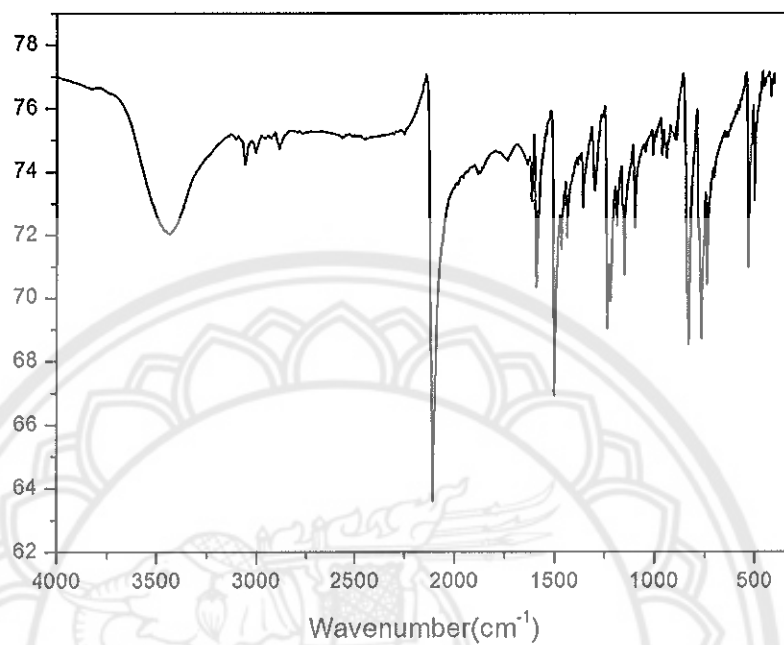


Figure 37 FTIR Spectrum of Compound Cu-1

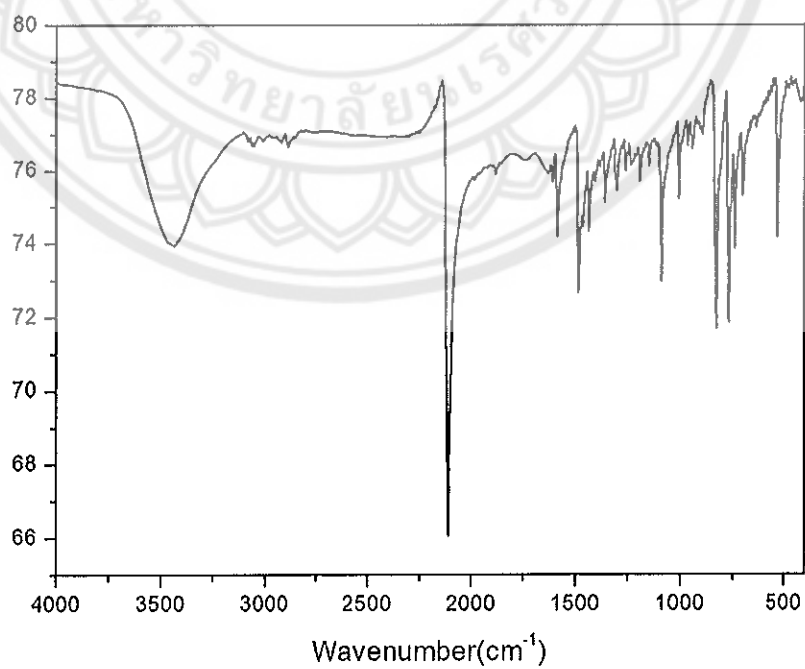


Figure 38 FTIR Spectrum of Compound Cu-2

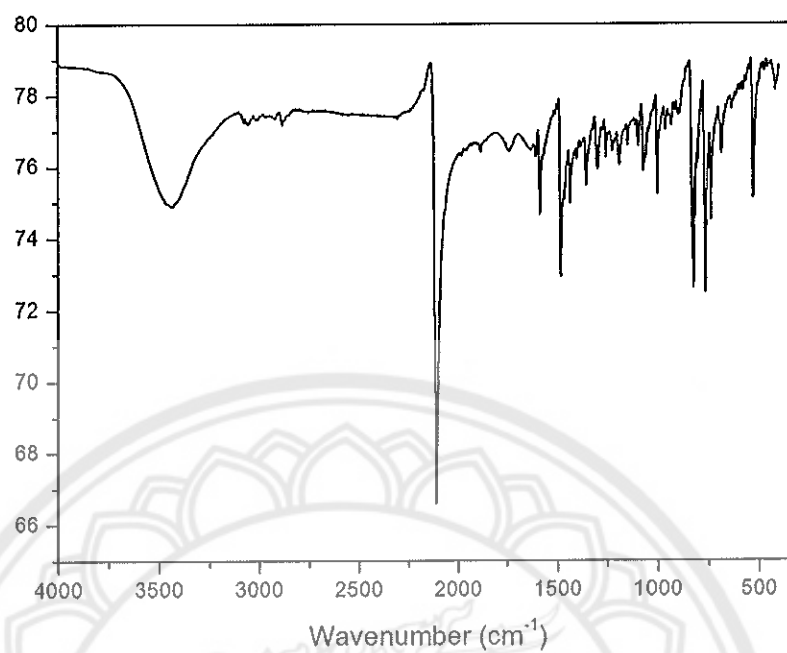


Figure 39 FTIR Spectrum of Compound Cu-3

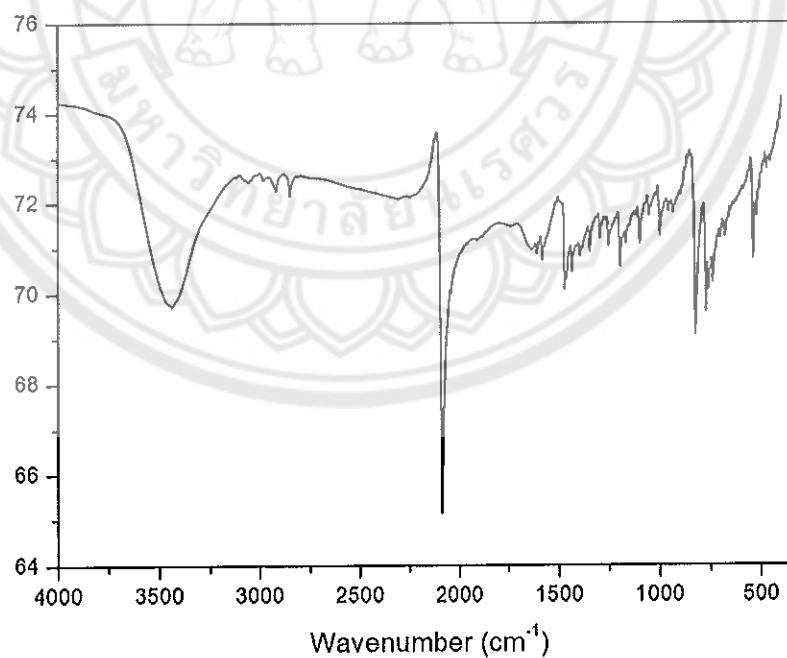


Figure 40 FTIR Spectrum of Compound Cu-4

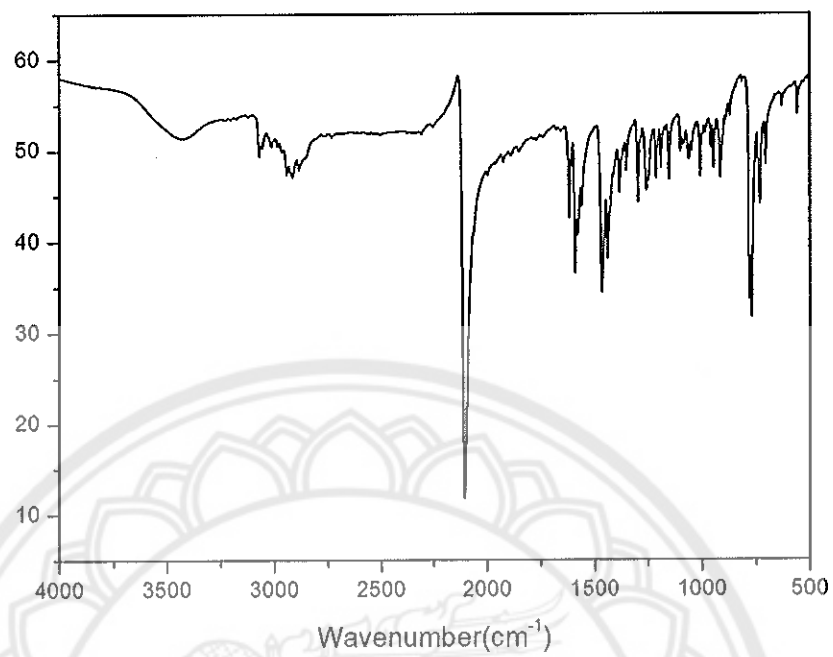


Figure 41 FTIR Spectrum of Compound Cu-5

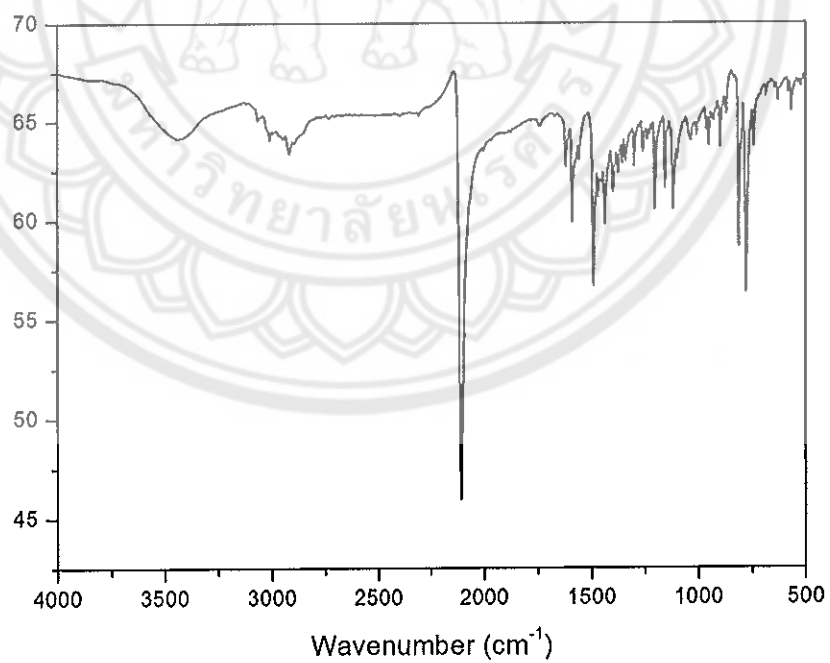


Figure 42 FTIR Spectrum of Compound Cu-6

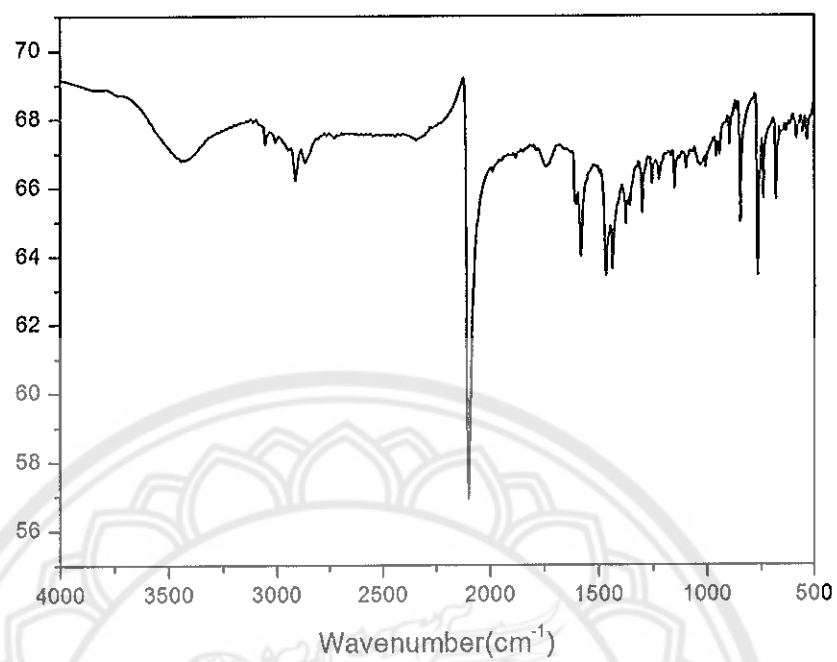


Figure 43 FTIR Spectrum of Compound Cu-7

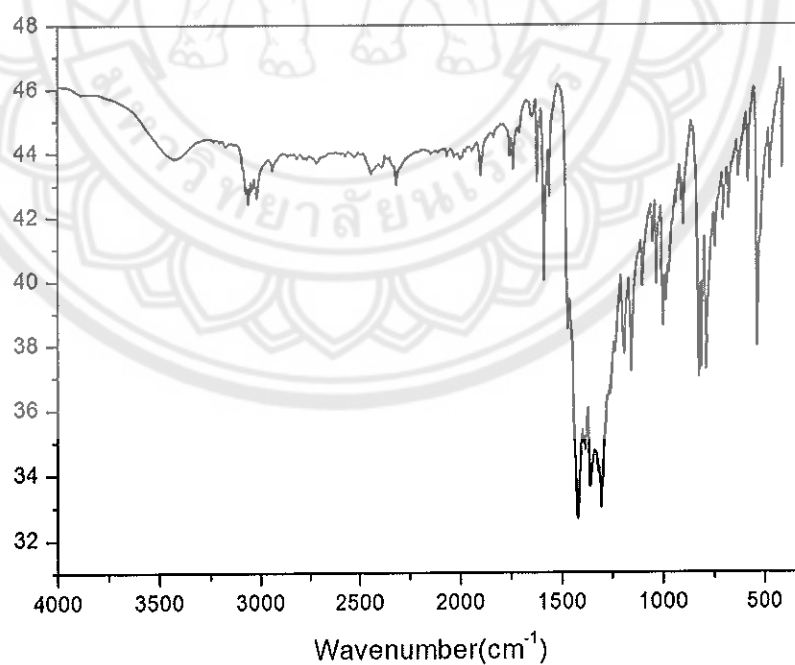


Figure 44 FTIR Spectrum of Compound Ag-1

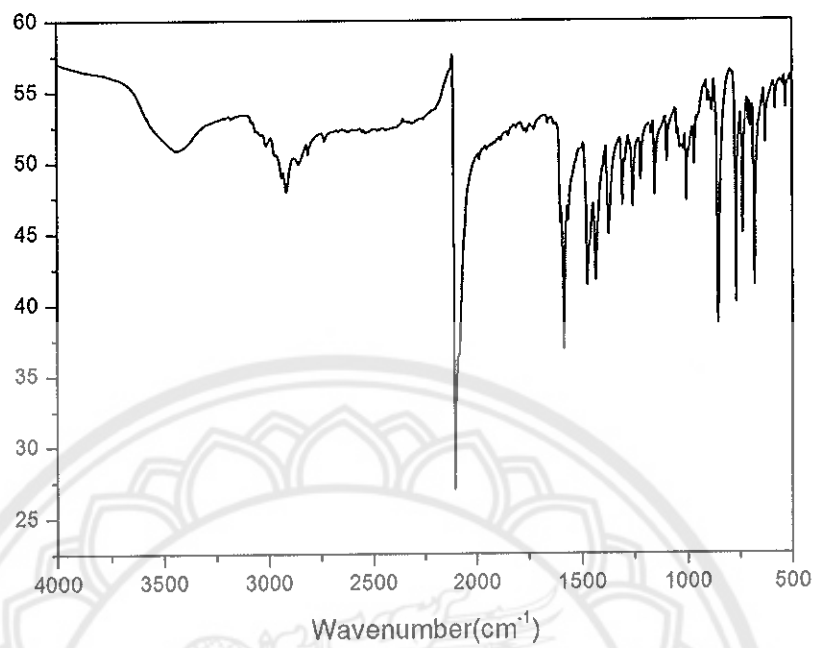


Figure 45 FTIR Spectrum of Compound Ag-2

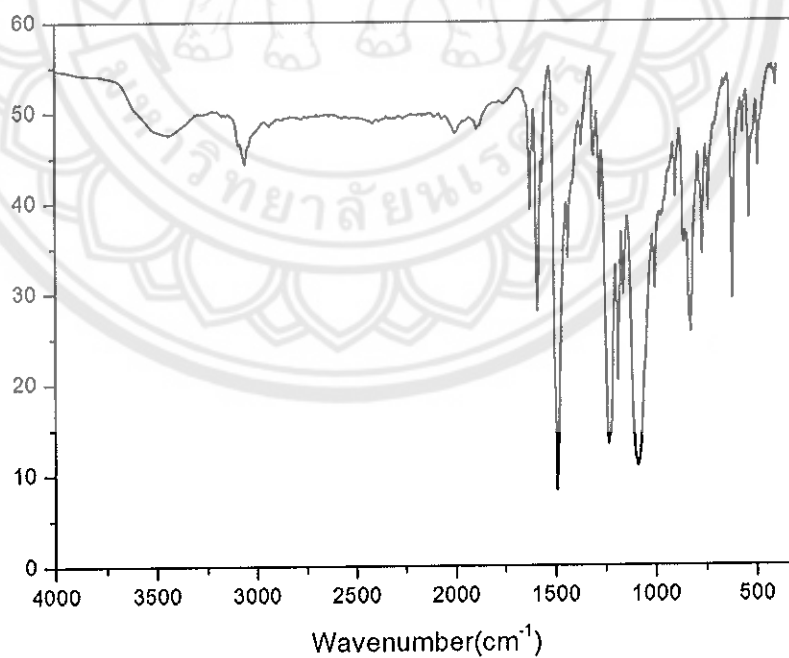


Figure 46 FTIR Spectrum of Compound Ag-3

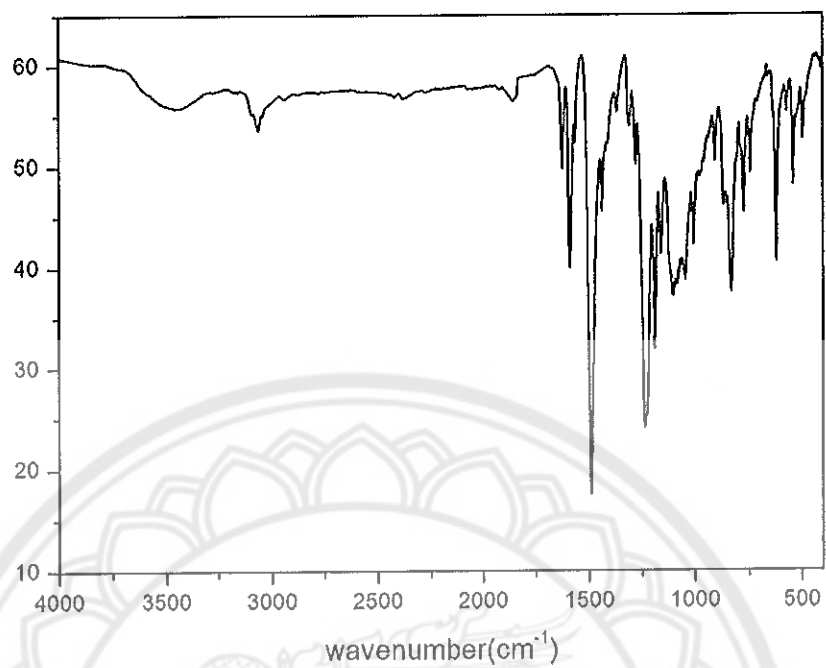


Figure 47 FTIR Spectrum of Compound Ag-4

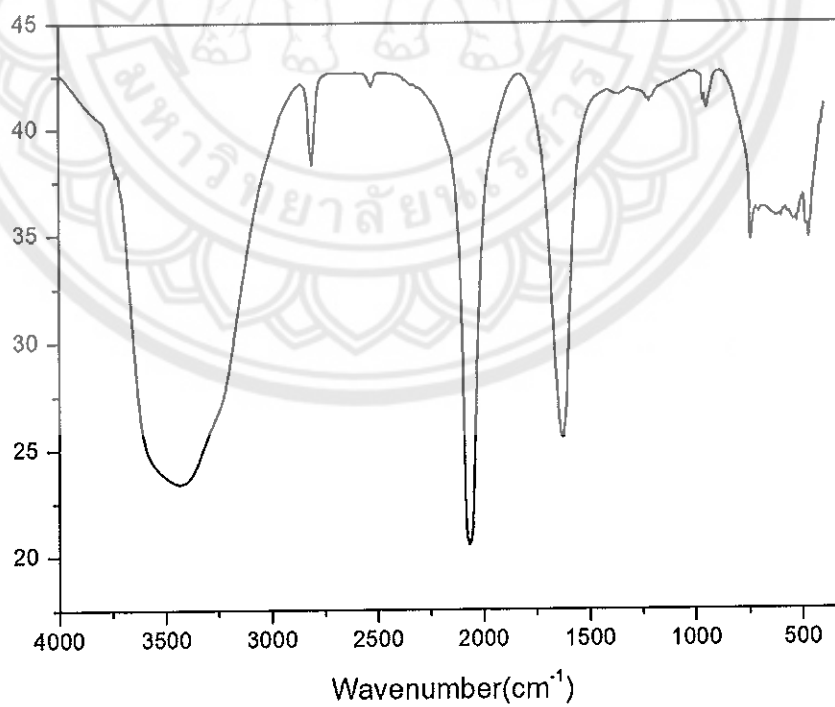


Figure 48 FTIR Spectrum of KNCS

APPENDIX B THERMAL GRAVIMETRIC ANALYSIS

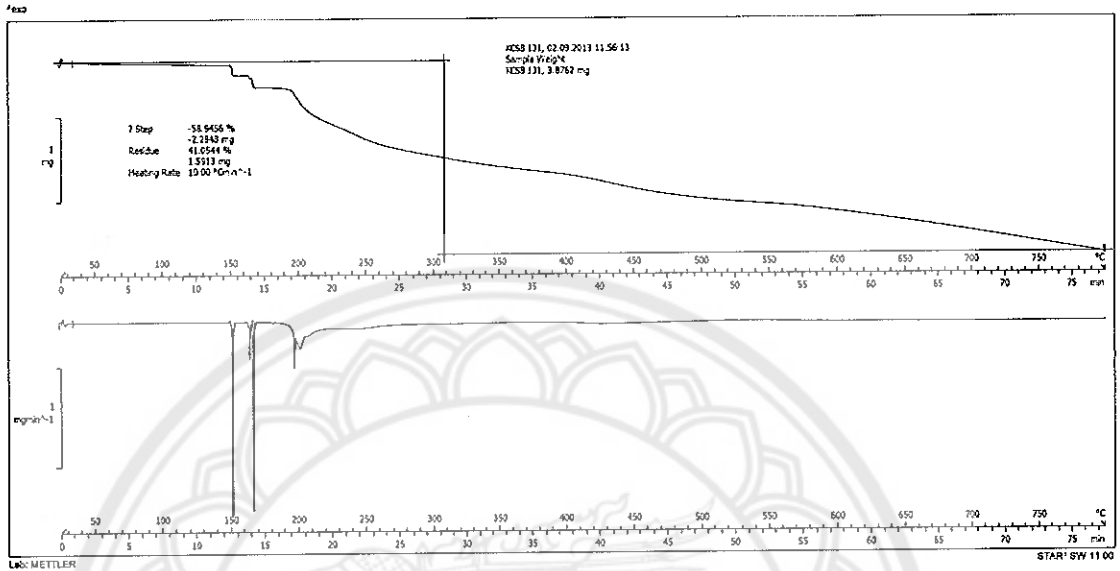


Figure 49 TGA Curve of Compound Cu-2

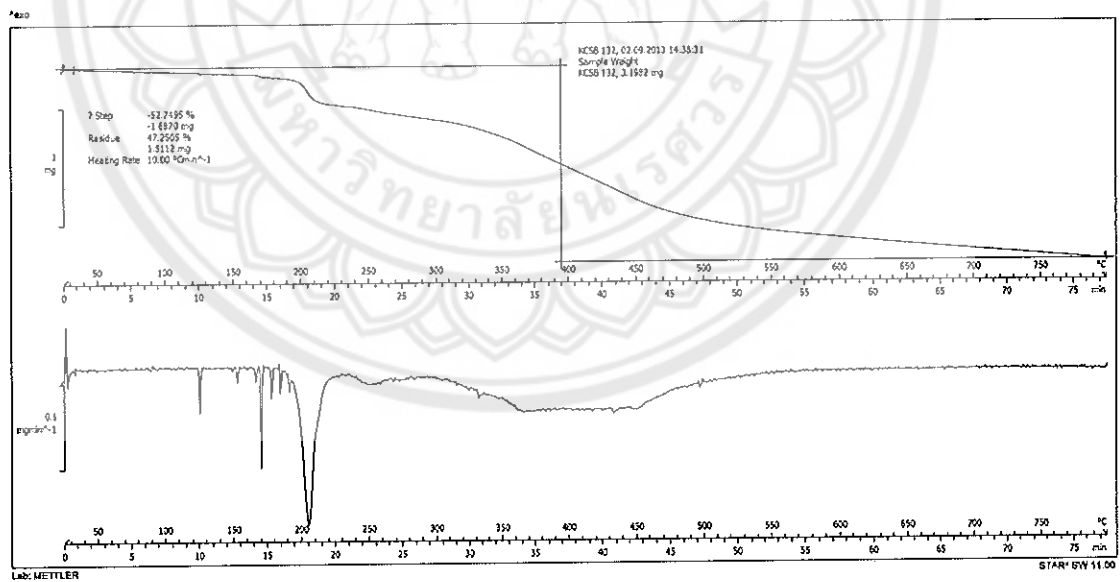


Figure 50 TGA Curve of Compound Cu-3

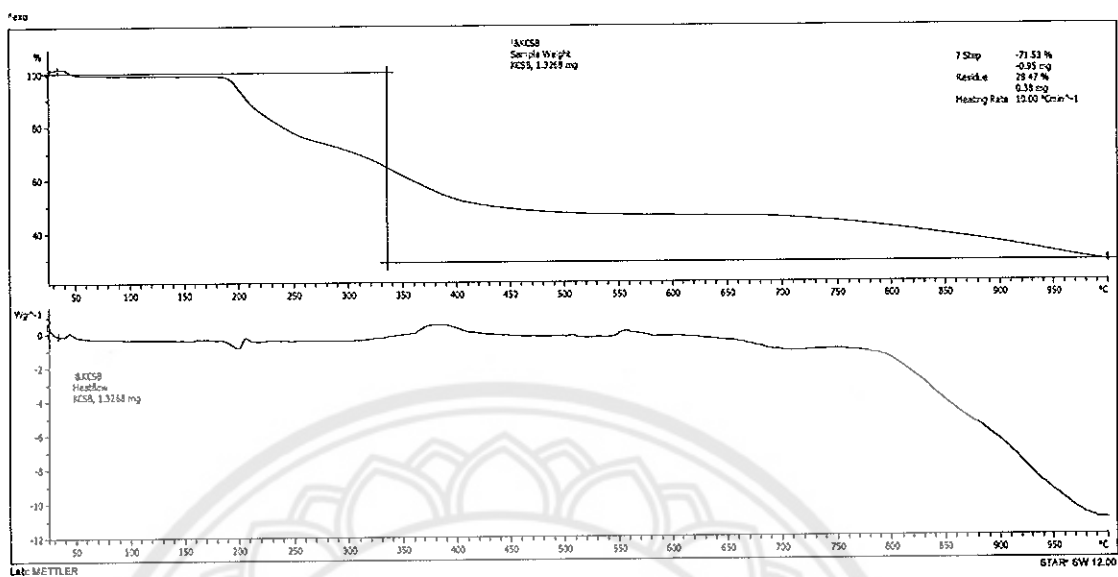


Figure 51 TGA Curve of Compound Cu-7

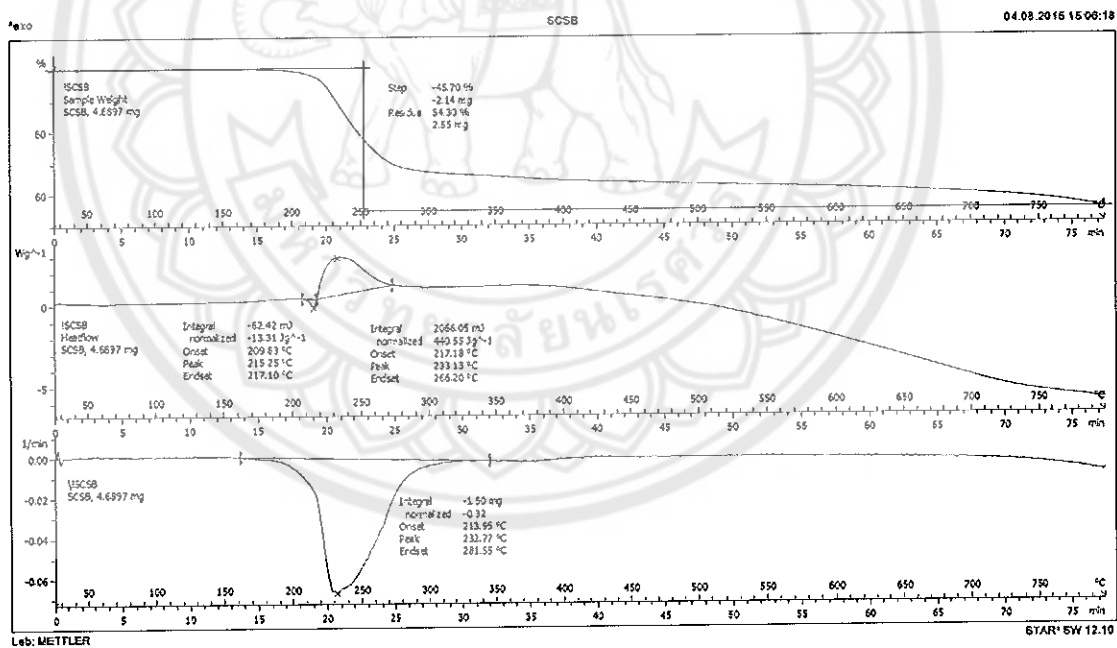


Figure 52 TGA Curve of Compound Ag-1

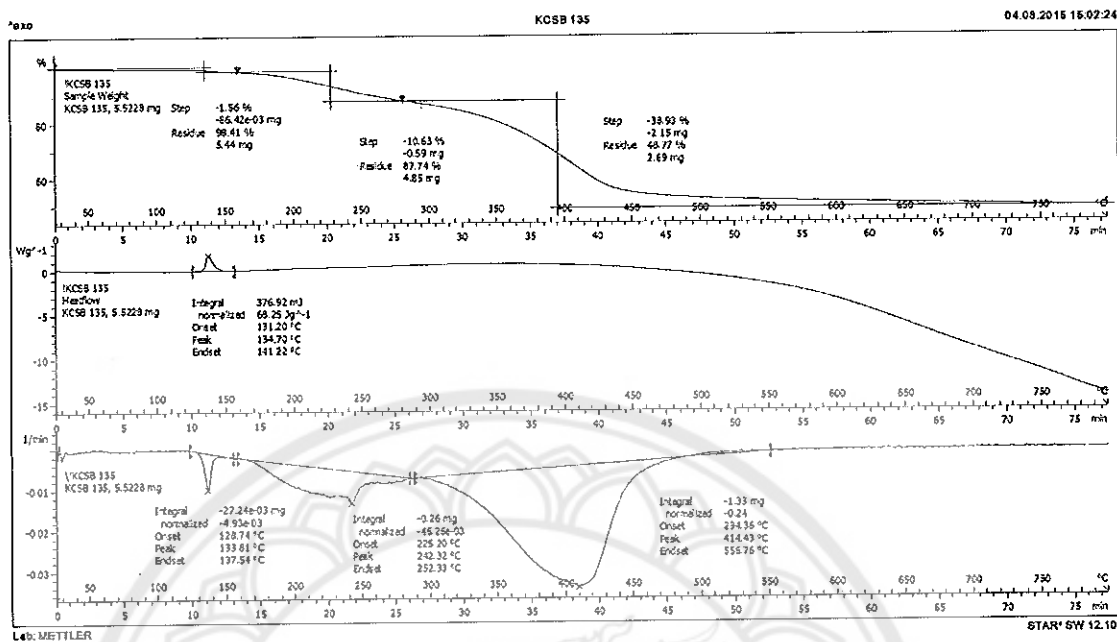


Figure 53 TGA Curve of Compound Ag-2

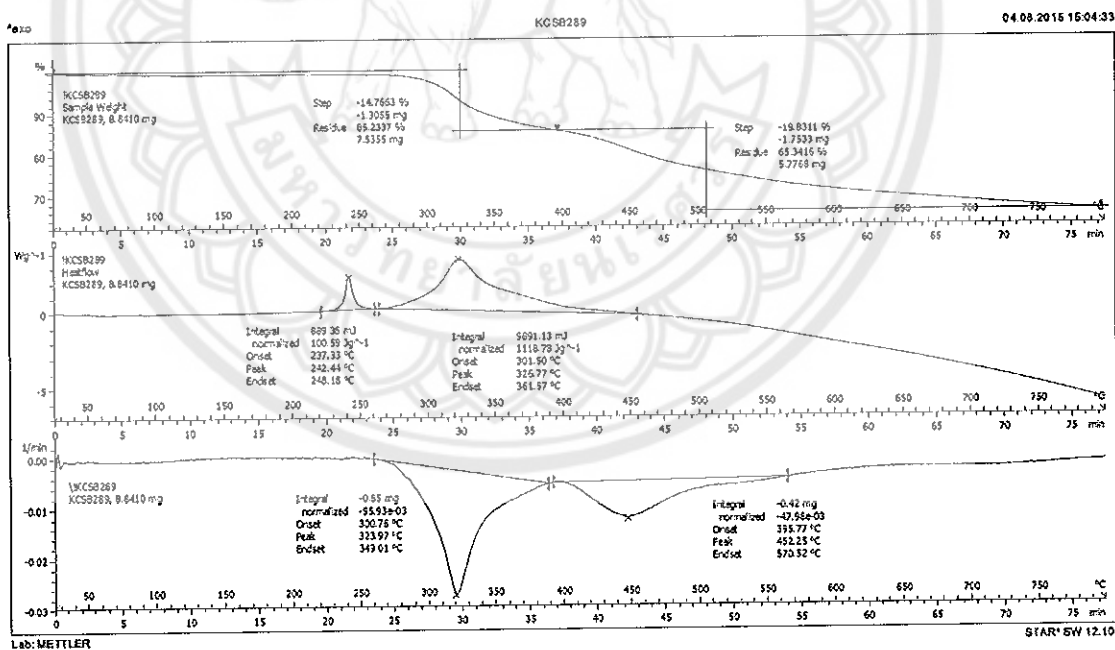


Figure 54 TGA Curve of Compound Ag-4